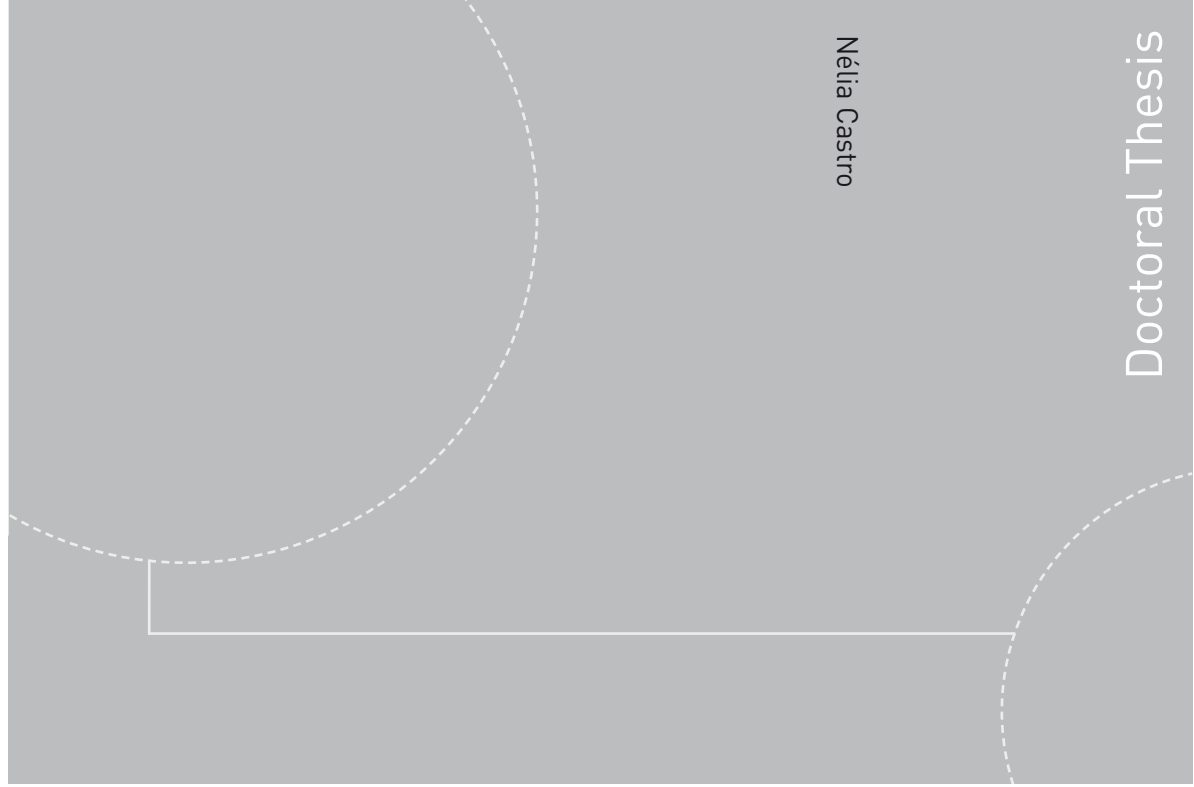


ISBN 978-82-471-4030-7 (printed version)  
ISBN 978-82-471-4031-4 (electronic version)  
ISSN 1503-8181



**NTNU – Trondheim**  
Norwegian University of  
Science and Technology



Doctoral theses at NTNU, 2012:351

Nélia Castro

Doctoral Thesis

NTNU  
Norwegian University of Science and Technology  
Thesis for the degree of Philosophiae Doctor  
Faculty of Engineering Science and Technology  
Department of Geology and  
Mineral Resources Engineering



**NTNU – Trondheim**  
Norwegian University of  
Science and Technology

Doctoral theses at NTNU, 2012:351

Nélia Castro

## Alkali-Aggregate Reactions in Concrete

Study of the relationship between  
aggregate petrographic  
properties versus expansion tests

Nélia Castro

# Alkali-Aggregate Reactions in Concrete

Study of the relationship  
between aggregate  
petrographic properties  
versus expansion tests

Thesis for the degree of Philosophiae Doctor

Trondheim, November 2012

Norwegian University of Science and Technology  
Faculty of Engineering Science and Technology  
Department of Geology and Mineral Resources  
Engineering



**NTNU – Trondheim**  
Norwegian University of  
Science and Technology

**NTNU**

Norwegian University of Science and Technology

Thesis for the degree of Philosophiae Doctor

Faculty of Engineering Science and Technology  
Department of Geology and Mineral Resources  
Engineering

© Nélia Castro

ISBN 978-82-471-4030-7 (printed version)

ISBN 978-82-471-4031-4 (electronic version)

ISSN 1503-8181

Doctoral theses at NTNU, 2012:351



Printed by Skipnes Kommunikasjon as

*In memory of my father  
Serafim Castro*





# Acknowledgements

First I would like to thank the two institutions that made this project possible: Fundação para a Ciência e Tecnologia - Portugal for the financial support through the doctoral grant SFRH/BD/41810/2007; The Norwegian University of Science and Technology (NTNU), Department of Geology and Mineral Resources Engineering, for accepting me as a PhD candidate.

I would also like to express my gratitude to my main supervisor Børge J Wigum for your constant support and motivation, and for the freedom you gave me to make my choices and my errors and learn from them. I really feel amazed and grateful with your readiness to answer my questions and especially with your ability to balance so many hats in your head at the same time. My thanks as well to my co-supervisors: Maarten ATM Broekmans for the scientific discussions, and critical review of my work; Mai Britt Mørk for the constant curiosity and enthusiasm about my work; Bjørn E Sørensen for invaluable help with laboratory work, and constant support and motivation.

For all the kind people and institutions that helped me with practical matters through the project my enormous thank you: Ingemar Borches at Verband Deutscher Zeitschriftenverleger (VDZ) for providing most of the samples used in this project and being so patient answering all my technical questions about them; Norcem for contributing with samples for this project as well; Isabel Fernandes at University of Porto for approving the use of samples from my Master thesis in this project; Jan Lindgård at SINTEF for receiving and storing some of my samples even before I started my project, for being always available to teach me about expansion data, and for the critical review of one of my papers; Peter Laugesen for the great work in preparing some of my samples; the NTNU laboratories and technicians at the Department of Geology and Mineral Resources Engineering and at the Department of Materials Science and Technology for sample preparation and analysis; the Norwegian Geological Survey (NGU) laboratories and technicians for analysis; and my colleague and friend Mahdi Shabanimashcool for the great help with statistics.

I sincerely thank the evaluation committee, Benoit Fournier, Per Hagelia, and Maria Thornhill, for their time, careful work, and valuable comments and suggestions.

I am grateful to all the friends and colleagues that made my stay in Trondheim wonderful and memorable. Your support, patience, and share of experiences, were nothing but essential to my success.

For being such important references in my career I have to extend my gratitude to my former supervisors Fernando Noronha and Isabel Fernandes for their long time support and advice.

And finally, most humble thanks to my wonderful family for long time support. My dear friends in Portugal (or anywhere else around the world), thanks for always believing I could do it even when I doubted. A special thanks to Tânia, for your advice, patience and knowledge, for the wonderful trips together, and for the hysterically funny adventures. Thank you, Pedro, for inspiration and growth, you show me I am much stronger than I thought. My extraordinarily beautiful mum and dad, I cannot thank you enough for your unconditional love and support. You gave me the courage to dream and the will to achieve. Dad, your wise words and proud eyes on me every step of the way were a great source of inspiration and are deeply missed every day, every moment. Mum, you are the strongest and more positive person I know. Thanks for teaching me that there is always a reason to smile.

Trondheim, November 2012

Nélia Castro

# Abstract

Alkali-Aggregate Reactions (AAR) is a deterioration mechanism in concrete that affects numerous structures worldwide. The most widespread type of AAR is the Alkali-Silica Reactions (ASR), a chemical reaction between silica *sensu lato* in the aggregates and the alkali hydroxides in the pore solution of concrete. Test methods to assess the potential alkali-reactivity of the aggregates have been under development for decades. The petrographic method shall always be the first step, followed by expansion tests (mortar bars and/or concrete prisms). The petrographic method has proven to be very effective, reliable, and time efficient when performed by experienced petrographers. However, some challenges in its application have been reported on a global scale for specific rock types. This thesis provides suggestions of test methods to be used as supplement to the petrographic method (RILEM-AAR-1, 2003) in order to overcome some of those challenges.

The mineral content of a variety of European aggregate samples was studied applying geology knowledge and techniques. Special focus was given to the characterization of the silica minerals within the aggregates. These results were critically reviewed against expansion results and experience in structures to ascertain the aggregate potential alkali-reactivity. As a result, a better understanding of some characteristics of the silica minerals that influence the potential alkali-reactivity of the aggregates was achieved. These findings were then used to develop methods able to quantify specific properties of the silica minerals that influence the aggregates reactivity under ASR environment. The developed methods are adapted to the characteristics of the aggregates: normally reactive or slowly reactive. The proposed methods are intended to overcome some of the limitations of the traditional petrographic method that have been reported in the literature with specific rock types. Therefore, their utilization may strengthen the petrographic method and improve its value as a tool to assess the potential reactivity of aggregates for concrete.

For slowly reactive aggregates, an image analysis petrographic method for quartz grain size and grain shape characterization was proposed. This method has proven to be more time efficient than the traditional point-counting method, while the results can be more accurate and precise. Not only a much larger number of points can be analysed, typical stereological problems such as the overestimation of the small grains produced by a two-dimensional representation of a rock (thin-section) can be easily and efficiently overcome. The correlation trends found between the grain size descriptors of quartz and expansion results confirm that the reactivity of slowly reactive aggregates is related to the total grain boundary area of quartz, which is strongly influenced by sub-granulation. This method has also great potential to be used

in thin-section from concrete structures in the assessment of the structure deterioration. Some inconsistencies between grain size descriptors and expansion data were found for samples with high degree of strain.

Electron backscatter diffraction (EBSD) analysis was applied to characterize the grain boundaries of quartz and investigate its influence on the reactivity of the slowly reactive aggregates for concrete. The initial results suggest that high angle boundaries increase quartz solubility, whereas low angle boundaries seem to have a lesser effect. This method bears a great potential to improve the understanding of the influence of strain in the potential alkali-reactivity of aggregates for concrete, especially when it comes to determining the role of different geometry and origin. The findings in this field can help to overcome the limitation found in the image analysis petrography method discussed above.

For normally reactive aggregates, the use of polished sections instead of the traditional powdered specimens to perform quantitative modal analysis by x-ray diffraction (XRD) was proposed. For fine-grained rock types without preferential orientation this alternative sample preparation has proven to be as accurate and precise as the traditional powdered specimens, while it offers several advantages in concrete petrography. By using polished section to investigate the mineral content by XRD in a number of normally reactive aggregates, it was possible to show that different polymorphs and species of silica have different impacts in the reactivity of normally reactive aggregates.

# Contents

<b>Acknowledgements</b> .....	i
<b>Abstract</b> .....	iii
<b>1 Introduction</b> .....	1
1.1 Motivations of the study.....	1
1.2 Objective of the study.....	4
1.3 Organization of the thesis.....	5
<b>2 Alkali-Aggregate Reactions in concrete</b> .....	7
2.1 Types of Alkali-Aggregate Reactions.....	7
2.2 Alkali-Silica Reactions mechanisms.....	8
2.3 Alkali-Silica Reactions controlling factors.....	12
2.3.1 Water.....	13
2.3.2 Alkalis.....	13
2.3.3 Reactive aggregates.....	15
<b>3 Test methods to assess the potential alkali-reactivity of aggregates for concrete</b> .....	21
3.1 General.....	21
3.2 Petrographic method.....	22
3.3 Accelerated mortar bar test.....	22
3.4 Concrete prism tests.....	23
3.5 The Danish methods.....	24
3.6 Field site test.....	25
3.7 PARTNER project conclusions.....	25
<b>4 Methodology</b> .....	29
4.1 General.....	29
4.2 Petrography of PARTNER samples.....	30
4.2.1 Materials.....	30
4.2.2 Methods for assessment and analysis.....	32
4.3 Grain size analysis of quartz.....	32
4.3.1 Materials.....	33

4.3.2	Methods for assessment and analysis .....	34
4.4	Characterization of the grain boundaries of quartz .....	38
4.4.1	Materials .....	39
4.4.2	Methods for assessment and analysis .....	39
4.5	Effect of polymorphs and other forms of silica .....	40
4.5.1	Materials .....	41
4.5.2	Methods for assessment and analysis .....	42
<b>5</b>	<b>Summary of results .....</b>	<b>47</b>
5.1	Petrography of PARTNER samples .....	47
5.2	Grain size analysis of quartz .....	53
5.3	Characterization of the grain boundaries of quartz .....	56
5.4	Effect of polymorphs and other forms of silica .....	58
	APPENDIX: Results from laboratory tests, field site test, and reported reactivity in structures .....	61
<b>6</b>	<b>Conclusions and recommendations for future work .....</b>	<b>65</b>
6.1	Conclusions .....	65
6.2	Recommendations for future work .....	67
	<b>References .....</b>	<b>69</b>

**Paper I:** Castro, N, Wigum, BJ (2012): *Grain size analysis of quartz in potentially alkali-reactive aggregates for concrete: a comparison between image analysis and point-counting*, in: Broekmans, MATM (Ed.), 10<sup>th</sup> International Conference on Applied Mineralogy, Trondheim, Norway, August 2011, Springer Verlag, Heidelberg/berlin, pp. 103-110.

**Paper II:** Castro, N, Sorensen, BE, Broekmans, MATM (2012): *Assessment of individual ASR-aggregate particles by XRD*, in: Broekmans, MATM (Ed.), 10<sup>th</sup> International Conference on Applied Mineralogy (ICAM), Trondheim, Norway, August 2011, Springer Verlag, Heidelberg/berlin, pp. 95-102.

**Paper III:** Castro, N, Wigum, BJ, Broekmans, MATM (2011): *Deleterious alkali-silica reaction in concrete: preliminary petrographical and microstructural characterisation of reacted and virgin materials from PARTNER project*, in: Mauko, A, Kosec, A, Tinkara, T, Gartner, N (Eds.), 13<sup>th</sup> Euroseminar on Microscopy Applied to Building Materials, Ljubljana, Slovenia, pp. 12.

**Paper IV:** Castro, N, Wigum, BJ, Broekmans, MATM (2012): *Deleterious alkali-aggregate reactions in concrete: relationship between mineralogical and microstructural characteristics of aggregates versus expansion tests*, in: Drimalas, T, Ideker, JH, Fournier, B (Eds.), 14th International Conference on Alkali-Aggregate Reactions in Concrete, Austin, Texas, USA, pp. 10.

**Paper V:** Castro, N, Wigum, BJ (2012): *Assessment of the potential alkali-reactivity of aggregates for concrete by images analysis petrography*, Cement and Concrete Research 42: 1635-1644.

**Paper VI:** Castro, N, Sorensen, BE, Broekmans, MATM (2012): *Quantitative assessment of alkali-reactive particles mineral content through XRD using polished sections as a supplementary tool to RILEM AAR-1 (Petrographic Method)*, Cement and Concrete Research 42: 1428-1437.

**Paper VII:** Castro, N, Sorensen BE, Wigum, BJ, Hjelen, J, Dall, W: *Potential contribution of EBDS to understand the role of quartz deformation in the alkali-reactivity of aggregates for concrete*, submitted to Materials Characterization (November 2012).



**Appendix A (on CD):** Additional papers

**Paper A:** Castro, N, Fernandes, I, Santos Silva, A (2009): *Alkali reactivity of granitic rocks in Portugal: a case study*, in: Bernhard, M, Just, A, Klein, D, Glaubitt, A, Simon, J (Eds.), 12th Euroseminar on Microscopy Applied to Building Materials, Dortmund, Germany, pp. 11.

**Paper B:** Lindgård, J, Haugen, M, Castro, N, Thomas, MDA (2012): *Advantages of using plane polished section analysis as part of microstructural analysis to describe internal cracking due to alkali-aggregate reactions*, in: Drimalas, T, Ideker, JH, Fournier, B (Eds.), 14th International Conference on Alkali-Aggregate Reactions in Concrete, Austin, Texas, USA, pp. 10.

# 1 Introduction

## 1.1 Motivations of the study

Alkali-Silica Reactions (ASR) is the most widespread type of Alkali-Aggregate Reactions (AAR) and causes damage in concrete structures worldwide. ASR can be defined as a chemical reaction that occurs when certain types of alkali-reactive silica minerals in the aggregate react with hydroxyl ions with associated alkalis, available from the cement paste, and/or the aggregates, and/or external sources, forming a hygroscopic gel. The alkali gel expands upon hydration and cracks up the surrounding concrete, thereby reducing the engineering properties of the concrete and the service lifetime of the structure. This can lead to the need of extensive repairing work or, in some extreme cases, to the replacement of the affected structures bearing extra costs for the society. Figure 1 shows examples of two concrete structures affected by ASR in Trondheim, Norway.

During the last century concrete has developed into the most important building material in the world. Concrete applications in the modern days are innumerable, ranging from residential and commercial construction to major infrastructure projects like e.g. tunnels, bridges and roads. This is partly due to the fact that concrete is produced from natural materials, available in all parts of the globe, and partly due to the fact that it is a versatile material, giving architectural freedom (ECO-SERVE, 2004).

In 2010, more than 369 millions of cubic meters of concrete were produced in Europe, which corresponds to an average of 0.70 cubic meters per capita (ERMCO, 2010). The EU-27's cement and concrete manufacturing sector employed more than 500 000 persons, or the equivalent of about one person in every three of those working in the activities of other non-metallic mineral products manufacturing. From a turnover of more than EUR 100 billion in 2006, the cement and concrete manufacturing sectors of the Member States together generated a total added value of more than EUR 35 billion, which represented ~44 % of the value added created by all the activities of other non-metallic mineral products manufacturing in the EU-27 (EUROSTAT, 2009). According to the statistics presented by the European Aggregates Association in their webpage (<http://www.uepg.eu/>), the annual aggregate production in Europe (EU-27 plus the EFTA countries) is estimated almost 3 billion tones, supplied by over 14,000 producers from 24,000 quarries and pits, employing about 250 000 people directly and indirectly. The total direct value of this production is estimated to be in the order of EUR 20 billion. These figures demonstrate the economic importance of the European cement and concrete, and aggregates industries.

Concrete is one of the most durable building materials. Most concrete buildings are design to a service life of ~30 years, but often last 50 to 100 years or longer. Nevertheless, concrete can be damaged by several processes, such as corrosion of the steel reinforcement bars, freeze/thaw deterioration, and chemical damage (carbonation, chlorides, sulfates, AAR). Giving the tremendous impact of concrete in the modern society, it is essential that the raw materials used in its manufacture are carefully selected in order to fulfill technical, economic and environmental requirements. This thesis focuses on the assessment of the potential alkali reactivity of aggregates for concrete.

Test methods to assess the ASR-potential of aggregates for concrete have been under development for several decades. To meet the needs of the building and construction industry, these test methods should be time and cost efficient, and yet provide accurate and precise results. The petrographic method shall always be the first step in the assessment of the potential alkali-reactivity of aggregates for concrete, followed by accelerated laboratory tests to confirm the results obtained (Sims and Nixon, 2003). Different European test methods were evaluated for their suitability for use with the wide variety of aggregates found across Europe in the EU-funded PARTNER project in 2002-2006. The overall experience from the PARTNER project is that the accelerated mortar bar test RILEM-AAR-2 (2000) and the accelerated concrete prism test RILEM-AAR-4.1 (to be published) are the most effective and have the best precision (Lindgård et al., 2010). It was also found that the petrographic method RILEM-AAR-1 (2003) can potentially provide effective and reliable results quicker than other method, but with some limitations. The petrographic method has proven to be very effective, reliable and time efficient method when performed by petrographers experienced both with the method and the local aggregates. However, when assessing specific rock types some challenges in the application of the petrographic method have been reported on a global scale. The limitations of the petrographic method and specific challenges in its application will be discussed in further detail in this thesis (Chapter III). It is however important to consider that if the petrographic method RILEM AAR-1 aims to be a reference method to assess the alkali reactivity of aggregates, both within Europe and worldwide; the quantification of the reactive silica within the aggregates may be an essential complement to the traditional application of nomenclature.

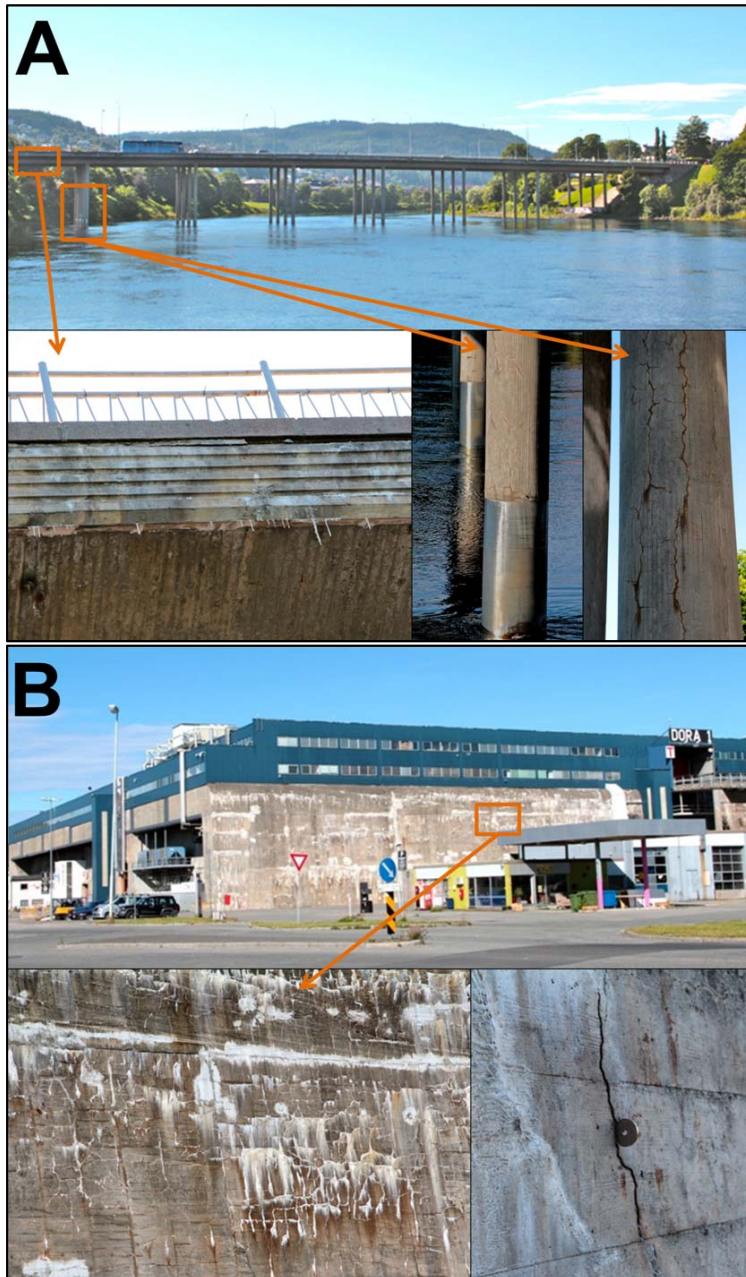


**Figure 1:** Examples of structures affected by ASR in Trondheim, Norway: (A) Elgeseter bridge: opened in 1951 after a construction period of 2 years; today, it represents a main entryway into Trondheim and is part of the European route E6 highway; (B) Dora 1: is a former German submarine base and bunker built during World War II; today is the home of the city and state archives and several businesses.

## 1.2 Objective of the study

The present project rose from the interest of applying techniques traditionally used by geologists like petrography, mineralogy, and geochemistry to the study of aggregates for concrete. A better knowledge of the aggregate properties will contribute to a better understanding of their performance when exposed to an extremely alkaline environment and consequently to a better understanding of the ASR mechanisms. A development of a full theoretical understanding on this very complex field is out of the scope of this work. The ASR phenomenon is so complex and there are so many parameters influencing its occurrence that, after more than half a century of research, many questions still remain unanswered. However, the findings of this work aim to contribute to the improvement of the test methods used to ascertain potential alkali reactivity of an aggregate, and to evaluate and set acceptable expansion limits of a reactive aggregate-cement combination.

The overall objective of this project is to provide basis to improve the precision and accuracy of the petrographic test RILEM AAR-1 for evaluating the alkali reactivity of aggregates across Europe. The project will achieve this by:

- Studying the mineral content of a variety of European aggregates using petrography, mineralogy and geochemistry techniques in order to investigate differences in the geological characteristics of the silica minerals within aggregates that proved to be reactive and non-reactive aggregates;
- Critically comparing the results of the silica minerals characterization with different test methods used across Europe to ascertain the alkali-reactivity of the aggregates in order to investigate possible correlation between them;
- Using the findings to develop a proposal to supplementary methods to improve the petrography method RILEM AAR-1, based on the quantitative measurement of specific properties of the reactive silica minerals within the aggregate.

### 1.3 Organization of the thesis

The thesis is divided as described in the following:

- **Chapters 2 and 3:** cover background topics and literature reviews on the alkali-aggregate reactions and the test methods to assess the potential alkali-reactivity of the aggregates for concrete.
  
- **Chapter 4:** describes the methodology used in the project.
  
- **Chapter 5:** present the main findings of the project and provides an overall discussion of the results.
  
- **Chapter 6:** conclusions and suggestions for future work are drawn.
  
- **Section of Original Papers:** full copies of the main papers I-VII can be found in this section.
  
- **Appendix A (on CD):** In addition to the seven main papers discussed in this thesis, contributions were made in two other papers that were included in this appendix.



## 2 Alkali-Aggregate Reactions in concrete

### 2.1 Types of Alkali-Aggregate Reactions

Alkali-Aggregate Reactions (AAR) can be defined as chemical reactions between the alkali hydroxides (sodium and potassium) in the pore solution of concrete and certain minerals in the aggregate. The product of the AAR is a hygroscopic gel that expands upon hydration and may introduce cracking in the surrounding concrete, thereby reducing the mechanical properties of concrete and structure service-life, and increasing cost for society. Expansive pressures of the alkali-silica gel as high as 14MPa were measured for mortars confined in a special container (Pike, 1967). Expansive pressures as high as 4MPa were obtained in concrete with reinforcing steel bars (Fujii et al., 1987). The incubation time needed before AAR damage starts ranges from a few months to several decades, much depending on aggregate type, binder type, and exposure conditions.

AAR was first mentioned in the literature by Thomas Stanton (1940) to explain the causes of map cracking which occurred in several structures situated in California. During the following decades several mineral and rock types were considered to be the cause of AAR. Gillott (1973) suggested the first systematic classification of AAR. His proposal was that AAR was divided in three main types:

#### *(1) Alkali-Silica Reaction (ASR)*

It was considered the most common and the most rapid of the AAR and described as a dissolution reaction that occurs as a result of the increased solubility in high pH conditions of amorphous, disordered or poorly crystallized forms of silica. This type of reaction was associated with the list of alkali-reactive rock types and minerals suggested by Mielenz (1946) (e.g. opal, chalcedony, volcanic glass, devitrified glass, tridymite, and possible hydromina);

#### *(2) Alkali-Silicate Reaction (ASiR)*

Distinguished from the “classical” ASR by a delayed onset of expansion of concrete prisms and the very long time span before cracking becomes evident in concrete structures. The reactive constituents were quartz bearing rocks, such as argillite, phyllite, greywacke, and possibly granitic rocks and quartzite;



### *(3) Alkali-Carbonate Reaction (ACR)*

A very deleterious and fast type of reaction associated with the presence of impure dolomitic limestone. As explained by Gillott (1964), expansion by ACR was associated with the presence of clays, either as intergranular material or as inclusions in the carbonate crystals.

In the late 80s, the Canadian Standard Association (CSA, 1986) renamed the ASiR to “Slow/Late-Expanding Alkali-Silicate/Silica Reaction (SLEASS)”. Some specialists (Hobbs, 1988; West, 1996) believe that in the case of the ASiR the reactive constituents in the aggregate were not free silica but the existence of silica in combined forms of phyllosilicates, often present in crystalline quartz-bearing rock types such as greywackes, phyllites, argillites or granites. In many of these rocks strained quartz is believed to be the reactive component.

Further research in the end of the 90s and beginning of the 00s, lead to the conclusion that both alkali-silica and alkali-silicate reactions should be generically called alkali-silica reactions (ASR), being the AAR divided only into two groups (Sims and Brown, 1998; RILEM-AAR-1, 2003): Alkali-Silica Reactions (ASR) and Alkali-Carbonate Reaction (ACR).

Recently, some researchers (Grattan-Bellew et al., 2008; Katayama and Sommer, 2008; Katayama, 2010, 2012) defend that ACR is most likely just a variant of ASR. According to the authors, ACR is a combination of deleteriously expansive ASR of cryptocrystalline quartz, and harmless dedolomitization of dolomitic aggregate which produces brucite and carbonate haloes without any accompanying expansion cracks. Other researchers accept ACR as formerly explained by Gillott (1964). Yet other authors believe that the dedolomitization process is the expansive and destructive mechanism and ASR is secondary regarding expansion (López-Buendía et al., 2008). The last editions of the International Conference on Alkali-Aggregate Reactions in Concrete (ICAAR) hosted interesting discussions on this topic. ACR is out of the scope of this thesis and will not be discussed further.

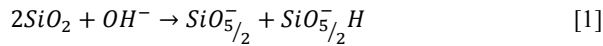
Jensen (2012) suggested a new classification system based on “reactive rate” and “negative lists” of reactive constituents and aggregates designated “very fast reactive AAR”, “fast reactive ASR” and “slow reactive ASR”.

## **2.2 Alkali-Silica Reactions mechanisms**

The chemical mechanisms of ASR were first described by Powers and Steinour (1955a, 1955b). Since then, different models have been discussed and proposed, being the most common to describe the reaction in two stages (Glasser and Kataoka, 1981a, 1981b; Wang and Gillott, 1991; Poole, 1992; Garcia-Diaz et al., 2006):

(1) Acid-base reaction

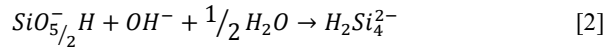
In contact to the pore solution of concrete, silanol groups (Si-OH) are created in the surface the silica minerals. The hydroxide ions (OH<sup>-</sup>) from the pore solution react with the acidic silanol groups as schematically represented in Figure 2 (yellow section), leading to a first bond break in the structure of the silica species present in the aggregate and water release. From a structural point of view, SiO<sub>2</sub> represents a Q4 silicon tetrahedron sharing 4 oxygens with 4 neighbours:



Note:  $\text{SiO}_{5/2}^-$  represents Q3 negatively charged tetrahedron in a basic solution.

(2) Dissolution of silica

The negatively charged Q3 tetrahedrons attract positive alkali cations such as sodium (Na<sup>+</sup>), potassium (K<sup>+</sup>), and calcium (Ca<sup>2+</sup>). The siloxane bonds are attacked by hydroxyl ions, leading to dissolution of silica in the pore solution and formation of silicate ions,  $\text{H}_2\text{Si}_4^{2-}$ ,  $\text{H}_3\text{SiO}_4^-$ , and small polymers, as schematically represented in Figure 2 (orange section):



Afterwards, precipitation of silicate ions by the cations of the pore solution of concrete leads to the formation of phases containing silica and different amounts of calcium and /or potassium and /or sodium and water (usually referred as alkali-silica gel). The alkali-silica gel by itself it is not deleterious, the problem is that when imbibes water its volume may increase considerably, creating high swelling pressure and consequent cracking of the concrete.

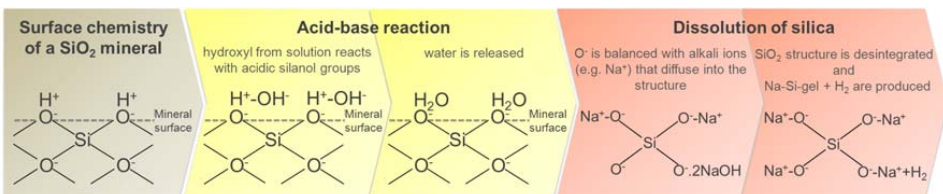


Figure 2: Schematic representation of ASR mechanisms.

Although the cracking of concrete by hydrated alkali-silica gel has been widely accepted, the swelling and cracking mechanisms are still under discussion. Different theories have been proposed to account for the swelling mechanism induced by ASR. According to Hansen (1944), the hardened cement paste act as a semi-permeable membrane that allows water molecules, hydroxyl ions, and alkali ions to “diffuse in”, but prevents silicate ions to “diffuse out”. As a result, an alkali-silicate is formed on the aggregate surface. This alkali-silicate would draw solution from the cement paste and form a liquid-filled pocket that would exert an osmotic pressure against the confining cement paste leading to cracking. McGowan and Vivian (1952) criticized this theory on the grounds that cracking in concrete should relieve the osmotic pressure and prevent any further expansion. Expansive pressure and eventually cracking in concrete are attributed by the authors to the growth of the alkali-silica gel caused by absorption of water. Expansion will depend on the volume concentration of the gel, its rate of growth and its physical properties. Tang (1981) supported this theory. Powers and Steinour (1955a) believed that both theories discussed above were fundamentally similar. The primary damage mechanism being swelling of the solid reaction product as controlled by the amount of calcium hydroxide it contained, but osmotic pressure might also develop as a results of the thermodynamic balance between the water held by the alkali-silica complex and the water external to the complex. The role of calcium hydroxide in the ASR mechanisms has been widely discussed in the literature and several theories have been proposed. The two main theories were proposed by Powers and Steinour in the middle 50s and by Chatterji et al. in the late 80s. Both theories agree that calcium hydroxide affects ASR, but disagree on how it affects the expansion mechanisms. Powers and Steinour (1955a, 1955b) postulated that the alkali-silica complex is expansive and that the lime-alkali-silica complex is non-expansive. Chatterji et al. (1989) did not accept the non-expansive nature of the lime-alkali-silica complex. Wang and Gillott (1991) summarized the most important functions of calcium hydroxide in the ASR and expansion processes. The first function of calcium hydroxide is its “buffering” capability for hydroxyl (OH-) ions; this function provides sufficient driving force to attack the disordered structure of siliceous mineral phases in the aggregate. The second function of the calcium hydroxide is its ability or potential to have ions exchange of calcium for alkalis. This can significantly re-generate alkalis for additional alkali-silica gel formation and increase expansion. Helmuth and Stark (1992) developed a model where gels in concrete are treated as mixtures of two end member phases of well-defined composition, one alkali-rich phase that is mobile and considered the traditional swelling gel, and one calcium-rich phase that is immobile and with limited or non-existing swelling capacity. Application to analysis of residual undissolved ASR gel in fully reacted natural opal sand grains performed by Diamond (2000), leads to unexpected

results that do not confirm Helmuth and Stark theory. Prezzi et al. (1997) and Rodrigues et al. (1999) proposed the electrostatic repulsion between diffuse double layers that form around the silica particles as responsible for generating expansive forces associated with ASR. Very high negative charges are observed at the surface of the silica grains (Rodrigues et al., 1999). To counterbalance the negative silica charges, an electric double layer of positive charges (cations) develop and absorb around the silica surface. These two layers are defined as the Gouy-Chapman layer and the Stern layer. They have a total thickness of a few nanometers, and can be composed of calcium, potassium, sodium, and some other anions. This system will form a colloidal suspension and then conglomerate into a gel which chemistry depends on the chemistry of the pore solution, pore structure in the concrete, and environmental conditions (Prezzi et al., 1997). The amount of repulsive forces and the thickness of the electric double layer depend on the valence of the cations in the gel and their concentration in the double layer (Prezzi et al., 1997; Rodrigues et al., 1999). Bivalent ions ( $\text{Ca}^{2+}$ ) will generate more repulsive forces and a larger electric double layer thickness than monovalent ions ( $\text{Na}^+$ ). Therefore, gels with high concentration of calcium will produce lower expansive forces than those containing high amounts of sodium and vice versa (Prezzi et al., 1997; Rodrigues et al., 1999). Dron (1990), Dron and Brivot (1993a, 1993b), and Dron et al. (1998) proposed that the hydrated gel is diffused far from the aggregate into micro pores and channels connecting the pores. The gel reacts with calcium ions and expands to induce the cracking of concrete. It not clear, however, why the gel generates an expansive pressure in the pores. Furthermore, the model cannot predict the cracking of the aggregate itself. Goltermann (1995) concluded that the expansive pressure due to the formation of hydrated gel is accumulated inside the reacting aggregate. The gel expands inhomogeneously causing tension in the aggregate, therefore causing cracking of both the aggregate and surrounding cement paste. Prince et al. (2001), demonstrated that the mechanisms governing the natural alteration of rocks also lead to the development of alkali-aggregate reaction. Their experiments with granites showed that existing minerals are transformed into minerals with expansive properties and the expansion occurs in the structural layers of the mineral and may cause relatively localized deterioration in the original material. Later, the mineral constituents are hydrolysed in the surrounding water, which gradually becomes saturated with silica, alumina and various cations. New phases evolve from this water, yielding gels or well crystallized products. Also Garcia-Diaz et al. (2006) proposed a swelling model based on the expansion of the aggregate. Ichikawa and Miura (2007) and Ichikawa (2009) defended that the alkali silica has no ability of generating expansive pressure unless the aggregate is tightly packed with a reaction rim. The reaction rim is slowly generated from the alkali silicate that covers the ASR-affected aggregate. Consumption of alkali hydroxide by the

ASR induces the dissolution of calcium ions into the pore solution. The alkali silicate then reacts with calcium ions to convert to an insoluble tight and rigid reaction rim. The reaction rim allows the penetration of alkaline solution but prevents the leakage of viscous alkali silicate, so that the alkali silicate generated afterwards by the ASR is accumulated in the aggregate to give an expansive pressure enough for cracking the aggregate and surrounding concrete.

In summary, though the exact mechanism of ASR is a matter of dispute, there is general consensus that at some point involves silica dissolution.

### 2.3 Alkali-Silica Reactions controlling factors

ASR can be influenced by several parameters, such as temperature, aggregate particle size/grading, use of air entrainment, paste porosity, water/cement ratio, but in order for expansion and cracking to result from ASR, the following three parameters have to be present at the same time: a sufficient supply of water, a sufficiently alkaline solution, and a critical amount of reactive aggregate (Figure 3). In this way, recommendations to avoid ASR are based on ensuring that at least one of those three major conditions is absent.

Comprehensive reviews on the parameters influencing ASR both in the structures and in the laboratory tests can be found e.g. in Wigum et al. (2006), Lindgård (2011), and Lindgård et al. (2012). The main focus in the literature survey has been to assess how various parameters may influence the laboratory/field correlation with respect to ASR performance testing, either directly or indirectly. A brief summary of the three most important parameters is included in the following sections.

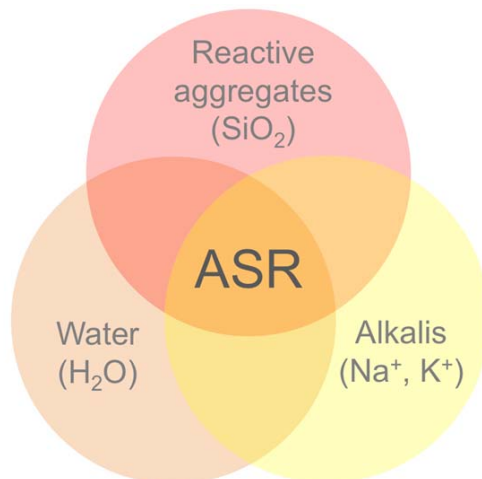


**Figure 3:** Illustration of the parameters necessary to the occurrence of ASR.

### **2.3.1 Water**

Water is generally accepted to be one of the main factors affecting ASR. As explained by Poole (1992), water plays a dual role in ASR. It works as a transport media for the alkali cations and hydroxyl ions, and when absorbed by the hygroscopic gel can make it swell and thereby causing concrete to crack. The sources of water in concrete could be either internal (e.g. excess of mixing water) or external.

The water content in ASR-affected structures is normally expressed as relative humidity (RH). However, the measurement of RH is notoriously very difficult and uncertain, particularly in the field (Lindgård et al., 2012). The degree of capillary saturation (DCS) may be a more suitable parameter to characterize the water content and the progress of damage on structures due to ASR (Lindgård, 2011). The relation between RH and DCS for different concretes, which is described by adsorption or desorption isotherms, varies depending on several factors, where the water-to-cementitious materials (w/cm) ratio (= water/binder (w/b) ratio) is the most important one.

The critical limit for developing ASR is reported to lie in the range 80-90% RH, depending on several factors, as discussed by Larive et al. (2000). Lindgård and Wigum (2003) and Wigum et al. (2006) found that DCS of Norwegian concretes with ASR was higher than 90%, with only a few exceptions.

Taking into account that the availability of moisture is an essential environmental factor for expansive ASR to occur, several researchers (CS, 1987; BCA, 1992; LCPC, 1994) propose different classifications of environmental risk of expansion due to ASR based on the exposure conditions. It is generally accepted that dams and bridges are long service life structures where the occurrence of deterioration due to ASR is unacceptable. More recently, Nixon et al. (2004) proposed a categorisation of the environmental risks both of the structures and of the concrete. According to the authors, the risks associated with the deterioration of the structure should be categorised in three levels: low risk, normal risk and high risk.

### **2.3.2 Alkalis**

The content of alkalis, i.e. sodium ( $\text{Na}^+$ ) and potassium ( $\text{K}^+$ ), in the concrete pore solution plays a major and complex role for development of ASR. Silica dissolves at extreme pH values in strongly acidic or strongly alkaline conditions, and less around neutral pH; and for this reason is designated as an amphoteric material. Increased alkali content leads to high pH of the pore solution necessary to dissolution of reactive silica from alkali reactive aggregates. Additionally, alkalis will react with the dissolved silica forming alkali silica gel.

The main contributor of alkalis to the concrete pore solution is usually the cement. Additional alkalis can be contributed by other sources such as supplementary cementitious materials, aggregates, mix water and external sources (e.g. de-icing salts). The alkalis in the cement are derived from the raw material (clay, limestone, chalk and shale) used in its manufacture. Supplementary cementitious materials (e.g. silica fume, fly ash, ground granulated blast furnace slag) sometimes have high alkali content but several studies suggest that they can be successfully used to prevent expansion due to ASR (Thomas et al., 2006). Past experience has demonstrated that the effectiveness of these materials depends on many factors such as their mineralogical and chemical composition, the percentage used as cement replacement, the reactive aggregates, and the concrete alkali content (Duchesne, 2006). Additional alkalis can be contributed by aggregates. In this case, the alkali is not in a free form but it is combined in silicates (e.g. feldspars, micas) and will be gradually released. Aardt and Visser (1977) were the first authors to propose the “solution theory” to explain the gradual release of alkalis from the silicates. According to this theory, the calcium hydroxide ( $\text{Ca}(\text{OH})_2$ ) reacts with the feldspar of the aggregates liberating alkalis in the form of potassium hydroxide (KOH) and sodium hydroxide (NaOH) and/or potassium and sodium silicate, the latter being gels and partially soluble in water. The same authors defend that feldspathic rocks should be carefully used as aggregates for concrete, especially the ones containing alkali feldspars such as granites, syenites. Bérubé and Fournier (2004) pointed out that there is still no consensus about the absolute amount that can be released by the aggregates into the concrete. However, considering that this can be an important factor in some cases, RILEM TC 219-ACS is developing a new test method (RILEM-AAR-8) regarding the release of alkalis from aggregates.

The content of alkalis in cement and concrete is usually expressed in terms of “sodium oxide equivalent”:  $\text{Na}_2\text{O}_{\text{eq}} = \text{Na}_2\text{O} + 0.658 \text{K}_2\text{O}$  (in weight percent). A limit of  $\text{Na}_2\text{O}_{\text{eq}} = 0.60\text{wt}\%$  of the cement, as proposed by Stanton (1940), has been used to minimize the risk of expansion by ASR. However, this limit ignores the fact that the alkali content of concrete is not determined solely by the alkali content of cement. Therefore, there are cases where the use of the sodium oxide equivalent to assess the potential reactivity of concrete mixtures can be misleading (Lindgård, 2011). A limit placed on the alkali content of concrete, expressed as  $\text{Kg Na}_2\text{O}_{\text{eq}}$  per  $\text{m}^3$  concrete, has been defended by several authors (CS, 1987; Hobbs, 1988; Bérubé et al., 2002). In Norway, concrete produced with Portland cement (CEM I, NS-EN 197-1) and alkali content  $\leq 3 \text{ Kg Na}_2\text{O}_{\text{eq}}$  per  $\text{m}^3$  of concrete shall be regarded as secure against deleterious ASR (NB-21, 2008).

The alkali distribution will also be of interest. It has been suggested that moisture mobility through concrete can cause alkali metal salts to migrate and create temporary or

permanent concentrations of these salts in some sections of the concrete structure. One example, of where this can occur is in foundation blocks where the tops are exposed, allowing water to evaporate from the surface (CS, 1987).

The alkali concentration in the concrete pore solution depends not only on the alkali content in the main constituents (cement, aggregates, and any additions), but also on the level of available alkalis that, to a high extent, is controlled by kinetics and mechanisms of release and fixation of these alkalis in reaction products (Lindgård, 2011). Various authors (Powers and Steinour, 1955a, 1955b; French, 1989), have observed the phenomenon of recycling of alkalis during the alkali aggregate reaction. The alkali gel formed within the aggregate particles changes composition when it comes in contact with the paste, and becomes richer in calcium, releasing alkalis to the pore water. According to this phenomenon, the reaction may theoretically continue until all alkali-reactive material is transformed into alkali silica gel.

### **2.3.3 Reactive aggregates**

There are two generalized classes of siliceous aggregates known to be potentially reactive with alkalis in concrete (Lindgård et al., 2010): the normally reactive aggregates (those that react in a time scale of 5 to 20 years) and the slowly reactive aggregates (those that react in a time scale greater than 15-20 years).

Normally reactive aggregates are characterized by the presence of very fine grained quartz and disorder forms of silica (e.g. opal, chalcedony). An important factor determining the reactivity of some normally reactive aggregates is the proportion of siliceous material. As defined by Hobbs (1988), for a given level of alkalis, the expansion of concrete increases with the reactive aggregate content to reach a maximum value. For aggregate content superior to the maximum, the expansion decreases due to an excess of reactive silica. The proportion of reactive aggregates corresponding to the peak expansion is called the “pessimum content”. Concretes based on both coarse and fine aggregate of very fast reactive forms of siliceous aggregates, like flint/chert, usually do not expand. Flint or chert-containing aggregates typically show pessimum behavior from 20-30vol%, with expansion reducing to negligible for flint/chert contents of 60vol% or over. For pure opaline silica, which is among the most alkali-reactive forms of silica, pessimum content is typically 2-5vol%, and self-inhibition from around 15vol% and up. However, experience shows that for certain rock types, there is no simple relationship between the proportion of any given reactive constituent in an aggregate and the magnitude of any resultant expansion due to ASR (Sims and Brown, 1998). Brouard (2012) defended the importance of correctly identify the potentially reactive aggregates with pessimum effect. These aggregates can be used safely in concrete structures as long as these aggregates are used alone



or mixed with potentially alkali-reactive aggregates. If they are mixed with non-reactive aggregates, the combination will likely lead to expansion and damage depending on the proportion of non-reactive aggregates.

Slowly reactive aggregates are typically crystalline quartz-bearing rock types such as mylonite, granite, gneiss, quartzite, greywacke, phyllite, and argillite. In many of these rocks, strained, microcrystalline or cryptocrystalline quartz is believed to be the reactive component. Gogte (1973) considered that the potential reactivity of slowly reactive rocks is related to the presence of strained quartz. Taking into account that the deformation of quartz is reflected on the undulatory extinction of quartz grains, Dolar-Mantuani (1981) measured the undulatory extinction angle of strained quartz and related this to the alkali reactivity of the material. However, many scientists have questioned the method and claimed that other factors have a greater influence on enhancing alkali reactivity of quartz than the undulatory extinction. West (1994) suggested that high undulatory extinction angles of quartz should be used as possible indicator rather than a diagnostic feature of potential alkali-silica reactivity in concrete aggregates. Grattan-Bellew (1986) defended that the presence of microcrystalline quartz in rocks that contain strained quartz is the key factor that makes them susceptible to alkalis. Thomson and Grattan-Bellew (1993) and Thomson et al. (1994) showed that the most reactive constituent appeared to be the microcrystalline quartz that has undergone significant sub-grain development, but not complete recrystallisation. It was also observed that zones of notable undulatory extinction were not significantly more alkali-reactive than non-deformed quartz. Kerrick and Hooton (1992) work about granitic rocks from Eastern United States shows that not only the microcrystalline quartz, which has formed by a recrystallisation process, but also texture properties of the rocks influence the alkali reactivity. Shayan (1993) obtained identical results with granitic rocks from Western Australia. Recently, the alkali-reactivity of granitic rocks in Portugal was also associated with the presence of strained, microcrystalline or cryptocrystalline quartz (Fernandes et al., 2004, 2007; Castro, 2008; Castro et al., 2009). Wigum (1995) and Wigum et al. (2000) have shown that grain size reduction of quartz (e.g. by subgranulation) enhances the aggregate reactivity by increasing the total grain boundary area available for reaction.

A main challenge regarding identification of aggregate reactivity is to find a test that can correctly classify all types of aggregates. The petrographic method shall always be the first step in the assessment of the potential alkali-reactivity of aggregates for concrete (Sims and Nixon, 2003), followed by expansion tests (e.g. mortar bars or concrete prisms) to confirm the results. Lists of potentially reactive rock types and minerals based on their nomenclature are present in literature and usually on standards (BS-7943, 1999; RILEM-AAR-1, 2003; CSA-A23.2-15A,

2004; ASTM-C-295, 2007; NB-21, 2008). However, it is now recognized that, the application of classifications based on rock and mineral nomenclature is too dependent of local experience and provide no guarantee to prevent deleterious ASR in concrete structures, as discussed in detail in the next chapter. Aggregate reactivity depends of many parameters. Mineralogy and microstructural texture of the rocks are the ones with more impact, but the mechanisms of formation of the rock and its degree of deformation have also great influence. Additionally, physical properties of the aggregate particles (e.g. particle size, shape and grading) can also influence the aggregate reactivity. Comprehensive descriptions of the parameters known to influence the potential alkali-reactivity of aggregates for concrete can be found in Wigum et al. (2006); Lindgård (2011); and Lindgård et al. (2012). While some parameters are easy to assess, others are more difficult to understand and cause numerous questions about the topic to remain unanswered. It is evident that further research is needed to understand the complex behavior of different rock types and minerals in “ASR environment”. Especial focus is required to the factors that influence the silica minerals dissolution as defended by Broekmans (1999, 2004). After all, silica dissolution is the starting point of ASR. Only a better understanding on this topics will make possible to develop tests capable of quantify the reactive components in the aggregates, which will considerably increase the precision and accuracy of the test methods.

Silica minerals are essential constituents of the Earth’s crust. At least nine silica polymorphs are known to exist. Best known are:  $\alpha$ -quartz,  $\beta$ -quartz, tridymite, cristobalite, coesite and stishovite. All have composition  $\text{SiO}_2$  but unique crystal structure. From a structural point of view, silica minerals are tectosilicates or framework silicates. Comprehensive reviews on silica polymorphs and varieties can be found e.g. in Heaney (1994), Rykart (1995), and Graetsch (1994). Each silicon atom (Si) is coordinated with four oxygen atoms (O), forming a tetrahedron ( $\text{SiO}_4$ ). The minerals structure is built from  $\text{SiO}_4$  tetrahedra linked by sharing each of their corners with another tetrahedron creating a 3D framework where every silicon has four oxygen and every oxygen has two silicon as nearest neighbours. Different silica polymorphs are stable in different pressure-temperature conditions but can be transformed into other polymorphs by breaking silicon-oxygen bonds, rearranging the tetrahedra into a new pattern. Different polymorphs can exist metastably for some time in other polymorphs stability fields. The predominant polymorph of silica within the crust is  $\alpha$ -quartz. It can be found as a major constituent of numerous igneous, metamorphic and sedimentary rocks. Therefore,  $\alpha$ -quartz is the most common of the silica polymorphs in aggregates for concrete, but metastable silica phases are not uncommon. For instance, both cristobalite and tridymite occur as metastable modifications at low temperature (Heaney, 1994).

Solubility of silica is different for different polymorphs. As a general rule, the lower the activity of silica, the lower the solubility. According to thermodynamic data experimentally confirmed in laboratory, quartz is the least soluble polymorph in contrast to glassy silica that is the most soluble, whilst others are intermediate (Robie et al., 1978). Thus, the predominant silica species largely governs the alkali-reactivity potential of the aggregate, a disordered silica structure being more reactive than cristobalite, which in turn is more reactive than ‘orderly quartz’ (Zhang et al., 1990). On the other hand, a number of SiO<sub>2</sub> species are of particular interest with respect to ASR: opal, flint/chert, chalcedony. Characterization of the predominant crystal structures is then essential to assess the effect of different silica species and polymorphs in the alkali-reactivity potential of aggregates for concrete, especially in rock types usually characterized as normally reactive.

Chemical impurities and foreign ions, including water and silanol groups, tend to be associated with crystal lattice defects: point defects, line defects or dislocations, and plane defects or boundaries. Within a defect and in a small volume embedding it, the crystal lattice is distorted and the inter-atomic bonds may be easier to break. Thus, the solubility of a solid at a crystal defect is increased relative to immaculate material. The most common point defects in quartz are replacements of Si<sup>4+</sup> for Al<sup>3+</sup> and Fe<sup>3+</sup>. These replacements leave uncompensated charges in the structure and to maintain electrical balance, small monovalent cations like H<sup>+</sup>, Li<sup>+</sup>, Na<sup>+</sup> and/or K<sup>+</sup> enter the quartz structure in interstitial spaces (Kronenberg, 1994). One other way to replace silicium in quartz is by four H<sup>+</sup> in a silanol group replacing one Si<sup>4+</sup> (Kronenberg, 1994). If a silanol group occur e.g. in dislocation defects, the entrance of water molecules in the quartz structure will be facilitated, causing the dislocation to grow. The effect of foreign and hydrous species in quartz solubility under ASR environment is poorly understood but deserves to be further investigated.

Deformation seems to be a key factor in the potential reactivity of slowly reactive aggregates. Deformation in rocks is achieved by a number of processes on the scale of individual grains. A comprehensive description of the deformation mechanisms on the scale of individual grains can be found e.g. in Passchier and Trouw (2005), and only a brief discussion of the main mechanisms influencing quartz deformation will be included here. Although quartz is one of the most common minerals in the crust, its deformation behavior is very incompletely understood. Temperature is an important factor in quartz deformation. The dominant deformation mechanisms and resultant structures change significantly from low to high temperature as schematically represented in Figure 4. However, quartz deformation behavior is also influenced by strain rate, differential stress and the presence of water in the lattice and along grain boundaries (Passchier and Trouw, 2005). Brittle deformation and cataclastic flow

are characteristic of the upper crust, while at deeper crustal levels, rock deform by ductile flow through a range of mechanisms of ductile grain scale deformation. Ductile deformation in rocks could not lead to high strain if not accompanied by mechanisms of recovery or recrystallization in order to reduce the damage imposed during the deformation process.

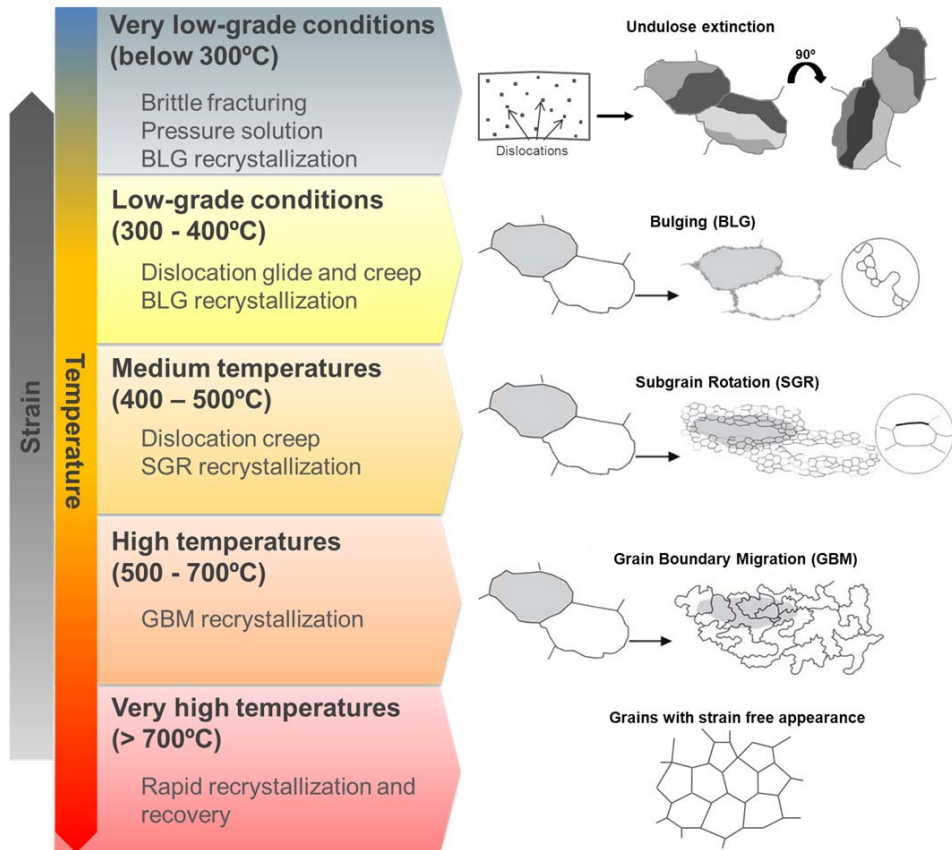


**Figure 4:** Schematic representation of quartz dominant deformation mechanisms and resultant structures with increase of temperature (some images adapted from Passchier and Trouw, 2005).

As discussed before, strained, microcrystalline or cryptocrystalline quartz is believed to be the reactive component in many slowly reactive aggregates. These structures can be the result of different deformation mechanisms as shown in Figure 4. The challenge is to quantify the potential-reactivity of each resultant structure, which is greatly influenced by the quality of the crystal lattice (e.g. dislocation density), grain size and shape, and extension and characteristic of the resultant grain boundaries. Although grain size and shape are not a fundamental material properties of quartz, they do affect its solubility, especially in combination with porosity and permeability of the aggregate particle. As shown by Wigum (1995) and

Wigum et al. (2000), aggregates containing quartz with a small initial grain size and/or coarse-grained quartz that suffered extensive grain size reduction and/or sub-graining due to geological deformation will be more prone to develop deleterious AAR due to an increase in available grain boundary surface area. However, it is not only the grain boundary area that determines the accessibility of the pore solution. The grain boundaries are characterized by two parameters with five degrees of freedom (Randle, 1992): the orientation of the boundary plane; and the misorientation between two neighbor grains which share the same grain boundary. If a grain boundary separates grains of the same mineral, they must have a significantly different lattice orientation. Sub-grains can be recognized as parts of a crystal that is separated from adjacent parts by discrete, sharp, low relief boundaries (usually  $<5^\circ$ ), and are often formed during ductile deformation of the rocks in order to achieve more stable energy stages. The characterization of grain boundaries geometry and their preferred orientation in different deformation contexts remain poorly understood due, mainly, to difficulties to determine all parameters required for a complete boundary characterization (Gonçalves and Lagoeiro, 2009). However, it would be essential to a better understanding of the effect of deformation in the potential-alkali reactivity of slowly aggregates for concrete.

# 3 Test methods to assess the potential alkali-reactivity of aggregates for concrete

## 3.1 General

Test methods to assess the potential alkali-reactivity of aggregate for use in concrete have been under development for several decades. A number of different test methods are used worldwide. While some methods assess the potential reactivity of the aggregate itself, others assess specific concrete job mixes (performance tests). To meet the needs of the building and construction industry, these test methods are required to provide an accurate and precise result that mirror the durability behavior in real structures designed for life time up to 100 years, in the shortest time possible, and with the lowest budget possible.

This chapter will describe several laboratory test methods to assess the potential alkali-reactivity of aggregates for concrete, with special focus on the test methods tested in the European research project PARTNER. As will be discussed in detail in Chapter 4, this doctoral project uses a number of samples previously applied in PARTNER project. Additionally, the results obtained with each of the methods used to characterize the aggregates in this doctoral thesis were critically reviewed against expansion data and field experience from PARTNER project.

PARTNER project was partly funded by the European Community and had the overall objective of establishing unified test procedure for evaluating the potential alkali reactivity of aggregates across the different European economic and geological regions. Nine laboratory test methods were evaluated for their suitability for use with the wide variety of aggregates and geological types found across Europe. The project had 24 partners from 14 countries, covering most of Europe, from Iceland to Greece. Were evaluated 22 different types of aggregates, including normally reactive, slowly reactive, and non-reactive aggregate types, from 10 different European countries. The aggregates were selected with the purpose of covering most types of reactive aggregates throughout Europe. In total, 413 tests were performed within the PARTNER project. Details of the test programme, the aggregates, the test methods and the results were given in a series of technical reports published by the Norwegian research institute SINTEF (Grekk, 2006; Jensen, 2006; Lindgård and Haugen, 2006; Nixon and Lane, 2006; Siebel et al., 2006; Wigum et al., 2006). These reports may be freely downloaded at the FARIN (Forum on Alkali-Aggregate Reactions in Norway) webpage ([www.farin.no/english](http://www.farin.no/english)) and at SINTEF webpage (<http://www.sintef.no>). Additionally, a petrographical atlas of the potentially

alkali-reactive rocks in Europe was published by the Belgian Geological Survey (GSB, 2006). The petrographic atlas was later integrated as part of the FARIN webpage. Four papers covering parts of the project in more detail were published in the 13<sup>th</sup> ICAAR conference in Trondheim (Borchers and Müller, 2008; Haugen et al., 2008; Nixon et al., 2008; Schouenborg et al., 2008). The final results and recommendations were published in Cement and Concrete Research (Lindgård et al., 2010). An update of the results of the field site test after 7 years was recently published in the 14<sup>th</sup> ICAAR conference in Texas (Borchers and Müller, 2012). This chapter contains a brief summary of each test method and an overview of the principal findings of the PARTNER project.

### **3.2 Petrographic method**

The petrographic method shall always be the first step in the assessment of the potential alkali-reactivity of aggregates for concrete (Sims and Nixon, 2003). The petrographic method RILEM-AAR-1 (2003) comprises two techniques: macroscopic petrography, and thin-section petrography. Macroscopic petrography is used in coarse aggregate fractions >4mm. Thin-section petrography is applied to all fine aggregate fractions <4mm (point-counting method), as well as to any coarse constituent that could not be unequivocally identified by macroscopic petrography (whole rock petrography). The objective is to identify the mineral and rock constituents of the aggregate according to acknowledge nomenclature and classify the alkali-reactivity potential of each mineral and rock type identified as: I – Very unlikely to be alkali-reactive; II – Alkali-reactivity uncertain; III – Very likely to be alkali-reactive. It is very important that the petrographic analysis is carried out by a qualified geologist or petrographer with experience of materials used for concrete and good local knowledge of alkali-reactive aggregates and minerals. When all samples have been studied, the modal content in volume percent for each identified lithology is calculated and the data used to classify the alkali-reactivity potential of the bulk aggregate material, applying criteria based on local (national, regional) experiences, recommendations and specifications. Different countries use different standards and methodologies to perform the petrographic method (BS-7943, 1999; RILEM-AAR-1, 2003; NB-21, 2008) and suggest different criteria for classification of the potential alkali-reactivity of the aggregates. All base their classification system in the application of mineral and rock nomenclature.

### **3.3 Accelerated mortar bar test**

The accelerated mortar bar test (AMBT) has duration of 14 days. Three mortar prisms made with the aggregate and a reference high alkali cement are stored in 1M NaOH at 80°C.

Differences in the mortar bar size, curing time and conditions, and storage time before zero reading are found when comparing different test procedures to this method (Oberholster and Davies, 1986; RILEM-AAR-2, 2000; ASTM-C-1260, 2007). A detailed discussion of these differences and their influence in the test result can be found in Paper V and will not be repeated here.

Results of less than 0.10% are likely to indicate non-expansive materials, whilst results exceeding 0.20% are likely to indicate expansive materials. Results between 0.10% and 0.20% are difficult to interpret and in the absence of additional local experience shall be regarded as potentially expansive. These critical limits are still under discussion for RILEM-AAR-2 (2000).

### **3.4 Concrete prism tests**

In general, concrete prism tests monitor the expansion and weight change of concrete specimens made with the test aggregates and high alkali cement and stored in conditions of high humidity and elevated temperature during weeks or years, depending of the method. In PARTNER project, five concrete prism tests were evaluated:

#### *Concrete prism test RILEM-AAR-3 (2000)*

This test has duration of 12 months. Wrapped concrete prisms (dimensions ranging between 250±50mm and 75±5mm) made with the aggregate and a reference high alkali cement are stored in individual containers within a constant temperature room at 38°C and measured at 20°C. The aggregate is considered reactive if expansion is higher than 0.050 % in the end of the test.

Note that further research lead to the conclusion that wrapping the concrete prisms enhances alkali leaching. Therefore, the new version of the method to be published this year uses unwrapped concrete prisms (more details in section 3.7).

#### *Accelerated concrete prism test RILEM-AAR-4.1 (to be published)*

This test has duration of 20 weeks. Concrete prisms (dimensions ranging between 250±50mm and 75±5mm) made with the aggregate and a reference high alkali cement are stored in individual containers within a reactor at 60°C and measured at 20°C. The aggregate is considered reactive if expansion is higher than 0.030 % in the end of the test.

#### *Alternative accelerated concrete prism test RILEM-AAR-4.1 (to be published)*

This test is similar in all aspects to the accelerated concrete prism test above but in this case the prisms are stored wrapped in a cotton cloth.



Note that this version of the method is no longer used since it was found that wrapping the prisms would enhance alkali leaching.

*German concrete prism method (DAfStb, 2007)*

This test has duration of 9 months. Three concrete prisms (100x100x500mm) and one cube (300x300x300mm) are stored in a fog chamber at 40°C with measurements taken immediately with no cooling down period. The aggregate is considered reactive if expansion is higher than 0.060 % in the end of the test.

*Norwegian concrete prism method (NB-32, 2005)*

This test has duration of 12 months. Three concrete prisms (100x100x450mm) made with the aggregate and a reference high alkali cement are stored in individual containers within a constant temperature room at 38°C and 100% relative humidity and measured at 20°C. The aggregate is considered reactive if expansion is higher than 0.040 % in the end of the test.

### **3.5 The Danish methods**

Two methods developed in Denmark were included in PARTNER project:

*The Danish mortar bar method TI-B51 (1978)*

This test has duration of 52 weeks. Mortar prisms (40x40x160mm) made with the aggregate are stored in saturated NaCl solution at 50°C. The aggregate is considered non-reactive if expansion is less than 0.04% after 20 weeks; late slow reactive if expansion is lower than 1.0% after 20 weeks and higher than 1.0% after 52 weeks; and fast highly reactive if expansion is higher than 1.0% after 20 weeks.

*The Danish Chatterji method (Chatterji and Jensen, 1988)*

This test has duration of 24 hours. Crushed and graded aggregate material is dried at 105°C to constant weight. Two dry samples of the aggregate to be tested and one sample of a non-reactive quartz sand (reference sample) of 100.0 g ± 0.2 g are placed in a conical flask with a KCl solution at 70°C ± 2°C. The degree of reaction is measured by the alkalinity after reaction, which is compared to the non-reactive standard. An index value ( $\Delta$ ) is calculated and evaluated according to criteria set by Chatterji and Jensen (1988).

### 3.6 Field site test

These tests were undertaken as a mean to evaluate the reliability of different laboratory tests (Lindgård et al., 2010). 100 concrete cubes (300mm length) were stored in 8 different sites from Norway (Figure 5) to Spain to test different environmental conditions. To investigate the effect of the storage conditions, one cube was stored with its base in a tray filled with water (wet storage) and the other was exposed only to ambient rainfall (dry storage). In Sweden specimens were stored in two field sites to study the influence of alkali supply by de-icing salts. Some specimens were stored alongside the highway 40, between Borås and Gothenburg; some specimens were stored in a nearby forest to work as a control group. Results after 7 years of exposure were recently published by Borchers and Müller (2012).



Figure 5: PARTNER field site test in Trondheim, Norway (photography kindly provided by Jan Lindgård).

### 3.7 PARTNER project conclusions

The overall experience from the PARTNER project is that in most cases the RILEM tests could successfully identify the reactivity of the aggregates or aggregate combinations tested (Lindgård et al., 2010). The RILEM concrete prism methods evaluated in the PARTNER project were most successful with normally reactive (those that react in a time scale of 5 to 20 years) and non-reactive aggregates. There was less certainty in identifying aggregates that react very slowly (in a time scale greater than 15-20 years) (Lindgård et al., 2010).

It was concluded that the accelerated mortar bar test (RILEM-AAR-2, 2000) and the accelerated concrete prism test (RILEM-AAR-4.1, to be published) are the most effective and have the best precision across the whole range of European aggregates. Moreover, these methods have the advantage of providing (relatively) fast results and are the most repeatable and reproducible. Whether these conclusions can be applied to all European regions will have to be verified by additional local examination. It is important to keep in mind that the mineralogical characteristics of the aggregates have a great influence in the expansion tests. Therefore, the results obtained in PARTNER project may be conditioned by the characteristics of the aggregates that were tested. RILEM-AAR-2 (2000), for example, was one of the most effective test methods in PARTNER project. However, several authors have shown that the limits usually applied are unable to detect some slowly reactive aggregates, such as granite, gneiss, and quartzite (Fernandes et al., 2004, 2007; Shayan, 2007; Castro, 2008; Castro et al., 2009). A reason for this problem may be the use of very fine aggregates that destroy the original microstructure characteristic of the rocks (Lu et al., 2006), underestimating the alkali reactivity of the rocks. On the other hand, non-reactive aggregates may be classified as reactive because the conditions of the test are too severe for some types of aggregates (Bérubé and Fournier, 1993; Shayan et al., 2008), or because the test is not able to detect non-reactive aggregates with pessimism effect. In PARTNER project, the method RILEM AAR-4 was the most effective in identify this type of aggregates (Lindgård et al., 2010). Ideker et al. (2006) and Shayan et al. (2008) verified that tests performed with different non-reactive natural sands mixed with the same coarse reactive aggregate show different results depending on the test methods applied. In PARTNER, the various tests gave results that agreed in most cases (Lindgård et al., 2010). The main exceptions were the differences between the RILEM AAR-3 and RILEM AAR-4 results when very slow reactive aggregates were tested. In these cases, the AAR-4 method identified more clearly the potential alkali-reactivity, even though it did not necessarily show that the expansion would be slow. In contrast to AAR-3 (38°C), the AAR-4 (60°C) method produced relatively higher expansions for slowly reactive aggregates compared with normally reactive aggregates. Recent studies developed in North America have reported that a significant reduction in expansion was observed when known reactive aggregates were tested in the accelerated concrete prism test (60°C) and compared to the standard concrete prism test (38°C) (Ideker et al., 2010).

PARTNER project findings also point out that the RILEM petrographic method (RILEM-AAR-1, 2003) can potentially provide effective and reliable results quicker than other methods, but with some limitations. Precision trials to RILEM petrographic method determined that the identification of the rocks and minerals is similar among different laboratories, but the

classification of the potential alkali-reactivity of the aggregates (i.e. class I, II, or III) varies a great deal, probably due to the regional experience (Haugen et al., 2008; Schouenborg et al., 2008; Lindgård et al., 2010). The spread between the four most experienced laboratories were rather low, though. The results show that the precision and reproducibility of the petrographic method strongly depends on the experience and expertise of the petrographer. Education, in combination with proficiency trials of individual laboratories, is therefore the way forward for future constructive development in this area. In summary, the petrographic method has proven to be very effective, reliable and time efficient method when performed by petrographers experienced both with the method and the local aggregates. In Norway, after more than 20 years of experience, the petrographic method (NB-21, 2008) is regarded as a very reliable tool for assessing the potential alkali reactivity of the Norwegian aggregates (Haugen et al., 2008). However, some challenges in the application of the petrographic method have been reported on a global scale. Some rock types have been identified as non-reactive in one place (country, region) and as reactive elsewhere. Granitic aggregates, for example, are considered non-reactive in several countries (RILEM-AAR-1, 2003), but ASR damage associated with granitic aggregates in large structures has been reported by several authors worldwide (Kerrick and Hooton, 1992; Shayan, 1993; Fernandes et al., 2004, 2007; Castro, 2008; Castro et al., 2009). Another problem often reported in the literature is that rock types that have shown significant variation in reactivity by expansion tests or field experience were given the same classification of the degree of alkali-reactivity by the petrographic method (class I, II, III). For example, in Norway, a local criteria of 20 vol% is used (NB-21, 2008). This means that if the aggregate contains 20 vol% or more of rock types considered reactive, the aggregate is classified as potentially reactive. The construction industry shall therefore use this information to take additional measures to avoid deterioration by ASR if this aggregate is to be used in construction. However, all rock types are counted the same, even though it is known that, for example, a mylonite is more reactive than a phyllite. Yet, another problem is the correct application of rock nomenclature. A mineral, textural, structural, and genetic meaning is contained in each rock name. But, sometimes, rock nomenclature is not consensual worldwide among geologists/petrographers. Taking again granite as an example, some geologists/petrographers consider that a granite can have a certain degree of deformation (strained quartz, subgranulation); while for others the definition of granite is more strict and if the rock exhibits deformation then it is no longer designated by granite but rather gneiss or mylonite, depending on the extent of deformation that the rock has suffered. If the petrographic method RILEM AAR-1 aims to be a reference method to assess the potential alkali reactivity of aggregates both in Europe and worldwide, the quantification of microstructural features within

the aggregates may be an essential complement to the traditional application of nomenclature when evaluating the potential alkali-reactivity of aggregates for concrete.

The results of the field site tests indicate that deleterious ASR occurs usually in the same way in northern and in southern Europe (Borchers and Müller, 2012). However, with some aggregates, the reaction may occur earlier in southern Europe, probably due to the higher average temperature. The specimens stored alongside a highway in Sweden to study the influence of alkali supply under severe conditions reveal, after 7 years of exposure, no difference in the performance when compared with the cubes stored in a nearby forest (without alkali supply).

It is intended that the results of the PARTNER project will be implemented in the form of new standard methods and specifications. The aim of RILEM TC 106-AAR (1998-2000) and RILEM TC 191-ARP (2001-2006) was to propose and validate test methods for classifying the potential alkali reactivity of concrete aggregates. All draft RILEM methods proposed by the former committees have been developed further by RILEM TC 129-ACS (2007-2013) and are planned to be published in a special issue of *Materials and Structures* during 2012/2013.

# 4 Methodology

## 4.1 General

The methodology followed in this doctoral study is schematically represented in Figure 6. The starting point of the project was the petrographic description of a number of samples previously tested in PARTNER project. A first assessment by detailed petrography was essential to identify reactive aggregate particles and select the properties and qualities of silica minerals that can contribute to its dissolution in ASR-environment relevant to investigate in the scope of the project. Thin section petrography shows the presence of two different groups of potentially alkali-reactive rocks in the aggregates studied. Some of the aggregates containing slowly reactive rock types were further assessed by petrographic image analysis to perform grain size and grain shape analysis of quartz. A number of samples from other two previous projects (Wigum, 1995; Castro, 2008; Castro et al., 2009) were also included in this study. Additionally, the misorientation angles of grain boundaries of quartz were investigated for three slowly reactive aggregates by Electron Backscatter Diffraction (EBSD). The effect of polymorphism and other forms of silica was investigated in normally reactive aggregates by X-ray Diffraction (XRD) using solid samples and a few powdered specimens. The results obtained with each method were compared with expansion data and field experience from PARTNER project to assess the reactivity of the aggregate.

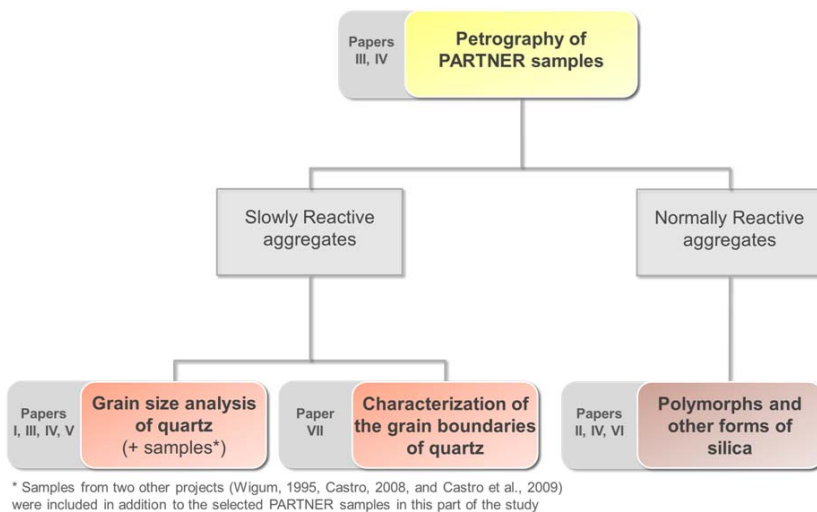


**Figure 6:** Methodology followed in the doctoral study.

## 4.2 Petrography of PARTNER samples

The petrographic description of a number of samples previously tested in the PARTNER project was the first step in this study. Main focus was given to the identification of potentially reactive particles within the aggregates that could be suitable to further microstructural and mineralogical characterization by analytical techniques of petrography and mineralogy.

### 4.2.1 Materials

A total of 22 post mortem expansion test specimens and 5 virgin aggregate samples previously tested in PARTNER project were used. These samples represent 14 different aggregate types from 8 different European countries. Normally reactive, slowly reactive, and non-reactive aggregates are included in this list. The laboratory Verband Deutscher Zeitschriftenverleger (VDZ) in Germany provided 19 of the 22 post mortem expansion test specimens used in this project. The laboratory Norcem in Norway provided the other 3. In total, 13 combinations of aggregates were tested in these 22 samples: 3 combinations with the AAR-3 method, 12 combinations with the AAR-4 method and 7 combinations with the German method (Table 1).

**Table 1:** List of the 14 aggregates, respective combinations of aggregates tested in each method and laboratory that provided the samples studied in this project.

Aggregate / country	Fraction / Combination	Expansion test method		
		AAR-3 (38°C)	AAR-4 (60°C)	German (40°C)
<i>Normally reactive aggregates</i>				
B1 - Belgium	C + F	Norcem	VDZ	VDZ
D1 - Denmark	C + F		VDZ	VDZ
D2 - Denmark	RF			
G1 - Germany	C + NRF		VDZ	VDZ
N1 - Norway	C + NRF	Norcem	VDZ	VDZ
UK1 - United Kingdom	C + F			VDZ
<i>Slowly reactive aggregates</i>				
It2 - Italy	C + F		VDZ	
N4 - Norway	C + F		VDZ	
N5 - Norway	C + F	Norcem	VDZ	
<i>Non-reactive aggregates</i>				
F1 - France	C + NRF		VDZ	VDZ
F2 - France	C + RF		VDZ	
	C + F		VDZ	VDZ
F3 - France	C + F		VDZ	
N3 - Norway	NRF			
S1 - Sweden	C + F		VDZ	

F = fine aggregate; C = coarse aggregate

NRF = non-reactive fine aggregate (=N3F); RF = reactive fine aggregate (=D2)

The 5 virgin aggregate samples used in this project were provided by VDZ (Table 2). To ensure the sample was representative of the aggregate in the context of this study, the amount of each sample to be used was calculated taking into account several parameters: the nature of the aggregate (natural aggregate was assumed to be ball shaped, while crushed aggregate was assumed to be cube shaped), the rock type predominant in the aggregate (in order to calculate the bulk density of the aggregate), nominal particle size (available at the laboratory that sent the sample), and potential reactivity (according to RILEM AAR-1 test results published in Lindgård et al., 2010). For example, for aggregate B1 was considered that 0.5 Kg of sample were enough for our research. This is a homogeneous aggregate, composed of silicified limestone, available in the fraction 2/4 mm. Assuming cube-shaped particles (because it is a crushed aggregate), of uniform density  $2.50 \text{ g.cm}^{-3}$ , and an average edge of 3 mm, each particle weighs  $\sim 0.07 \text{ g}$ . Thus, 1 Kg sample of that particulate material counts at least 14 815 cube shaped particles. According to point-counting results for the fraction 2-4 mm published in Lindgård et al. (2010), all constituents of this aggregate are potentially alkali-reactive. Therefore, it was considered that 0.5 Kg of this material is enough for the purposes of this project. On the other hand, for aggregate It2, 1 Kg of sample was considered to be necessary. This is a polymictic aggregate, composed mainly by quartzite and gneiss, available in the fraction 16/30mm. Assuming ball shaped particles (because this is a river gravel), of average density  $2.70 \text{ g.cm}^{-3}$ , and an average radius of 115 mm, each particle weighs  $\sim 17 \text{ g}$ . Thus, 1 Kg sample of that particulate material counts at least 59 ball-shaped particles. Particle separation results according to RILEM AAR-1 for the coarse fraction 16/30 mm of this aggregate is 84 vol% (Lindgård et al., 2010). This means that, in 58 particles, 49 will be reactive and 9 non-reactive. Therefore, it was considered that 1 Kg of this material would be suitable for the purposes of this project. Note that if the samples were to be used in other type of analysis (e.g. bulk geochemistry analysis) different amounts of the same materials could be necessary in order to obtain a representative sample (see e.g. Broekmans (2006) for further details on this topic).

**Table 2:** List of the virgin aggregate samples used in this project.

<b>Aggregate / country</b>	<b>Fraction (mm)</b>	<b>Amount of sample (Kg)</b>
<i>Normally reactive aggregates</i>		
B1 - Belgium	2/4	0.5
G1 - Germany	11/16	1.0
<i>Slowly reactive aggregates</i>		
It2 - Italy	15/30	1.0
N4 - Norway	0/4	0.5
<i>Non-reactive aggregates</i>		
F2 - France	4/20	1.0



### **4.2.2 Methods for assessment and analysis**

Two sections, ~20 mm in thickness, were cut off from each post-mortem expansion-test specimen. One section was impregnated with fluorescence epoxy and polished according to Danish standard DS-423.39 (2002) with minor adaptations, while the other remained unprepared. Both sections were observed under the stereomicroscope Wild Leitz Heerbrugg using incident normal and fluorescent illumination in order to identify signs of AAR and potentially reactive aggregate particles. Impregnated polished thin sections were prepared from the unprepared section using standard procedures (Humphries, 1992). Then, the thin-sections were analysed under a Nikon Eclipse E600 microscope using transmitted illumination in plane-polarized light (PPL), cross-polarized light (XPL), and incident fluorescent illumination (FL).

Virgin aggregate materials were weighed and washed. The particles were counted and separated by lithology using a stereomicroscope Wild Leitz Heerbrugg. Polished thin-sections of potentially alkali-reactive lithologies, as well as some unidentified particles, were prepared using standard procedures (Humphries, 1992). Then, the thin-sections were analysed under a Nikon Eclipse E600 microscope using transmitted illumination in plane-polarized light (PPL) and cross-polarized light (XPL).

A total of 168 thin-sections were studied, 110 from post mortem expansion test specimens and 58 from virgin aggregate materials.

### **4.3 Grain size analysis of quartz**

Although grain size in itself is not a fundamental material property of quartz, it does affect its solubility. Aggregates containing quartz with a small initial grain size and/or coarse-grained quartz that suffered extensive grain size reduction and/or sub-graining due to geological deformation will be more prone to develop deleterious ASR due to an increase in available surface, provided that the increased surface is sufficiently accessible for the pore solution.

Experience within some regions and with particular materials (i.e. highly metamorphic rocks) has shown that a determination of the quartz grain size within a particle it is important in the assessment of the reactivity potential of that aggregate (Haugen et al., 2008). Wigum (1995) demonstrated by theoretical approach and experimental work that the alkali reactivity of cataclastic rocks is clearly related to the total grain boundary area of quartz. The study showed a direct relationship between the quartz grain size, using the inverse of the  $d_{50}$  (mm), the total grain boundary of quartz ( $m^2/cm^3$ ) and the accelerated mortar bar expansion after 14 days for some mylonites, granites, and gneisses. Wigum et al. (2000) analysed more samples, including more rock types, and observed the same trend. Alaejos and Lanza (2012) studied the reactivity of aggregates containing different quartz crystal sizes (0-10 $\mu$ m; 10-60  $\mu$ m; 60-130  $\mu$ m),

measured by point-counting, proposing a unique limit for all of them applied to their weighted sum (Equivalent Reactive Quartz). Although the method seems to tackle the problem in an interesting way, more research is needed to overcome some limitations of the method and confirm the proposed limits. Both authors (Wigum, 1995; Alaejos and Lanza, 2012) suggested that image analysis procedure could help to establish standard/automatized procedures, hence making the grain size analysis more repeatable and reproducible.

In the present study, image analysis was used to quantify microstructural parameters of different rock types usually considered slowly reactive. Size and shape parameters were calculated. In a first step, the precision of the petrographic image analysis method was assessed by studying the grain size of the same samples with image analysis and with point-counting and comparing the results. This study is described in detail in paper I. Later, the focus of the application of the petrographic image analysis was to obtain accurate results for grain size analysis of quartz and to investigate grain shape. Initial results of this study are presented in papers III and IV. In paper V, the final results of grain size and shape for all the 11 aggregates were critically compared with expansion data to identify possible correlation.

### **4.3.1 Materials**

This study uses selected samples of virgin aggregate and post-mortem expansion tests prisms previously tested in three different projects (Wigum, 1995; Castro, 2008; Castro et al., 2009; Lindgård et al., 2010). Rock types usually regarded as slowly reactive were selected. It was also important that results of laboratory tests were available to use as assessment of their potential reactivity. When available, reported reactivity with structures was also taken into account. The final list contained 11 aggregates, from 3 countries (Italy, Norway, and Portugal), including reactive and non-reactive rock types (Table 3).

The assessment of the precision of the petrographic image analysis method described in paper I was performed using aggregates A, B and C. Papers III and IV present initial results of the investigation of more aggregate samples. Finally, paper V uses the 11 aggregates listed in Table 3 for a detailed characterization of quartz grain size and shape.

**Table 3:** List of the aggregates used to perform grain size analysis of quartz.

Aggregate Country	Brief petrographic description	Sample	Reported field experience	Reference
A Norway	Porphyritic granite from North Norway.	Virgin aggregate	-	Wigum (1995) (Note: original designation of these aggregates was 1.4, 3.3 and 5.1, respectively)
B Norway	Mylonite from the Southeastern Precambrian region in Norway.	Virgin aggregate	-	
C Norway	Mylonite from the Southwest part of Norway.	Virgin aggregate	-	
D Portugal	Granite from a Pre-orogenic pluton, North Portugal.	Virgin aggregate	-	
E Portugal	Granite from a Syn-orogenic, Syn-D3 pluton, North Portugal.	Virgin aggregate	Reactive	Castro (2008); Castro et al. (2009) (Note: original designation of these aggregates was Belver, Bemposta, S. Tomé de Castelo, Alpendurada, and Vila Flor, respectively)
F Portugal	Granite from a Syn-orogenic, Late-D3 pluton, North Portugal.	Virgin aggregate	Reactive	
G Portugal	Granite from a Syn-orogenic, Late-D3 pluton, North Portugal.	Virgin aggregate	-	
H Portugal	Granite from a Late to Post-orogenic pluton, Centre Portugal.	Virgin aggregate	Non-reactive	
I Italy	Polymictic river gravel mainly composed by quartzite. Other lithologies observed include: gneiss, granite, flint/chert, gabbro, and eclogite. ASR was associated with the presence of quartzite and gneiss particles.	Concrete prism (tested with RILEM AAR-4)	Reactive	
J Norway	Natural gravel/sand from a moraine deposit. Rock types observed in this aggregate include: sandstone, siltstone, cataclasite, quartzite, granite, gneiss, gabbro, basalt. ASR was associated with the presence of cataclasite and quartzite particles.	Concrete prisms (tested with RILEM AAR-3 and RILEM AAR-4)	Reactive	Lindgård et al. (2010) (Note: original designation of these aggregates was It2, N4, and N5, respectively)
K Norway	Sand/gravel from a glaciofluvial deposit mainly composed by quartzite. Other rock types identified include: rhyolite, granite, gneiss, sandstone. ASR was associated with the presence of quartzite and rhyolite particles.	Concrete prisms (tested with RILEM AAR-3 and RILEM AAR-4)	Reactive	

### 4.3.2 Methods for assessment and analysis

A detailed description of the petrographic image analysis method used in this part of the study is presented in papers I, III, IV and especially in paper V.

The Lazy Grain Boundary (LGB) method (Heilbronner, 1999, 2000) was used for creating grain boundary maps of the quartz contained in the aggregates. The LGB method is

based on a set of macro commands programmed for Image SXM (Barrett, 2008), a public domain image processing and analysing software. The procedure makes use of multiple input images. Sets of input images (stacks) composed by six polarization micrographs were acquired with crossed polarizers and  $\lambda$ -plate rotated  $0^\circ$  -  $150^\circ$  at  $30^\circ$  increments in a Leica DM 2500P polarizing microscope with a Jenoptik ProgRes digital camera system. For reliable analysis, the image set must comprise a statistically sufficient number of grains, which is a combined function of microscope magnification, grain size, and rock heterogeneity. The preparation of the input images included the elimination, by gradient filtering, of all minerals present in the sample except quartz. In the studied samples, this procedure was effective to filter even feldspars due to the fact that sets of multiple input images acquired with crossed polarizers and  $\lambda$ -plate rotated at different angles were used. The majority of the image sets were processed fully automated by the LGB method (Figure 7). A few sets required additional minor manual corrections (e.g. repairing discontinuous grain boundaries and/or erasing pending relics). After segmentation, the quartz grains were analysed for major and minor axis length of the best fit ellipse, cross-sectional area and perimeter. A spread-sheet program was used to calculate grain size and grain shape descriptors.

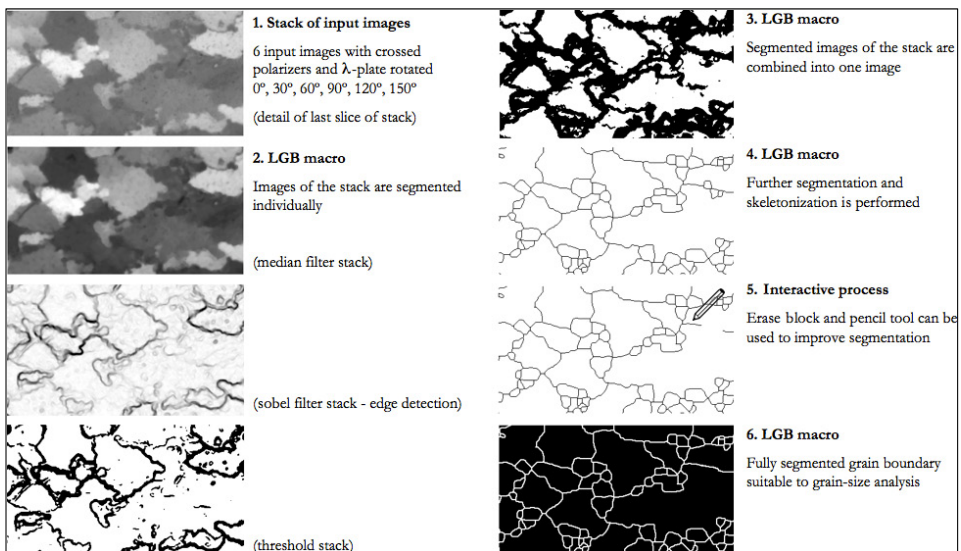


**Figure 7:** Schematic representation of automated image segmentation using the LGB macro for Image SXM.

A number of measurements can be made in order to characterize the size of a grain. In point-counting studies, usually the maximum grain length is measured and used as the diameter. In this case, it is considered that the grain is a sphere (equivalent) of this maximum dimension. When using image analysis, other quantities such as minimum length, volume or area can be

used; however, this will produce a different result for the grain size. Each answer will be correct, giving a valid result for the property being measured. Independently of the method used to make the measurements (point-counting or image analysis), it is important to keep in mind that a two dimensional image (like the one obtained from the examination of a rock under the microscope) will produce an overestimation of small grain sizes. To obtain a more accurate estimation of the grain size, one uses stereology (the extrapolation from two- to three-dimensional space). Numerous analytical procedures are available for determining grain size distribution of spheres from section size distributions (Underwood, 1970). In other words, stereology is used to correct the typical overestimation of small grains obtained from measurements in a plane (thin-section), which in turn leads to a more accurate estimation of the grain size distribution.

In the present work three different measurements were used to calculate the grain size:

*(1) The length of the major axis of the best fit ellipse ( $d_E$ )*

In order to mirror the results obtained by Wigum (1995) and Wigum et al. (2000) with point counting, the  $d_E$  was used as diameter of the particle. In this case, it is thus considered that the grain is a sphere (equivalent) of this maximum dimension.

*(2) The equivalent circle diameter ( $d_A$ )*

The areas of the grains measured by image analysis were used to calculate the  $d_A$ , which means that the grain size is defined as the diameter of a circle having the same area.

*(3) The equivalent spherical diameter ( $d_V$ )*

The equivalent circle diameters were then grouped into histograms of 20 classes, where the bins are delimited by their upper bound. The program StripStar (Heilbronner, 1998) was used to calculate the parent distributions of spheres from the histograms of equivalent circle diameters; or, in other words, to calculate the  $d_V$ . In this case, the grain size is defined as the diameter of a sphere having the same volume, which represents a more accurate estimation of the grain size distribution than the previous two measurements.

A granular structure is better characterized by the distribution of grain sizes (e.g. the grain size distribution cumulative curve). However, for practical reasons a system of grains is often represented by numerical parameters that will define the distribution curve. The mean grain size of quartz ( $d_{50}$ ) and the total grain boundary area of quartz (TGBA) were used as size descriptors (Table 4). These descriptors were calculated following the same assumptions of Wigum (1995)

with minor changes. For determination of the mean grain size of quartz, the  $d_{50}$  (mm) read from the cumulative grain size distribution curve was used. In order to estimate the total grain boundary area of quartz, each grain, including subgrains, was assumed to be spherical in shape. The average grain size between two selected fractions was used to calculate the specific surface area ( $SS$ ) for this specific part of the grading. The specific surface area obtained was multiplied by the amount of grains in that fraction ( $f$ ). This was done for all the selected fractions in the grading and all results summed up in order to obtain the grain boundary area for the entire grading. The total amount of quartz in the rock ( $Qz_r$ ) was obtained by a visual estimation from the thin-section using volume % estimation diagrams. By multiplying the grain boundary area with the total amount of quartz in the rock an estimate for the total grain boundary area of quartz ( $m^2/cm^3$ ) in each sample was achieved. In paper I, the size descriptors were calculated using the  $d_E$  as diameter of the particle. In paper V, the size descriptors were calculated using the  $d_E$ , the  $d_A$  and the  $d_V$  as diameter of the particle. In this way, it was possible to compare the difference in the results of the grain size descriptors that would result from the use of different measurements for the grain size.

**Table 4:** Size descriptors (adapted from Wigum, 1995).

Name	Definition	Unit	Observations
Mean grain size	$d_{50}$	mm	50% of the analysed grains have diameters smaller than this value
Total grain boundary of quartz	$TGBA = \left( \sum_{i=1}^n SS_i \times f_i \right) \times Qz_r$	$m^2/cm^3$	$n$ = number of fractions $SS = \frac{SA}{V} = \frac{\pi d^2}{\pi \frac{d^3}{6}} = \frac{6}{d}$

Notation:  $SS$  = specific surface area (surface area per unit of volume);  $SA$  = surface area;  $V$  = volume;  $f$  = amount of grain in this fraction (in percentage);  $Qz_r$  = amount of quartz in the rock

Intuitively, the shape of an object can be described by comparison with another one. Thus, in image analysis, shape is commonly characterized by quantifying the difference between a given object and a reference shape. A number of shape factors have been described in the literature (Underwood, 1970; ISO-9276-6, 2008). Shape factors are dimensionless parameters derived from the basic geometrical measurements (e.g. best fit ellipse, cross sectional area, perimeter) and generally vary between 0 and 1, the maximum value corresponding to perfect geometric shapes and the minimum corresponding to irregular shapes. In the present work, axial ratio and circularity were employed for shape characterization according to ISO-9276-6 (2008) (Table 5). Axial ratio is defined as the ratio between the minor diameter of the best fit ellipse ( $b$ ) and the major diameter of the best fit ellipse ( $a$ ). This shape

descriptor is sensible to the elongation of the grains. Circularity is the ratio between the perimeter equivalent ( $P_{equ}$ ), that corresponds to the perimeter of a circle with the same area as the analysed grain, and the perimeter of the particle ( $P$ ), measured by image analysis. This descriptor is sensible to the irregularities of the contour of the grain. Note that the names and definitions of these parameters may vary in the literature.

**Table 5:** Shape descriptors used in the present study (adapted from ISO-9276-6, 2008).

Name	Definition	Sensitivity
Axial ratio	$E = \frac{b}{a}$	Elongation
Circularity	$C = \sqrt{\frac{4\pi A}{P^2}} = \frac{P_{equ}}{P}$	Circular shape and contour irregularities

Notation: A = area; P = perimeter;  $P_{equ}$  = perimeter equivalent (perimeter of a circle with the same area as the analysed grain); a = best fit ellipse major diameter; b = best fit ellipse minor diameter

#### 4.4 Characterization of the grain boundaries of quartz

The grain boundary surfaces represent the adjustment between neighbor lattices and can be seen as discontinuities between adjacent grains. This means that within a grain boundary and in a small volume embedding it, the crystal lattice is distorted and deviates significantly from the proper quartz structure increasing its solubility, therefore making it more susceptible to react with the alkali hydroxides from the pore solution of concrete.

The grain boundaries are characterized by two parameters with five degrees of freedom (Randle, 1992): the orientation of the boundary plane; and the misorientation between two neighbor grains which share the same grain boundary (the parameter in focus in this study). The characterization of grain boundaries geometry and their preferred orientation in different deformation contexts remain poorly understood due, mainly, to difficulties to determine all parameters required for a complete boundary characterization (Gonçalves and Lagoeiro, 2009).

In the present study, Electron Backscatter Diffraction (EBSD) was used to investigate the influence of the misorientation grain boundary angles in the potential reactivity of aggregate for concrete. Particles of quartzite with different strain degrees of the quartz crystals were analyzed. Initial results of this part of the research are presented in paper VII.

#### **4.4.1 Materials**

This study uses selected samples of virgin aggregate and post-mortem expansion tests specimens previously applied in PARTNER project (Lindgård et al., 2010). Three slowly reactive aggregate samples (It2, N4, and N5), from 2 different countries (Italy and Norway), were studied. After initial petrographic assessment, 4 particles were selected for further characterization by EBSD. One of the studied particles (It2-1) is from a virgin aggregate sample, the other three particles included in this study (It2-2, N4, and N5) are from post-mortem expansion specimens.

#### **4.4.2 Methods for assessment and analysis**

A detailed description of the EBSD method used in this part of the study is presented in papers VII.

EBSD, also known as backscatter Kikuchi diffraction, is a Scanning Electron Microscope (SEM) based microstructural-crystallographic technique to measure crystallographic orientation that has become well known as a powerful and versatile experimental tool for materials scientists, geologists and other scientists and engineers (Randle, 2009). In EBSD, a stationary electron beam strikes a tilted crystalline sample and the diffracted electrons form a pattern on a fluorescent screen. This pattern is characteristic of the crystal structure and orientation of the sample region from which it was generated. It provides the absolute crystal orientation with submicron resolution, which makes it a very powerful tool for microstructural characterization. It allows, among other things, grain and boundary characterization and strain determination. Originally, EBSD was applied exclusively to materials (mostly metals) having cubic crystal structure, but nowadays, it is applied to materials with more complex structures, including geological materials. Comprehensive reviews on EBSD principles, data acquisition, and processing may be found in Dingley and Randle (1992) and Randle (2009).

Sample preparation is crucial for EBSD analysis. The analysed sample surface must be perfectly flat and free of any type of mechanical damage resulting from polishing. The thin-sections used in this study were polished using a colloidal silica suspension for 2 minutes and then plasma cleaned for 10 minutes. Full crystallographic orientation data were obtained using a Hitachi SU6600 probe SEM fitted with a field emission gun at the Department of Materials Science and Engineering at NTNU. Images of EBSD patterns were streamed to a hard disc using the NORDIF Data Collection 1.4 and later indexed offline. The SEM equipment was running at low vacuum mode with chamber pressure of 15 Pa. EBSD working conditions were: 20 kV acceleration voltage, 20 nA beam current and 22 mm working distance with a tilt of 70°.



The samples were mapped by automatic scans on a square grid with a fixed step size of 5  $\mu\text{m}$  for samples It2-1 and It2-2, and 10  $\mu\text{m}$  for samples N4 and N5. The acquired orientation maps contain 240x240 pixel for samples It2-1 and It2-2, and 250x250 pixel for samples N4 and N5. Acquisition time per map was  $\sim$ 8:00 min for maps It2-1 and It2-2, and  $\sim$ 3:30 min for maps N4 and N5. All EBSD patterns were stored and used to perform offline indexing and reanalyses to obtain orientation maps with reduced total amount of non-indexed points by using the program TSL OIM Data Collection 5.32. Offline indexing offers some advantages over the traditional online indexing, especially in geological materials that are so sensitive to the Hough transform settings. With the current offline system, every diffraction pattern is available for re-indexing as many times as needed until finding optimized settings. In this case, the centre of a minimum of 6 and maximum of 14 Kikuchi bands was automatically detected using the Hough parameters described in detail in Paper VII. The solid angles calculated from the patterns were compared with the quartz specific match unit containing 18 reflectors to index the patterns. Indexing time was  $\sim$ 2h30min for maps It2-1 and It2-2, and  $\sim$ 1h00min for maps N4 and N5. Extrapolated orientation maps were produced by applying a clean-up routine of grain dilation (grain tolerance angle 5 and minimum grain size 5) to the raw data maps. Misorientation angle histograms were produced by using only boundaries between identified grains and by removing noise at low angles ( $< 2^\circ$ ).

#### **4.5 Effect of polymorphs and other forms of silica**

Solubility of silica under ASR environment is different for different polymorphs as discussed in section 2.3.3. As a general rule, the lower the activity of silica, the lower the solubility. Thus, the predominant silica polymorph largely governs the alkali-reactivity potential of the aggregate, a disordered silica structure being more reactive than cristobalite, which in turn is more reactive than ‘orderly quartz’ (Zhang et al., 1990). On the other hand, a number of silica species are of particular interest with respect to ASR: opal, chert, chalcedony. Characterization of the predominant crystal structures is then essential to assess the effect on the alkali-reactivity potential of aggregates for concrete, especially in rock types usually characterized as normally reactive.

A popular method to perform such characterization is X-ray Diffraction (XRD). Major texts on XRD analysis (Klug and Alexander, 1974; Bish and Reynolds, 1989; Buhrke et al., 2001; Cullity and Stock, 2001) generally discourage the use of material without prior comminution and/or disaggregation for a range of reasons, primarily (too coarse) particle size, (poor) particle count statistics, (preferred) orientation issues, among many others. However, in materials like e.g. polycrystalline virgin aggregate, field concrete, and post-mortem mortar bars and

concrete prisms, traditional sample preparation by pulverization can present a real challenge, for various reasons. Reliable mineralogical analysis of bulk (concrete, aggregate) material is compromised by limited sample size and hence unsatisfying representativeness (Broekmans, 2006), whereas analysis of individual particles as identified in thin section petrography is challenged by preparation issues and access to limited amounts of material too, albeit on a different size scale. On the other hand, sample and specimen preparation both do introduce artifacts affecting diffraction by attributing lattice deformation, contamination from equipment wear, etc. Thus, minimizing material treatment before analysis bears a strong potential to improve the result, especially for intrinsically fine-grained lithologies without (optically discernible) preferred orientation, e.g. chert, siltstone, rhyolite, and siliceous limestone.

In the present study, selected particles of normally reactive aggregates were investigated using XRD on powdered sample material as well as on polished sections. In a first step, results from XRD on a polished section were critically reviewed against results from traditionally powdered specimen for the same particle as described in paper II. Additional results from Inductively Couple Plasma – Atomic Emission Spectroscopy (ICP-AES), X-ray Fluorescence (XRF) and Electron Probe Micro-Analyzer (EPMA) for the same particle were critically reviewed against XRD results to validate the data obtained. Later, XRD, EPMA and Cathodoluminescence (CL) were used to assess mineral content and silica speciation in a number of aggregates previously tested in PARTNER project. Data on mineral content and silica speciation were compared with expansion data from PARTNER to identify possible correlation. Initial results of this part of the research are presented in paper IV and the final results are presented in paper VI.

#### **4.5.1 Materials**

This study uses selected samples of virgin aggregate and post-mortem expansion tests specimens previously tested in the PARTNER project (Lindgård et al., 2010). Paper II uses an individual particle of siliceous limestone selected from the virgin aggregate G1. Further research, described in paper IV and especially in paper VI, uses five aggregates (F1, F3 – non-reactive; B1, D1, G1 – normally reactive) from 4 different countries. After initial petrographic assessment, 25 individual particles were selected for further characterization by XRD (Table 6). One particle of aggregate D1 (D1-01) was selected to further characterization by EPMA-CL.

**Table 6:** List of the aggregates particles selected for characterization by XRD.

Aggregate / Country	Brief petrographic description	Sample	Specimen type
B1 / Belgium	This aggregate is composed of several types of siliceous limestone.	B1-11	polished section
		B1-12	polished section
		B1-13	polished section
		B1-14	polished section
		B1-15	polished section
D1 / Denmark	Glaciofluvial sand/gravel mainly containing flint/chert, siliceous limestone.	D1-00	polished section
		D1-01	polished section
		D1-02	polished section
		D1-03	polished section
		D1-04	polished section
F1 / France	Polymictic river gravel mainly composed by flint/chert.	F1-40	polished section
		F1-41	polished section
		F1-42	polished section
		F1-43	polished section
		F1-44	polished section
F1-45	polished section		
F3 / France	Polymictic river gravel mainly composed by flint/chert.	F3-77	polished section
G1 / Germany	Partly crushed polymictic river gravel with considerable variation in constituent lithologies. Main constituents are flint/chert and siliceous limestone.	G1-75	polished section *
		G1-76	pulverized material *
		G1-26	pulverized material
		G1-27	pulverized material
		G1-28	pulverized material
		G1-29	polished section
		G1-30	polished section
G1-31	polished section		

\* These two specimens belong to the same aggregate particle (the particle tested in Paper II).

## 4.5.2 Methods for assessment and analysis

A detailed description of all analytical method used in this part of the study is presented in papers II, IV and VI.

### *X-ray Diffraction (XRD)*

After an optical petrographic microscope using polarized light, an XRD is arguably among the most widely available analytical instruments suitable for identification of crystalline substances, hereunder minerals. Moreover, data collections of confirmed quality on natural minerals and numerous synthetic crystalline substances are publicly available from an independent body, the International Center for Diffraction Data ([www.ICDD.com](http://www.ICDD.com)). Both optical properties and XRD data enable unequivocal identification of mineral species, as demonstrated by the fact that both are essential parts in the approval of new-identified mineral species. Finally, XRD analysis can be automated to a large extent.

A number of virgin aggregate particles were prepared for XRD analysis by powdering. These particles were pre-crushed using a percussion mortar to pass a 400 $\mu$ m sieve, and charged to a McCrone Micronizer with corundum grinding elements, adding 10 ml of ethanol as a

grinding agent. They were ground for 5 minutes, extracted from the grinding jar, rinsed with ethanol, and subsequently dried overnight at 50 °C in a covered petri dish. Pulverized sample material was put in a polymethyl methacrylate (PMMA) specimen holder following standard procedures described in Buhrke et al. (2001) with minor adaptations. The powder surface was finished with a carrier glass for microscopy to ensure planarity and flatness.

In addition, this study uses polished specimens. When the particles of interest come from post-mortem expansion test specimens, the selected particles were liberated from the unprepared counterparts of the thin-sections that were used to select them. When particles from virgin aggregate samples were being used, the selected particle was simply cut in two with a diamond blade. Then, the particles surface was manually plane polished in several steps and finished with 0.25 $\mu$ m diamond paste. Planarity and flatness of the polished surface were verified by putting a carrier glass for microscopy on the surface and observing presence/absence of an optical interference pattern. Next, the polished aggregate particle was mounted on a PMMA holder using plasticine, as commonly used for observation of polished ore specimen for reflected light petrography. Figure 8 shows a polished specimen prepared according to this procedure. After manually charging the sample holder containing the polished specimen to the instrument, specimen height was carefully adjusted to the focal point of the goniometer to minimize offset and error in the apparent diffraction angle.

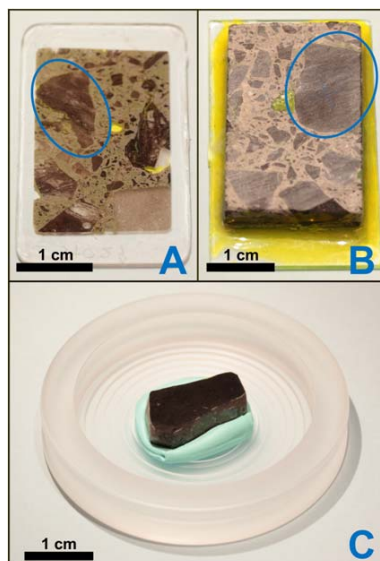


**Figure 8:** Schematic representation of the steps needed to prepare the polished specimens to XRD analysis: (A) Thin-section used to select the particle of interest; (B) Unprepared thin-section counterpart; (C) particle liberated from the unprepared thin-section counterpart, manually plane polished and mounted on a PMMA holder using plasticine. Note that due to the thickness of the diamond blade, a ~3mm mismatch exists between thin-section versus unprepared counterpart which explains the particle shape variation indicated by the blue ellipsoids.

All specimens were analysed spinning at 60 rpm in a Bruker D8 Advance X-ray diffractometer at the Department of Geology and Mineral Resources Engineering at NTNU. For both specimen types (ie. powdered or polished), the projected primary beam had a diameter maximum of 12mm, never exceeding the perimeter of the prepared specimen. Operating conditions were set to 40 kV and 40 mA, using CuK $\alpha$  radiation of wavelength  $\lambda=1.54178\text{\AA}$ . Radiation was applied without monochromator, but K $\beta$  was removed by a Ni-foil filter in the incident/primary beam. Diffractograms were recorded using a Lynxeye CCD linear detector from 2 - 80°2 $\theta$ , in 0.01°2 $\theta$  increments with 1s counting time per increment, with total scan time 2h10m. Phase quantification was performed using the Rietveld refinement software TOPAS 4.2 with the fundamental parameter approach, using as few parameters as possible to fit the data in order to get better precision in the quantification.

#### *Inductively coupled plasma – atomic emission spectroscopy (ICP-AES)*

ICP-AES is a type of mass spectrometry which is capable of detecting metals and several non-metals at concentrations as low as one part per trillion (10<sup>12</sup>). This technique has great precision, and sensitivity, while the amount of sample necessary for analyse is very small, which in this study represented an advantage since less than 0.5 grams of material were available to analyse.

For chemical analysis by ICP-AES, used in paper II, 0.471g of powdered sample material (=all available) from a single aggregate particle (from aggregate G1) was digested in 10mL of 7N HNO<sub>3</sub> (nitric acid). The solution was fed into a Perkin Elmer Optima 4300 Dual View instrument at the Norwegian Geological Survey, operated at standard settings. The solution was analysed for main elements Na, K, Ca, Mg, Mn, Fe, Al, Ti, P, and a number of trace elements including heavy metals, for a total of 30 elements.

#### *X-ray fluorescence (XRF)*

XRF is an analytical method widely used for elemental analysis and chemical analysis by geologist around the world. The method is fast, accurate and non-destructive, and usually requires only a minimum of sample preparation.

Chemical analysis by XRF was used in paper II. Powdered sample material of the selected aggregate particle (from aggregate G1) was used to produce a fused disc. The powdered sample material was first pre-dried at 105°C and then ignited at 850°C. Next, 0.5g of powdered sample material was added to 5g of lithium borate flux (66wt% tetra, 34% meta) and 60 $\mu$ L of lithium iodide. The mixture was fused for ~10 min in Pt crucible using a Claisse-type device, producing a transparent bead. Bulk lost on ignition (LOI) was determined

gravimetrically in the same digestion procedure. Weight loss was assumed to include CO<sub>2</sub> from carbonate only, as minerals possibly containing hydrous species (e.g. clays) were not identified in thin section. As the sample is very light in color, organic matter was considered negligible or absent.

The bead was analyzed in a Bruker S8 Tiger at the Department of Geology and Mineral Resources Engineering at NTNU, for Na<sub>2</sub>O, K<sub>2</sub>O, MgO, CaO, MnO, Al<sub>2</sub>O<sub>3</sub>, Fe<sub>2</sub>O<sub>3</sub>-total, TiO<sub>2</sub>, SiO<sub>2</sub>, and P<sub>2</sub>O<sub>5</sub>. Operating conditions of the XRF instrument were set at 60kV max and 50mA.

*Electron probe micro-analyzer – cathodoluminescence (EPMA-CL)*

EPMA is an analytical tool used to non-destructively determine the chemical composition of small volumes of solid materials (typically 10-30 cubic micrometers or less). A CL detector attached to EPMA is capable of producing high-resolution digital cathodoluminescent images of luminescent materials. CL emissions can provide general information on e.g. the trace elements contained in minerals or the production of mechanically induced defects in the crystals. In this study, it was expected to provide information on the presence of different silica polymorphs within the sample.

For element mapping by EPMA, polished thin sections were prepared, and sputter coated with ~270Å carbon. The coated sections were loaded in a JEOL JXA-8500F thermal field-emission electron-probe micro-analyzer at the Department of Materials Science and Engineering at NTNU. The instrument is equipped with five wave dispersive spectrometers (WDS) and one electron dispersive spectrometer (EDS), allowing simultaneous acquisition of 5+16 elements Be U, in addition to BE and SE imaging modes. The instrument also includes a WDS-based CL detector by XCLent, enabling simultaneous per-pixel analysis of CL spectrum and intensity as well as element composition. The instrument was operated at 10<sup>-5</sup>Torr or better, 15.0kV accelerating voltage, 20nA beam current, and 250ms dwell time, with an effective beam diameter of ~1µm (i.e. current density >25nA·µm<sup>2</sup>).

In paper II, only elemental mapping was used to characterize the selected siliceous limestone particle of aggregate G1. To obtain sufficient data for statistical assessment, a total of 15 maps were acquired distributed over the thin section. Element maps were acquired at 400×400 pixel resolution (1pixel=1µm) for Si, O, Ca, C, Fe, Mg, Al and P. Each area was scanned twice to suit the number of available spectrometers, here 4 for each run. The acquisition time was 88 minutes per map, and 22h for the 15 maps altogether.

In paper VI, both elemental mapping and cathodoluminescence were used to characterize the particle D1-01. To obtain sufficient data for statistical assessment, a total of 3 maps were acquired distributed over the particle. Each area was scanned only once to preserve the

luminescent properties of quartz, which often change with extended beam exposure (Götze et al., 2001). Two element maps were acquired at 400×400 pixel resolution (1pixel=2.5μm) for Si, Ca, Fe, and Mg. Total acquisition time was 12h22m per map. One element map was acquired at 512×512 pixel resolution (1pixel=1μm) for Si, Ca, Fe, and Mg, with total acquisition time ~20h12m.

## 5 Summary of results

### 5.1 Petrography of PARTNER samples

Observations made during the petrographic examination of post-mortem expansion-test specimens and virgin aggregates with focus to the identification of potentially reactive particles within each aggregate were published in papers III and IV.

Tables 7A, 7B and 7C summarize petrography results for aggregates classified as normally reactive, slowly reactive, and non-reactive by PARTNER (Lindgård et al., 2010) respectively. A first assessment by detailed petrography was essential to identify reactive aggregate particles and select the properties and qualities of silica minerals that can contribute to its dissolution in “ASR-environment” relevant to investigate in the scope of the project. Original descriptions elaborated during the PARTNER project have been limited to a few lines in the final PARTNER report, and therefore important information essential to the present work was lacking.

After thin section petrography, the particles selected for further investigation were divided into two different groups of potentially alkali-reactive rocks. The first group comprises slowly-reactive rock types, like gneiss, rhyolite, granite, cataclasite, greywacke, and quartzite and correspond to the aggregates N3, S1, N1, UK1, It2, N4, and N5. The second group comprises normally reactive flint/chert and silicified limestone and correspond to the aggregates F1, F3, B1, D1, D2, and G1. Some of the aggregates containing slowly reactive potentially reactive rock types were further assessed by petrographic image analysis to perform grain size and grain shape analysis of quartz. Additionally the quality of the crystal lattice was investigated with EBSD in some of those aggregates. Some of the aggregates containing normally reactive potentially reactive rock types were further investigated by XRD to identify and quantify silica polymorphs and other species of silica. The results obtained with each method were critically compared with expansion data and field experience from PARTNER project to assess the reactivity of the aggregate. A summary of the results from laboratory test methods, field site test, and reported experience in structures, obtained during PARTNER project for these samples, can be found in Tables A1, A2, and A3, in the Appendix in the end of this chapter.



**Table 7A:** Summary of petrography results for normally reactive aggregates with focus to the identification of potentially reactive particles within each aggregate. These results reflect the observations made in post-mortem expansion-test specimen and virgin aggregate.

<b>Aggregate / Country</b>	<b>Brief description</b>	<b>Potentially reactive lithologies</b>
B1 / Belgium	This aggregate contains several types of siliceous limestones (mudstones, wackestones and packstones) with fossils (foraminifera). Alkali-silica gel was found in all the thin-sections partly filling cracks (Figure 9A-A).	Siliceous limestone Reactive minerals are micro- and crypto- crystalline quartz, sometime with fibrous habit.
D1 / Denmark	Glaciofluvial sand/gravel containing: flint/chert (some particles are dense while others are partly porous), siliceous limestone, greywacke, quartzite, granite, gneiss, and mafic rocks. Alkali-silica gel was found filling cracks and air voids (Figure 9A-B) almost always associated with flint/chert particles.	Flint/chert, siliceous limestone, (greywacke, quartzite, gneiss) Reactive minerals are micro- and crypto- crystalline quartz, and presumably opal.
D2 / Denmark	Sea dredged, polymictic gravel originally derived from glaciofluvial sediments. This aggregate is mainly composed of monomineralic particles of quartz and feldspar. Among the rock types identified the most abundant is flint/chert. Other rock types identified include: quartzite, granite, sandstone, and gabbro. Alkali-silica gel is found frequently associated with flint/chert particles.	Flint/chert Reactive minerals are micro- and crypto- crystalline quartz.
G1 / Germany	Partly crushed polymictic river gravel from upper Rhine valley. This aggregate presents considerable variation in constituent lithologies. Observed rock types include: flint/chert, siliceous limestone with foraminifera and braquiopod fossils, quartzite, sandstone, greywacke, granite, and mafic rocks. Alkali-silica gel is frequently observed in cracks and air voids associated with several rock types but more frequently with flint/chert, siliceous limestone and sandstone (Figures 9A-C and 9A-D).	Flint/chert, siliceous limestone, (sandstone) Reactive minerals are micro- and crypto- crystalline quartz.
N1 / Norway	This aggregate is mainly composed of cataclasite (Figure 9A-E). Other rock types observed include: granite and mylonite. Alkali-silica gel is found frequently in cracks and air voids associated with cataclasite particles.	Cataclasite Reactive minerals are strained quartz with extensive sub-granulation
UK1 / United Kingdom	This aggregate is mainly composed by greywacke (Figure 9A-F). Other lithologies observed include: sandstone, siltstone, mudstone, and basalt. Alkali silica gel was found in cracks and air voids associated with greywackes in all the thin-sections.	Greywacke Reactive minerals are micro- and crypto- crystalline quartz, and possibly volcanic glass

Rock types between brackets were identified in this sample but in minor quantities and /or not directly associated with reactivity, and therefore, were not object of further study.

**Table 7B:** Summary of petrography results for slowly reactive aggregates with focus to the identification of potentially reactive particles within each aggregate. These results reflect the observations made in post-mortem expansion-test specimen and virgin aggregate.

Aggregate / Country	Brief description	Potentially reactive lithologies
It2 / Italy	Polymictic river gravel mainly composed by quartzite (Figure 9B-A). Other lithologies observed include: gneiss (Figure 9B-B), granite, flint/chert, gabbro, and eclogite. Alkali-silica gel can be found in cracks and air voids mainly associated with quartzite and gneiss particles.	Quartzite, gneiss Reactive minerals are strained quartz with extensive sub-granulation and highly sutured quartz.
N4 / Norway	Natural gravel/sand from a moraine deposit. Rock types observed in this aggregate include: cataclasite (Figure 9B-C), sandstone (Figure 9B-D), siltstone, quartzite, granite, gneiss, gabbro, basalt. Alkali-silica gel was observed in cracks and air voids associated with particles of cataclasite, sandstone and quartzite.	Cataclasite, quartzite, (sandstone) Reactive minerals are strained quartz with extensive sub-granulation and micro- and crypto- crystalline quartz.
N5 / Norway	Sand/gravel from a glaciofluvial deposit mainly composed by quartzite (Figure 9B-E). Other rock types identified include: rhyolite, granite, gneiss, sandstone. Alkali-silica gel is found partly and/or totally filling cracks and air voids (Figure 9B-F) usually associated with quartzites and rhyolites.	Quartzite, Rhyolite Reactive minerals are microcrystalline and fine grained quartz.

Rock types between brackets were identified in this sample but in minor quantities and /or not directly associated with reactivity, and therefore, were not object of further study.

**Table 7C:** Summary of petrography results for non-reactive aggregates with focus to the identification of potentially reactive particles within each aggregate. These results reflect the observations made in post-mortem expansion-test specimen and virgin aggregate.

Aggregate / Country	Brief description	Potentially reactive lithologies
F1 / France	Polymictic river gravel mainly composed by flint/chert (Figure 9C-A). Other rock types observed are siliceous limestone, mudstone, and greywacke. Alkali-silica gel observed in some thin-sections associated with flint/chert particles.	Flint/chert Reactive minerals are micro- and crypto- crystalline quartz.
F2 / France	This aggregate contains several types of limestones. These include: mudstone, wackestone, packstone and grainstone. Braquiopode and foraminifera fossils, ooids and peloids are frequently observed (Figure 9C-B). No signs of AAR reaction were observed.	None
F3 / France	Polymictic gravel from Rhine valley. Rock types observed include: flint/chert (Figure 9C-C), siliceous limestone, granite, sandstone (Figure 9C-D), greywacke, quartzite, rhyolite. Alkali-silica gel was found in 2 of 7 thin-sections associated with porous flint/chert particles.	Flint/chert, siliceous limestone, (greywacke, sandstone, quartzite, rhyolite) Reactive minerals are micro- and crypto- crystalline quartz.
N3 / Norway	Natural sand from a glaciofluvial deposit. Consists mainly of monomineralic particles of quartz and rock fragments of granite and gneiss. No alkali-silica gel was found associated with this aggregate.	Gneiss, (granite) Reactive minerals are strained quartz with sub-granulation.
S1 / Sweden	Polymictic glaciofluvial gravel and sand. Rock types identified include: rhyolite (meta-rhyolite) (Figure 9C-E), granite (Figure 9C-F), ganodiorite, gabbro, basalt. Alkali-silica gel was found partly filling an air void in 1 of 3 thin-sections, apparently associated with a very altered fragment of rock (basalt ?).	Rhyolite (meta-rhyolite), granite Reactive minerals are strained quartz with sub-granulation, micro- and crypto- crystalline quartz.

Rock types between brackets were identified in this sample but in minor quantities and /or not directly associated with reactivity, and therefore, were not object of further study.

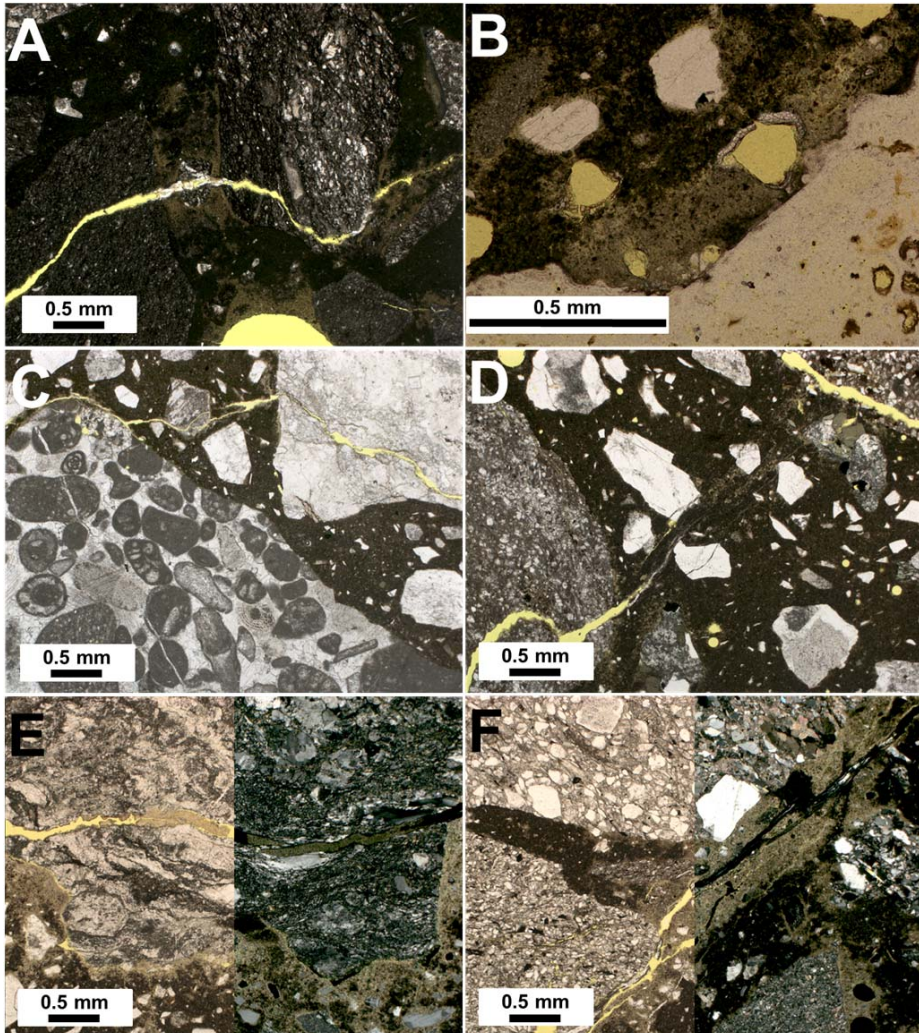


**Figure 9A:** Normally reactive aggregates: A) Aggregate B1, crack partly filled with gel crossing particles of siliceous limestone in PPL; B) Aggregate D1, air voids partly filled with gel around a chert particle in PPL; C) Aggregate G1, crack partly filled with gel crossing and around aggregate particles of siliceous limestones in PPL; D) Aggregate G1, crack starting in a particle of siliceous limestone is releasing gel into the cement paste in PPL; E) Aggregate N1, particle of cataclasite with a crack partly filled with gel in PPL on the left side and XPL on the right side; F) Aggregate UK1, cracks partly filled with gel around particles of greywacke in PPL on the left side and XPL on the right side.



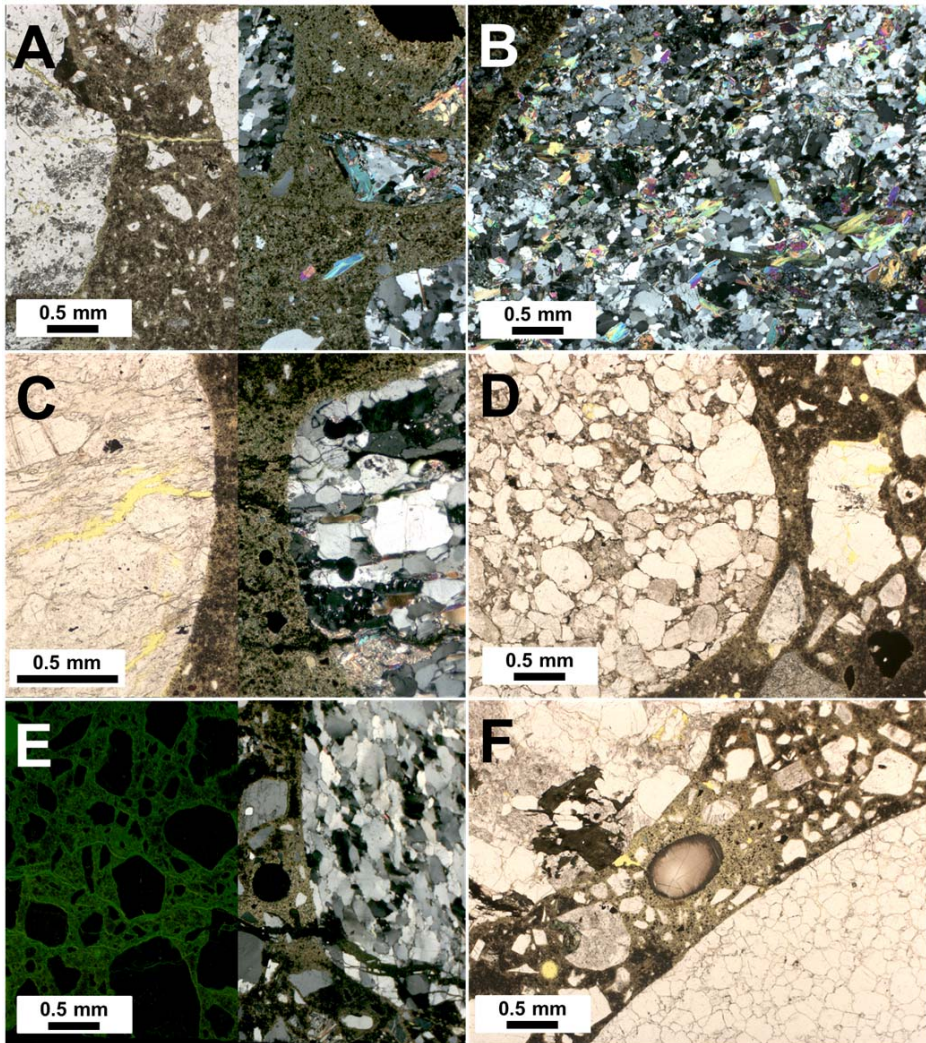


**Figure 9B:** Slowly reactive aggregates: A) Aggregate It2, crack partly filled with gel crossing different particles of quartzite and gneiss in PPL on the left side and XPL on the right side; B) Aggregate It2, particle of gneiss in XPL; C) Aggregate N4, crack crossing particles of cataclasite and quartzite in PPL on the left side and XPL on the right side; D) Aggregate N4, particle of sandstone in PPL; E) Aggregate N5, cracks crossing a particle of quartzite and around several fine particles and the cement paste in FL on the left side and XPL on the right side; F) Aggregate N5, air void filled with gel in PPL.

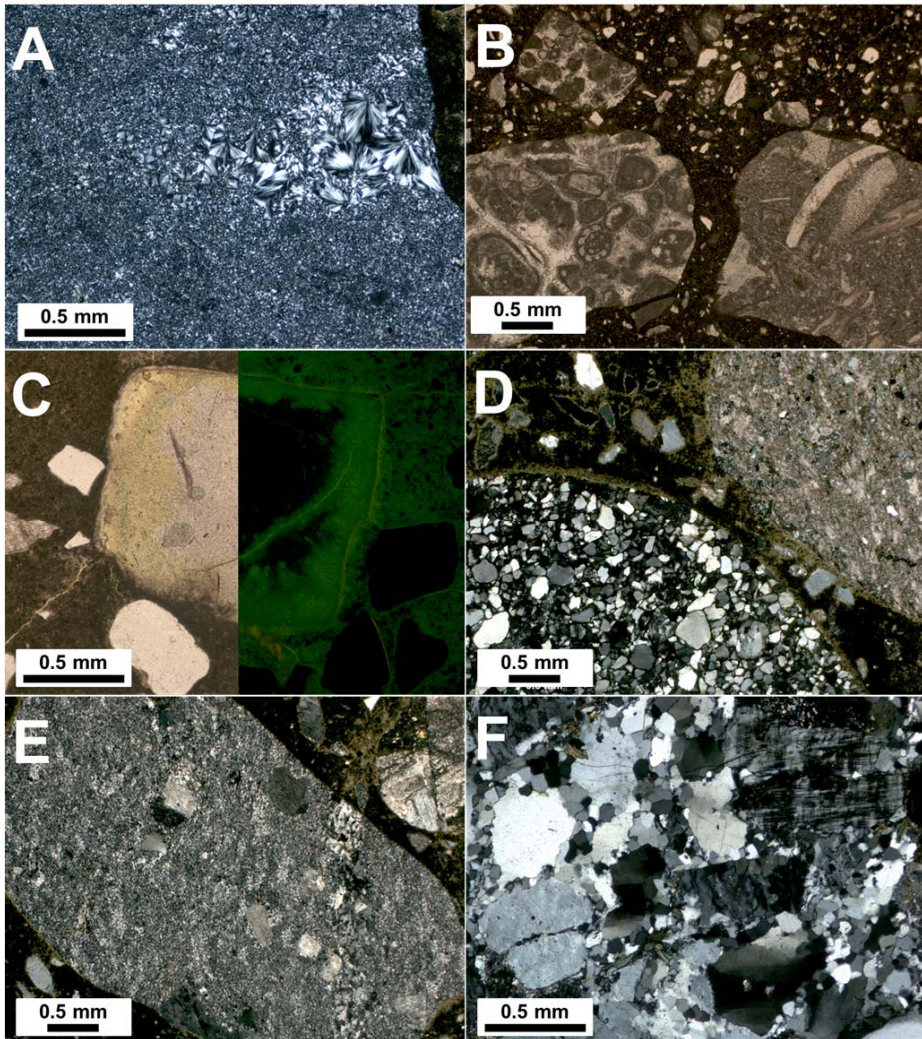


**Figure 9C:** Non-reactive aggregates: A) Aggregate F1, chert particle in XPL; B) Aggregate F2, limestones with braquiopode and foraminifera fossils in PPL; C) Aggregate F3, porous chert particle with cracks in PPL on the left side and FL on the right side; D) Aggregate F3, sandstone and siliceous limestone particles in XPL; E) Aggregate S1, rhyolite particle in XPL; F) Aggregate S1, granite particle with strained quartz and subgranulation in XPL.



## 5.2 Grain size analysis of quartz

A detailed description of the results obtained for this part of the study is presented in papers I, III, IV and V. Therefore, only an overview of the most relevant results will be included in this section.

Paper I assesses the precision and speed of the petrographic image analysis method by studying the grain size of three samples previously applied in Wigum (1995) with image analysis and with point-counting and comparing the results. The length of the major axis of the best fit ellipse ( $d_E$ ) was used as diameter of the particle in the petrographic image analysis method in order to mirror the measurements made with point counting. The number of individual grains assessed by image analysis is higher (up to 5 times higher for this three samples) than by point-counting. Total segmentation time for single samples was approximately 30-110 min, in contrast to point-counting assessment requiring several hours for a single thin-section. The results to mean grain size of quartz and total grain boundary area of quartz obtained by image analysis and by point-counting are consistent with each other. The degree of agreement between the two methods assessed by the square of the correlation coefficient is 0.99 for the mean grain size of quartz and 0.69 for the total grain boundary area of quartz. In summary, the results show that petrographic image analysis method allows the assessment of a higher number of grains in a shorter time without compromising the precision of the results.

Initial results of grain size and grain shape analysis of quartz by image analysis for more samples are presented in papers III, and IV. Final results for 11 aggregates are presented in paper V. In this case, the number of individual quartz grains assessed by the petrographic image analysis method ranges from 186 to 27606, whereas the point-counting method suggested by Wigum (1995) typically assesses ~200 grains. Total segmentation time for single samples was approximately 10–120 min. As expected, the use of different grain size measurements ( $d_E$ ,  $d_A$ ,  $d_V$ ) led to different values for the size descriptors (the mean grain size of quartz and the total grain boundary area of quartz). The values obtained with the  $d_E$  and the  $d_A$  will be similar if the grains have higher circularity and increasingly different with the increasing irregularity of the grains. However, the calculation of these diameters does not take into account the overestimation of small grains produced by a two-dimensional planar section of a rock (thin-section). The equivalent spherical diameter ( $d_V$ ), being calculated with base on the volume weighted distribution of radii of spheres, represents a more accurate estimation of the grain size distribution (Heilbronner and Bruhn, 1998). Therefore, the size descriptors calculated from this measurement are also more accurate. Even though both size descriptors are calculated using the

cumulative grain size distribution curve obtained from the thin section examination by image analysis, only the total grain boundary area of quartz takes into account the shape of the cumulative curve. Hence, the total grain boundary area of quartz gives a better relationship with the reactivity of the aggregate than the mean grain size of quartz. Further correlations use the total grain boundary area of quartz calculated with the  $d_v$ . A summary of the results from laboratory test methods, field site test, and reported experience in structures, used to assess the potential reactivity of the aggregates included in this study, can be found in Tables A2, and A4, in the Appendix in the end of this chapter.

Samples with lower mean grain size and higher total grain boundary area of quartz correspond indeed to the rock types that exhibits higher deformation features in their microstructure. Overall, there is good agreement between the size descriptors, the potential reactivity of the aggregate by RILEM-AAR-1 (2003), and the field experience reported in structures to 6 aggregates. Figure 10 shows the correlations between the total grain boundary area of quartz and the results obtained with the AMBT at 14 days. A reasonable logarithmic correlation was found ( $R^2 = 0.79$ ). The best fit line follows the same trend as the ones obtained by Wigum (1995) and Wigum et al. (2000) even if the rock types included in the present study have a more limited range of grain sizes. These results suggest that the reactivity of the slow reactive aggregates is related the total grain boundary area of quartz, which is strongly influenced by sub-grain development. These results can also be interpreted as evidence that grain size analyses by petrographic image analyses has similar precision to grain size analysis by the traditional point-counting method. Aggregate sample A was regarded as outlier and was not included in the statistical model. Wigum (1995) attributed the anomalous behaviour found for sample A to the presence of strain lamellae and myrmekite. More outliers have been detected in the studies of Wigum (1995), and especially of Wigum et al. (2000). These may be explained, at least in part, by the influence of micas, feldspars, and other mineralogical parameters. Hagelia (1999) showed that mylonite formed at higher temperature exhibited unexpected low expansion when compared with mylonites formed at lower temperatures possible due to the presence of feldspars. Grattan-Bellew and Beaudoin (1980) and Broekmans and Jansen (1997, 1998) found evidences of enhanced silica dissolution in the presence of mica and possible silica minerals. The catalytic effect of other minerals in silica dissolution must be investigated further before some rock types are included into the model. The results of the concrete prism test (RILEM-AAR-3, 2000) and the Danish mortar bar TI-B51 (1978) do not correlate well with the total grain boundary area of quartz. Reasons for this lack of correlation will be discussed in section 5.3.

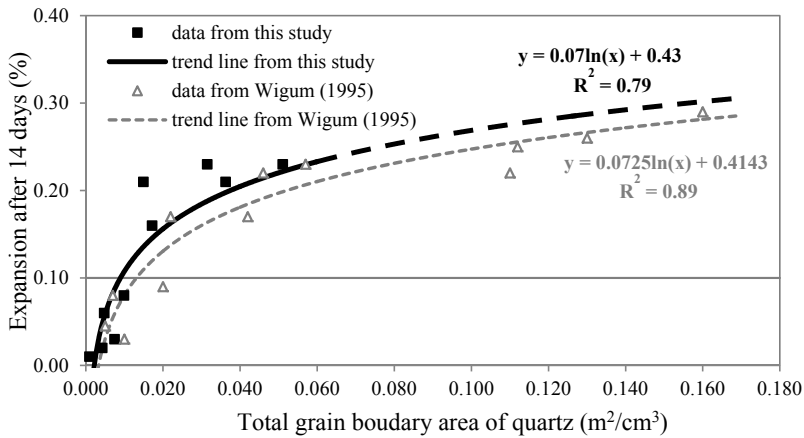


**Figure 10:** Total grain boundary area of quartz versus accelerated mortar bar expansion results.

Minimum, maximum and average values for shape descriptors were calculated. The averaging of shape over all grains in a sample has shown to be an ineffective approach with no correlation with the expansion tests. Distributions of other characteristics were attempted, for example grain size distribution. A correlation was found when comparing circularity with grain size distribution (Figure 11). It was observed that smaller grains tend to be more regular than bigger grains. This can be explained by the fact that smaller grains result from recrystallization while bigger grains have suffered ductile strain effects and deformation. Even though that is not evident from the data obtained with the studied samples, the grain shape can enhance the aggregate reactivity by increasing the surface area of the grain.

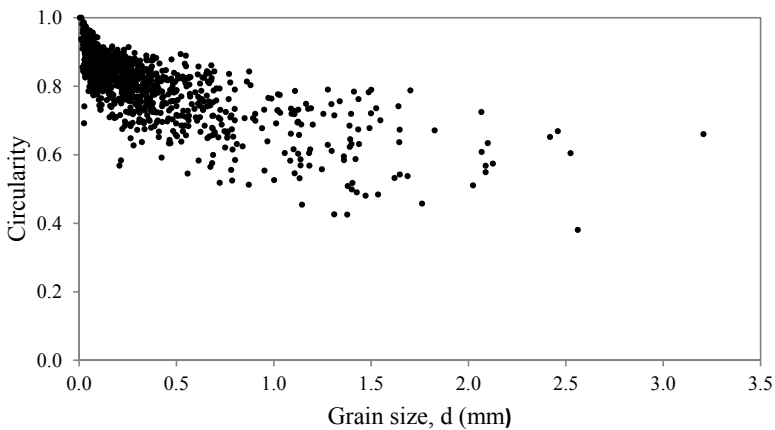


**Figure 11:** Typical distribution of circularity according to grain size distribution for the studied aggregates.



### 5.3 Characterization of the grain boundaries of quartz

A detailed description of the results obtained for this part of the study is presented in paper VII. Therefore, only an overview of the most relevant results will be included in this section.

Raw orientation maps obtained by EBSD have between 99.4% (It2-1) and 98.0% (N5) of points indexed as quartz, which means that the non-indexed points (EBSD patterns with no solution) are  $\leq 2\%$ . The non-indexed points correspond to grain boundaries, secondary phases and defects in the sample surface. Between 1.0% and 8.8% of points were changed in the clean-up routine to produce the extrapolated orientation maps, much depending on the total number of points analysed and of the percentage of non-indexed points per map. Misorientation angle histograms from samples It2-1 and It2-2 have a higher incidence of low angle boundaries than the histograms from samples N4 and N5 (Figure 12). It is important to refer that the use of offline indexing and re-analyses to obtain orientation maps with reduced total amount of non-indexed points was a key point to the very low percentage of non-indexed points obtained in the raw orientation maps. In geological materials like the ones included in this study, the use of optimized Hough transform settings it is essential to the success of the analyses.

Thin-section petrography shows that the quartzite particle samples It2-1 and It2-2 are characterized by elongated grains with irregular grain boundaries and extensive sub-granulation, suggesting high strain. The particle samples N4 and N5 are characterized by quartz grains with shape more regular and smoother grain boundaries and to exhibit less extensive sub-granulation, suggesting lower strain than the previous samples. EBSD data confirms that low boundary angles are predominant in the particle samples It2-1 and It2-2, which can be explained by the extensive sub-granulation observed by thin-section petrography. On the other hand, particle samples N4 and N5 have predominantly high angle boundaries.

The number of particles analysed by EBSD per aggregate sample are very far from being statistically significant. Furthermore, it is improbable that only the quartzite component in the aggregates is responsible for reaction. Therefore, a detailed critical review of the EBSD results against expansion results was not attempted. However, it is interesting to mention that Castro and Wigum (2012a, 2012b) performed grain size analysis to these three aggregate by image analysis petrography, and their results are in apparent contradiction with the EBSD results presented here. Aggregate It2, has higher total grain boundary area of quartz when compared with aggregates N4 and N5, which should mean higher potential to exhibit reactive behaviour, but that is not always evident from expansion data and field experience. For example, non-reactive results were found to aggregate It2 in RILEM AAR-3 and TI-B51, while both

aggregates N4 and N5 tested reactive in the same tests. These results suggest that high angle boundaries, by representing discontinuities between adjacent crystals, may increase quartz solubility by making it more susceptible to be attacked by the alkali hydroxides in the pore solution of concrete. Low angle boundaries, on the other hand, seem to be less susceptible to attack by the alkali hydroxides in the pore solution of concrete, even when the total grain boundary area is higher. However, these results are based on the analysis of a reduced number of samples and therefore require validation by further investigation.

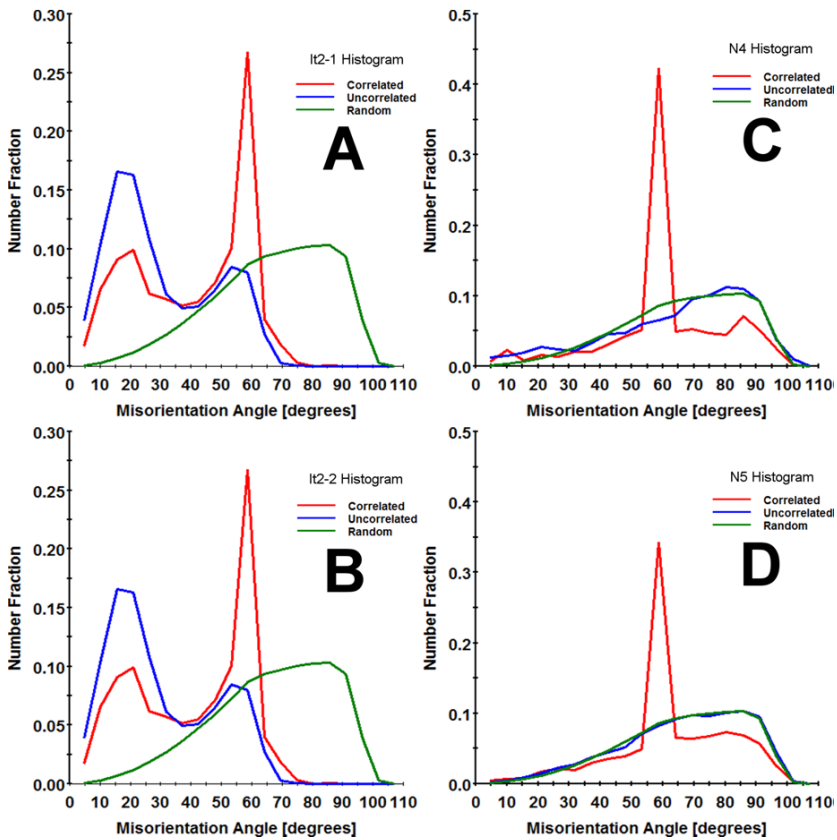


**Figure 12:** Misorientation angle histograms: A) sample It2-1; B) sample It2-2; C) sample N4; D) sample N5.

## 5.4 Effect of polymorphs and other forms of silica

A detailed description of the results obtained for this part of the study is presented in papers II, IV and VI. Therefore, only an overview of the most relevant results will be included in this section.

In Paper II, the precision of the method was assessed by comparing the XRD results obtained on a polished section and on powdered sample material for the same particle. Quartz, calcite and dolomite were identified in both polished section and powdered specimen. The corundum identified in the powdered sample material was regarded as contamination from the crushing process. Figure 13 shows a good fit between the results obtained with polished section and powder material. Additional analytical techniques were used to confirm the precision and accuracy of the XRD analysis. A discrepancy was found between the mineralogical characterization by XRD and the chemical characterization by ICP-AES. The amount of quartz calculated by XRD is in the range 61-65wt%, while the amount of quartz calculated by ICP-AES is ~81wt%. The authors decided to investigate this discrepancy by chemical characterization by other two techniques, XRF and EPMA elemental mapping. The results of XRD, XRF and EPMA elemental mapping are consistent with each other and suggest that the sample sent to ICP-AES was not representative, has suffered segregation or had some heterogeneity. In summary, results from this paper suggest that the precision of the XRD analyses was not compromised by the use of a polished section instead of the traditional powdered sample. In fact, the results of the powdered sample show a corundum contamination due to sample preparation that is not present in the solid sample.

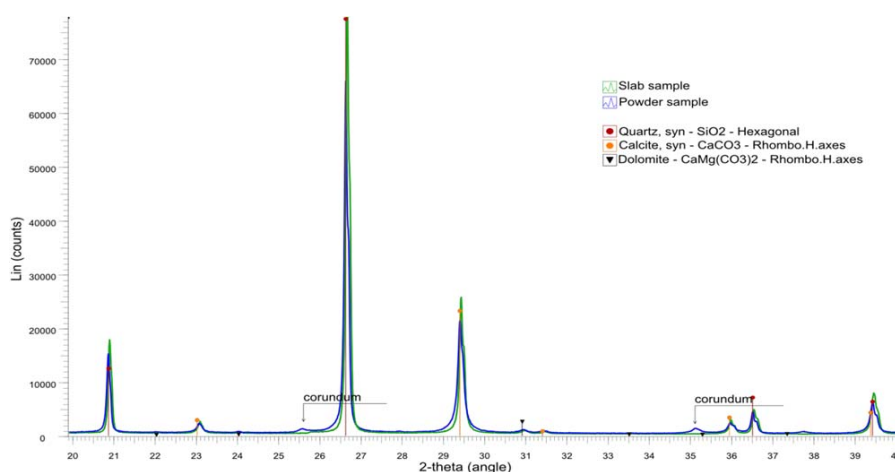


**Figure 13:** XRD spectra of polished section (green) and powder sample (blue) of the same particle of siliceous limestone.

Initial results of XRD analysis with polished sections and powdered material for more samples are presented in paper IV. Final results for 5 aggregates are presented in paper VI. Results from the XRD analysis identified quartz and calcite as main rock forming constituents for the particles analysed. The corundum identified in some of the powdered sample material was regarded as contamination from the comminution process. Particles D1-01 and D1-05 appear to contain a substantial volume of light silica polymorphs cristobalite and tridymite, presumably representing fine-grained intergrowths in opal-CT. Figure 14 shows a good fit between real data and calculated curve to the applied model. For the chert/flint and siliceous limestone investigated in this project, possible effects from sample/specimen preparation such as particle count statistics, particle size and distribution, surface amorphization and sample mounting, seem to balance out rather evenly as thoroughly discussed in paper VI. Presence and spatial distribution of opal CT in sample D1 was assessed by element and CL mapping on the EPMA instrument. CL mapping shows that different types of silica are present in the sample, but reliable quantification was not possible due to its very small grain size below the spatial resolution of the instrumentation. However, the combined amount of quartz, tridymite and cristobalite determined by XRD (56 wt%) is consistent with the amount of SiO<sub>2</sub> determined by EPMA (64 wt%) in D1-01. A summary of the results from laboratory test methods, field site test, and reported experience in structures obtained during PARTNER project for these samples, can be found in Tables A1, and A3, in the Appendix in the end of this chapter. When comparing the results from PARTNER to the results obtained in this study with XRD, some interesting considerations can be drawn. A recent investigation by Garcia-Diaz et al. (2010) with siliceous limestones concluded that contrary to the pure siliceous aggregates, the content of silica in siliceous limestones is too low to consume a maximum of alkalis in non-expansive adsorption process and to obtain non-expansive concretes. This is in agreement with the results obtained for the aggregates B1 and G1. Both have variable amounts of carbonates and higher reactivity than the aggregate F1. On the other hand, Zhang et al. (1990) defend that the phase in which silica occurs plays the dominant role in determining the reactivity, with disordered structures more reactive than structures containing cristobalite, which are in turn more reactive than structures containing quartz. Although more research is needed to confirm experimentally this theory, it is interesting to observe that aggregate D1, where opal-CT was identified by XRD in two particles, was ranked as highly reactive by field experience but expansion after 14 days with RILEM-AAR-2 (2000) was lower than other aggregates like F1 and G1 that showed lower reactivity in the field than aggregate D1. Another interesting fact about aggregate D1 is that it has shown pessimum behaviour despite its composition that is not the typical “pure siliceous aggregate”.

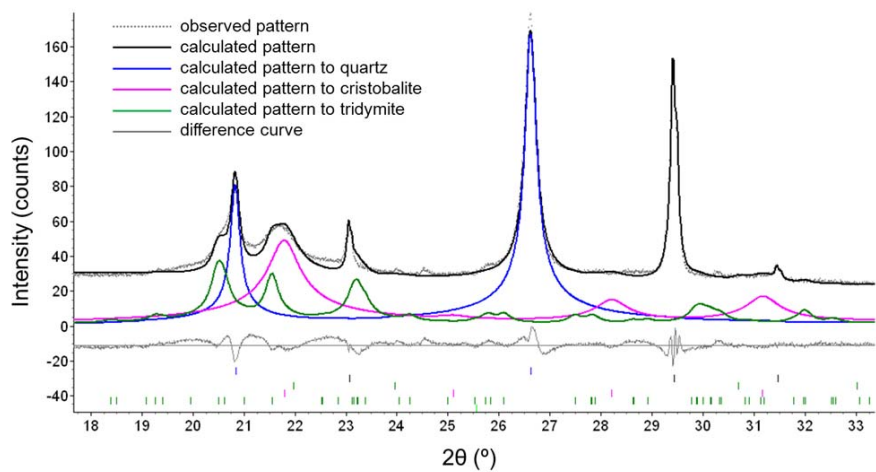


**Figure 14:** Example of XRD fit for aggregate particle with opal.

## APPENDIX: Results from laboratory tests, field site test, and reported reactivity in structures

This appendix summarizes results from laboratory tests, field site tests, and reported reactivity in structures, for the aggregates included in the study presented in this thesis. These results were used to assess the potential reactivity of the studied aggregates and critically compared with the results from the different techniques used to characterize the silica minerals within the aggregates, as explained in detail in Chapters 1, 4 and 5. The results presented here were obtained in three previous projects (Wigum, 1995; Castro, 2008; Lindgård et al., 2010).

**Table A1:** Summary of results of laboratory test methods, field site test, and reported reactivity in structures for the normally reactive aggregate combinations tested in the PARTNER project (adapted from Lindgård et al., 2010, and Borchers and Müller, 2012).

Aggregate	Fraction / Combination	Reactivity / evaluation							
		AAR-1	AAR-2	AAR-3	AAR4 / AAR-4 Alt.	TI-B51 / Chatterji	German / Norwegian	Field site test after 7 years**	Reported reactivity in structures?
Normally reactive aggregate combinations									
B1 – Silicified limestone	F	R	R			R/R			Yes
	C	R							
	C+F			R	R/R		R/R	R	
	C+NRF			R	R/R			R	
UK1 - Greywacke	F	R	R			R/R			Yes
	C	R							
	C+F			R	R/R		R/R	R	
G1 – Gravel with siliceous limestone and chert	C	R	R			R/-			Yes
	C+NRF			R	R/R		R/-	R	
	C	R	R						
	C+F			R	R/R				
N1 - Cataclasite	C	R	R			R/R			Yes
	C+NRF			R	R/R		R/R	R	
D1 – Gravel with opaline flint	F	R	R						Yes, but pessimum effect
	C	R	R			R/R			
	C+F			?*	NR/NR		NR/-		
D2 – sea gravel semi-dense flint	F	R	R						Yes, but 10-15 years
	C	R	R						
	F+NRC			NR/MR?	NR/MR			R	

F = fine aggregate; C = coarse aggregate

NRF = non-reactive fine aggregate (=N3F); NRC = non-reactive coarse aggregate (=F2C)

R = reactive (according to the critical limits in the different testing methods); NR = non-reactive (according to the critical limits in the different testing methods); MR = marginally reactive (i.e. expansions just above the critical limits in the different testing methods)

p.r. = possibly reactive aggregate combination; n.r. = no rating yet possible

\* = one result strongly reactive, second non-reactive

\*\* = the evaluation of the preliminary results from the field sites is based on measurements of crack widths after about 7 years of exposure and of expansions during the last 6 years (the expansion measurements were re-started in 2005 due to problems with the zero measurements at some field sites).

\*\*\* = first indication of reactivity in at least one field site.

**Table A2:** Summary of results of laboratory test methods, field site test, and reported reactivity in structures for the slowly reactive aggregate combinations tested in the PARTNER project (adapted from Lindgård et al., 2010, and Borchers and Müller, 2012).

Aggregate	Fraction / Combination	Reactivity / evaluation							Field site test after 7 years**	Reported reactivity in structures?
		AAR-1	AAR-2	AAR-3	AAR4 / AAR-4 Alt.	TI-B51 / Chatterji	German / Norwegian			
<b>Slowly reactive aggregate combinations</b>										
It2 (I in paper V) – Gravel with quartzite	F	R	R			NR/-				Yes 50 years
	C	R	R							
	C+F			NR	R/R			n.r.		
N4 (J in paper V) – gravel with sandstone and cataclastic rocks	F	R	R			R/R				Yes 20-25 years
	C	R	R							
	C+F			MR	R/-		MR/MR	R***		
N5(K in paper V) – Gravel with rhyolite and quartzite	F	R	R			R/R				Yes 20-25 years
	C	R	MR							
	C+F			MR	R/-		MR/MR			

Regarding abbreviations: see legends to Table A-1.

**Table A3:** Summary of results of laboratory test methods, field site test, and reported reactivity in structures for the non-reactive aggregate combinations tested in the PARTNER project (adapted from Lindgård et al., 2010, and Borchers and Müller, 2012).

Aggregate	Fraction / Combination	Reactivity / evaluation							Field site test after 7 years**	Reported reactivity in structures?
		AAR-1	AAR-2	AAR-3	AAR4 / AAR-4 Alt.	TI-B51 / Chatterji	German / Norwegian			
<b>Non-reactive aggregate combinations</b>										
F1 – Gravel with flint	C	R	NR			NR/R				No, but known pessimum effect
	C+NRF			NR	NR/NR		NR/-	R***		
F2 – Non-reactive limestone	F	NR	NR							No
	C	NR								
	C+F			NR	NR/NR		NR/NR	n.r.		
F3 – Gravel with quartzite, flint, greywacke and granitoids	F	R	R			NR/R				No, but likely pessimum effect
	C	R								
	C+F			NR	NR/NR					
S1 – Gravel with meta-rhyolite and greywacke	F	R	R			R/R				Yes, but source variable in composition
	C	R								
	C+F			NR	MR/-		NR/MR	R***		
N3 – Granitic sand	F	NR	NR			NR/NR				No
	C	NR								
	C+NRF			NR	NR/NR		NR/NR			

Regarding abbreviations: see legends to Table A-1.

**Table A4:** Summary of results of laboratory test methods and reported reactivity in structures for the aggregates tested in the projects Wigum (1995), and Castro (2008).

<b>Reactivity / evaluation</b>				
<b>Aggregate</b>	<b>AAR-I</b>	<b>AMBT</b>	<b>Reported reactivity in structures?</b>	<b>Project</b>
A - Porphyritic granite	NR	R		Wigum (1995)
B - Mylonite	R	R		
C - Mylonite	R	R		
D - Granite	R	NR		Castro (2008)
E - Granite	R	NR	Yes, > 40 years	
F - Granite	R	NR	Yes, > 10 years	
G - Granite	R	NR		
H - Granite	NR	NR	No, > 30 years	

R = reactive; NR = non-reactive





## 6 Conclusions and recommendations for future work

### 6.1 Conclusions

This thesis provides suggestions of different test methods that, when used as a supplement to the petrographic method (RILEM-AAR-1, 2003), can help to overcome some of the limitations of the traditional petrographic method that have been reported in the literature, and improve its value as a tool to evaluate the potential reactivity of aggregates for concrete. The suggested methods are dependent on the aggregate type.

The petrographic image analysis method presented in papers I, III, IV and V, has proven to be a precise and accurate method for grain size and grain shape analysis of slowly reactive aggregates for concrete. Not only is it possible to analyse samples much faster than with point-counting, a much larger number of grains can be analysed. Typical stereological problems such as the overestimation of the small grains produced by a two-dimension representation of a rock (thin-section) can be easily and efficiently overcome. Very good correlation was found between the grain size descriptors and the petrographic method RILEM-AAR-1 (2003) and the reported reactivity in structures. Good correlation was also found with the results of the accelerated concrete prism test RILEM-AAR-4.1 (to be published), although only three results are available. The correlations found between grain size descriptors and the AMBT follow the same trends by Wigum (1995) and Wigum et al. (2000), confirming that the reactivity of the slowly reactive aggregates is related the total grain boundary of quartz, which is strongly influenced by sub-grain development. No correlation was found between the average values of the grain shape descriptors and the laboratory tests to assess the potential reactivity of the aggregates or reported reactivity in structures, but it was observed that overall the small grains are more regular than bigger grains. This method has also the great potential to be used not only in the assessment of aggregates for concrete but as well as in the assessment of deterioration in real structures, since concrete thin-sections can also be analysed.

Characterization of the grain boundaries of quartz by EBSD has shown to have a great potential to improve the understanding of the influence of strain in the potential alkali-reactivity of aggregates for concrete. With the offline indexing system used in paper VII, it is possible to re-index each pattern as many times as needed until finding optimized settings. This option is

especially useful when analysing geological materials since these are extremely sensitive to the Hough transform settings. The initial results presented in this paper for 4 particles of quartzite suggest that high angle boundaries of quartz, by representing discontinuities between adjacent crystals, increase its solubility by making it more susceptible to be attacked by the alkali hydroxides in the pore solution of concrete.

The results presented in papers II, IV, and VI with normally reactive aggregates, show that for fine-grained rock types with grain size below  $\sim 5\mu\text{m}$  and without preferred orientation, the assessment of mineral content by XRD using polished sections represents an advantage over traditional powdered specimens in materials like e.g. polymictic virgin aggregate, field concrete, and post-mortem mortar bars and concrete prisms. Traditional sample preparation by pulverization can present a real challenge in these materials, for various reasons. In concrete petrography, use of polished solid samples offers several advantages. Rather than extracting fragile and often already cracked material (problematic in hardened concrete) and subsequent comminution, the particle of interest is cut in situ and polished with diamond. Then, prepared polished sections can be assessed in a petrographic microscope using incident illumination, SEM, and XRD, whereas the unpolished counterpart can be sacrificed for additional analysis by destructive methods. XRD analysis of the chert/flint and siliceous limestone investigated here using polished sections provides results that are indistinguishable from results obtained using powdered material. The presence of other species of silica in addition to quartz was confirmed by cathodoluminescence using a FEG EPMA instrument. XRD analysis implies these might represent 'cristobalite and/or tridymite', presumably present as opal-CT. Expansion data from PARTNER coincide with the presence of known deleterious alkali-reactive silica species, notably fine grained quartz. The identification of 'additional silica species other than quartz' in sample D1 coincides with the unexpected pessimum behavior and very high expansion in the field although non-reactive results in several other tests have been observed pessimum as reported by PARTNER project.

## 6.2 Recommendations for future work

*“An answer is always the part of the road that is behind you.*

*Only questions point out the future.”*

Jostein Gaarder

The petrographic image analysis method presented in this thesis is currently limited to rock types with grain sizes resolvable under the optical microscope. The grain size problem is easily overcome by adapting the method to input images obtained with other microscopes with higher resolution (for example a scanning electron microscope - SEM). Some problems were also found with rock types where the quartz grains exhibited high degree of strain. At this point, the authors consider that more research is also needed to establish criteria limits on the total grain boundary area of quartz that determines an aggregate reactivity. Future research should focus on the investigation of more rock types and on the use of precise and reliable expansion tests.

The EBSD method used here to characterize the grain boundaries of quartz is not suitable to be used as a standard method in the characterization of aggregates for concrete. However, it bears a great potential to be used to improve our understanding about the role of the grain boundary quality in the potential alkali-reactivity of aggregates for concrete, and consequently to help developing simple and time efficient techniques that can take such characterization into account. Future work shall focus on combining energy-dispersive x-ray spectroscopy (EDS) with EBSD so that multiple mineral phases can be analysed at the same time, and therefore, a much larger number of rock types could be analysed. If a statistically significant number of aggregate samples are investigated and the results critically reviewed against expansion results and experience in structures it is expected that:

- A better understanding of the effect of strain in the grain boundaries of quartz and how this influences the potential reactivity of aggregates for concrete is achieved;
- Optical techniques and image analysis edge detection logarithms are improved in such way that characterization of the grain boundary features are included, which will significantly improve the image analysis petrography technique suggested by Castro and Wigum (Castro and Wigum, 2012a, 2012b).

The assessment of mineral content by XRD using polished sections has proven to be precise and accurate for the flint/chert and siliceous limestone included in this study. However, extending the results obtained here to samples from other locations, or to other (very) fine grained lithologies (eg. siltstone, greywacke, rhyolite) is likely to produce different results. Therefore, future work should focus on the assessment of XRD analysis using polished sections from samples of flint/chert and siliceous limestone of different origin and nature, as well as of different lithologies to clearly understand the limitations of the method.

A number of parameters that affect the solubility of the silica minerals under ASR environment have been discussed in this thesis; however, many other deserve our attention. Any defect in the crystal lattice of quartz (e.g. replacement, dislocation, grain boundary) will have a substantial impact in its solubility and therefore will affect aggregate reactivity. It is essential to understand the extent of the distortion introduced in the crystal lattice of quartz by foreign and hydrous species and in which way this will affect its solubility. A better understanding of the effect of different deformation mechanisms of quartz in the aggregate reactivity it is also very important. A number of parameters (e.g. grain size and shape, grain boundaries area and characteristics, dislocations density in the crystal, etc.) will be influenced by the deformation mechanisms and they need to be studied and understood in a holistic way. The development of improved test methods to assess the potential alkali-reactivity of aggregates for concrete is a complex and challenging task. To meet the needs of the building and construction industry the tests shall be time and cost efficient, and yet provide an accurate and precise prediction of the aggregate behaviour in a structure for the next 50 to 100 years. Such exigent requirements can only be achieved by the development of test methods capable of quantifying the reactive component in the aggregate; which, in turn, can only be achieved by a better understanding of the properties of the silica minerals that affect its dissolution under ASR environment. Such advances in the scientific knowledge are essential to the comfort and security of the modern society due to the huge importance that concrete as a building material has on our lives.

## References

- ALAEJOS, P, and LANZA, V (2012) *Influence of equivalent reactive quartz content on expansion due to alkali silica reaction*. Cement and Concrete Research, 42, 99-104.
- ASTM-C-295 (2007) *Standard guide for petrographic examination of aggregates for concrete*. The American Society for testing and Materials. Philadelphia, 8.
- ASTM-C-1260 (2007) *Standard test method for potential alkali-aggregates (Mortar bar method)*. American Society for Testing and Materials. Philadelphia, 4.
- BARRETT, SD (2008) *Image SXM*. <http://www.ImageSXM.org.uk>.
- BCA (1992) *The diagnosis of alkali-silica reaction. Report of a working party*. British Cement Association Publication (45.042), 44.
- BÉRUBÉ, M, and FOURNIER, B (1993) *Canadian experience with testing for alkali-aggregate in concrete*. Cement and Concrete Composites, 15, 27-47.
- BÉRUBÉ, MA, DUCHESNE, J, DORION, JF, and RIVEST, M (2002) *Laboratory assessment of alkali contribution by aggregates to concrete and application to concrete structures affected by alkali-silica reactivity*. Cement and Concrete Research, 32, 1215-1227.
- BÉRUBÉ, MA, and FOURNIER, B. (2004) *Alkalis releasable by aggregates in concrete – significance and test methods*. In: M. TANG, DENG, M. , ed. 12th International Conference on Alkali-Aggregate in Concrete, Beijing, China, 17-30.
- BISH, DL, and REYNOLDS, RC (1989) *Sample Preparation for X-Ray-Diffraction*. Reviews in Mineralogy, 20, 73-99.
- BORCHERS, I, and MÜLLER, C. (2008) *Field site tests established in the PARTNER project for evaluating the correlation between laboratory tests and field performance*. In: M. A. T. M. BROEKMANS, and WIGUM, B. J., eds. 13th International Conference on Alkali-Aggregate Reaction in Concrete, Trondheim, Norway, 10.
- BORCHERS, I, and MÜLLER, C (2012) *Seven years of field tests to assess the reliability of different laboratory test methods for evaluating the alkali-reactivity potential of aggregates*. In: T. DRIMALAS, IDEKER, J. H., and FOURNIER, B. (eds.) *14th International Conference on Alkali-Aggregate Reactions in Concrete*. Austin, Texas, USA, 10.
- BROEKMANS, MATM. (1999) *Classification of the alkali-silica reaction in geochemical terms of silica dissolution*. In: H. PIETERSEN, LARBI, J., and JANSSEN, H., eds. 7th Euroseminar on Microscopy Applied to Building Materials, Delft, 155-170.
- BROEKMANS, MATM (2004) *Structural properties of quartz and their potential role for ASR*. Materials Characterization, 53, 129-140.
- BROEKMANS, MATM. (2006) *Sample representativity: effects of size and preparation on geochemical analysis*. In: B. FOURNIER, ed. Marc-André Bérubé Symposium on alkali-aggregate reactivity in concrete. 8th CANMET / ACI International Conference on Recent Advances in Concrete Technology Montréal, 1-19.
- BROEKMANS, MATM, and JANSEN, JHB (1997) *ASR in impure sandstone: mineralogy and chemistry*. In: E. L. SVEINSDÓTTIR (ed.) *6th Euroseminar on Microscopy Applied to Building Materials*. Reykjavik, Iceland, 161-176.
- BROEKMANS, MATM, and JANSEN, JHB (1998) *Silica dissolution in impure sandstone: application to concrete*. In: S. P. VRIEND, and SZIJLSTRA, J. J. P. (eds.) *Geochemical Engineering: Current Applications and Future Trends*. Journal of Geochemical Exploration, Special Volume, 311-318.
- BROUARD, E (2012) *Potentially reactive aggregates with a pessimum effect. Pessimism effect mechanisms, review of PRP qualification tests and conditions of use of these aggregates*. In: T. DRIMALAS, IDEKER, J. H., and FOURNIER, B. (eds.) *14th International Conference on Alkali-Aggregate Reactions in Concrete*. Austin, Texas, 10.

- BS-7943 (1999) *Guide to the interpretation of petrographical examinations for alkali-silica reactivity*. British Standard, 20.
- BUHRKE, VE, JENKINS, R, and SMITH, DK (2001) *A practical guide for the preparation of specimens for X-ray fluorescence and X-ray diffraction analysis*, New York, Wiley-VCH, 360.
- CASTRO, N. (2008) *Granitic aggregates for concrete. Attempt of correlation between the granite age and the potential reactivity to alkalis of concrete*. Master in Science, Porto, 122.
- CASTRO, N, FERNANDES, I, and SANTOS SILVA, A. (2009) *Alkali reactivity of granitic rocks in Portugal: a case study*. In: M. BERNHARD, JUST, A., KLEIN, D., GLAUBITT, A., SIMON, J., ed. 12th Euroseminar on Microscopy Applied to Building Materials, Dortmund, 11.
- CASTRO, N, and WIGUM, BJ. (2012a) *Grain size analysis of quartz in potentially alkali-reactive aggregates for concrete: a comparison between image analysis and point-counting*. In: M. A. T. M. BROEKMANS, ed. 10th International Conference on Applied Mineralogy, August 2011, Trondheim: Elsevier, 103-110.
- CASTRO, N, and WIGUM, BJ (2012b) *Assessment of the potential alkali-reactivity of aggregates for concrete by image analysis petrography*. Cement and Concrete Research, 42, 1635-1644.
- CHATTERJI, S, and JENSEN, AD (1988) *A Simple Chemical-Test Method for the Detection of Alkali-Silica Reactivity of Aggregates*. Cement and Concrete Research, 18, 654-656.
- CHATTERJI, S, THAULOW, N, and JENSEN, AD (1989) *Studies of Alkali-Silica Reaction. Verification of a Newly Proposed Reaction-Mechanism*. Cement and Concrete Research, 19, 177-183.
- CS (1987) *Alkali-silica reaction: minimising the risk of damage to concrete. Guidance notes and model specification clauses*. Technical Report n° 30, 3rd Edition. London: Concrete Society, 34.
- CSA-A23.2-15A (2004) *Petrographic examination of aggregates*. Canadian Standard Association.
- CSA (1986) *Supplement no. 2 to CSA Standards CAN3-A23.1 and CAN3-A23.2*. Canadian Standard Association
- CULLITY, BD, and STOCK, SR (2001) *Elements of X-ray diffraction*, Upper Saddle River, New Jersey, Prentice Hall, 664.
- DAFSTB (2007) *Vorbeugende Maßnahmen gegen schädigende Alkali-reaktion im Beton : Alkali-Richtlinie*. Beuth, Berlin, (DAFstb-Richtlinie). Deutscher Ausschuss für Stahlbeton.
- DIAMOND, S (2000) *Chemistry and other characteristics of ASR gels*. In: M. A. BÉRUBÉ, FOURNIER, B., and DURAND, B. (eds.) *11th International Conference on Alkali-Aggregate Reaction in Concrete*. Québec City, Canada, 31-40.
- DINGLEY, DJ, and RANDLE, V (1992) *Microtexture Determination by Electron Back-Scatter Diffraction*. Journal of Materials Science, 27, 4545-4566.
- DOLAR-MANTUANI, L. (1981) *Undulatory extinction in quartz used for identifying potentially alkali-reactive rocks*. In: R. E. OBERHOLSTER, ed. 5th International Conference on Alkali-Aggregate Reactions in Concrete, Cape Town, S252/236.
- DRON, R (1990) *Thermodynamique de la réaction alcali-silice*. Bull. de Liaison des Lab. Ponts et Chaussées, 166, 55-59.
- DRON, R, and BRIVOT, F (1993a) *Study of Some Synthetically Prepared Hydrous Alkali Calcium Silicates - Discussion*. Cement and Concrete Research, 23, 1001-1002.
- DRON, R, and BRIVOT, F (1993b) *Thermodynamic and Kinetic Approach to the Alkali-Silica Reaction .2. Experiment*. Cement and Concrete Research, 23, 93-103.
- DRON, R, BRIVOT, F, and CHAUSSADENT, T (1998) *Mécanisme de la réaction alcali-silice*. Bull. Liaison Lab Ponts et Chaussées, 214, 61-68.
- DS-423.39 (2002) *Concrete testing - hardened concrete - production of fluorescence impregnated plane sections (in Danish)*. . Danish Standards Association 8.

- DUCHESNE, J. (2006) *ASR Mitigation by the use of supplementary cementing materials: evaluation of the available alkali content*. In: B. FOURNIER, ed. Marc-André Bérubé symposium on alkali-aggregate reactivity in concrete, Montréal, Canada, 129-138.
- ECO-SERVE (2004) *Baseline Report for the Aggregate and Concrete industries in Europe*. ECO-SERVE Network, Cluster 3: Aggregate and Concrete Production, 68.
- ERMCO (2010) *Ready-Mixed Concrete Industry Statistics*. European Ready Mixed Concrete Organization, 16.
- EUROSTAT (2009) *European Business facts and figures*. Statistical Office of the European Communities, 567.
- FERNANDES, I, NORONHA, F, and TELES, M (2004) *Mictoscopic analysis of alkali-aggregate reaction products in a 50-year-old concrete*. Materials Characterization, 53, 295-306.
- FERNANDES, I, NORONHA, F, and TELES, M (2007) *Examination of the concrete from an old Portuguese dam: Texture and composition of alkali-silica gel*. Materials Characterization, 58, 1160-1170.
- FRENCH, W. (1989) *Maintenance of mobile alkali concentration in cement paste during Alkali-Aggregate reactions*. 8th International Conference on Alkali-Aggregate Reactions in Concrete, Kyoto, Japan, paper distributed at the conference.
- FUJII, M, KOBAYASHI, K, KOJIMA, K, and MAEHARA, H. (1987) *The static and dynamic behavior of reinforced concrete beams with cracking due to alkali-silica reaction*. . In: P. E. GRATAN-BELLEW, ed. 7th International Conference on Alkali-Aggregate Reactions in Concrete, Ottawa, Canada, 126-130.
- GARCIA-DIAZ, E, BULTEEL, D, MONNIN, Y, DEGRUGILLIERS, P, and FASSEU, P (2010) *ASR pessimum behaviour of siliceous limestone aggregates*. Cement and Concrete Research, 40, 546-549.
- GARCIA-DIAZ, E, RICHE, J, BULTEEL, D, and VERNET, C (2006) *Mechanism of damage for the alkali-silica reaction*. Cement and Concrete Research, 36, 395-400.
- GILLOTT, J (1964) *Mechanisms and kinetic of expansion in the alkali-carbonate rock reaction*. Canadian Journal of Earth Science, 1.
- GILLOTT, J (1973) *Alkali-aggregate reaction in Nova Scotia IV. Character of the reaction*. Cement and Concrete Research, 3, 521-535.
- GLASSER, LSD, and KATAOKA, N (1981a) *The Chemistry of Alkali-Aggregate Reaction*. Cement and Concrete Research, 11, 1-9.
- GLASSER, LSD, and KATAOKA, N (1981b) *Some Observations on the Rapid Chemical-Test for Potentially Reactive Aggregate*. Cement and Concrete Research, 11, 191-196.
- GOGTE, BS (1973) *Evaluation of Some Common Indian Rocks with Special Reference to Alkali-Aggregate Reactions*. Engineering Geology, 7, 135-153.
- GOLTERMANN, P (1995) *Mechanical prediction of concrete deterioration - part 2: classification of crack patterns*. ACI Materials Journal, 92, 1-6.
- GONÇALVES, CP, and LAGOEIRO, LE (2009) *U-stage and EBSD technique as complementary methods*. Revista Brasileira de Geociências, 39, 112-128.
- GRAETSCH, H (1994) *Structural characterizatics of opaline and microcrystalline silica minerals*. In: P. HEANEY, PREWITT, C., and GIBBS, G. (eds.) *Silica: physical behaviour, geochemistry and materials applications*. Reviews in Mineralogy, 209-232.
- GRATTAN-BELLEW, P, and BEAUDOIN, J (1980) *Effect of phlogopite mica on alkali aggregate expansion in concrete*. Cement and Concrete Research, 10, 789-797.
- GRATTAN-BELLEW, PE. (1986) *Is high undulatory extinction in quartz indicative of alkali-expansivity of granitic aggregates?* In: P. E. GRATAN-BELLEW, ed. 7th International Conference on Alkali-Aggregate Reactions in Concrete, Ottawa: Noyes Publications, 434-439.
- GRATTAN-BELLEW, PE, MARGESON, J, MITCHELL, L, and MIN, D. (2008) *Is ACR just another variant of ASR? Comparison of acid insoluble residues of alkali-silica and alkali-carbonate reactive limestones and its significance for the ASR7ACR debate*. In: M. A. T.



- M. BROEKMANS, and WIGUM, B., eds. 13th International Conference on Alkali-Aggregate Reactions in Concrete, Trondheim, Norway, 706-717.
- GRELK, B (2006) *PARTNER Report No. 3.4. Experience from testing of the alkali reactivity of European aggregates according to two Danish laboratory test methods*. SINTEF Report SBF52 A06022 / ISBN 82-14-04082-5 / 978- 82-14-04082-5, 18 + appendices.
- GSB (2006) *Petrographic Atlas of the Potentially Alkali-Reactive Rocks in Europe*. In: G. LORENZI, JENSEN, J., WIGUM, B., SIBBICK, R., HAUGEN, M., GUÉDON, S., and ÅKESSON, U. (eds.). Geological Survey of Belgium 63 + 192 photographs.
- GÖTZE, J, PLÖTZE, M, and HABERMANN, D (2001) *Origin, spectral characteristics and practical applications of the cathodoluminescence (CL) of quartz - a review*. *Mineralogy and Petrology*, 71, 225-250.
- HAGELIA, P (1999) *Samanlikning av tre testmetodar for alkalireaktivitet (in Norwegian)*. *Prosjekt-496-DP2. Internrapport 2076*. Oslo, Norway: Vegteknisk avdeling (Norwegian Public Road Administration, Geology and Tunnel Division), 21.
- HANSEN, WC (1944) *Studies relating to the mechanism by which the alkali-aggregate reaction produces expansion in concrete*. American Society of Civil Engineering, 66, 1781-1811.
- HAUGEN, M, LINDGÅRD, J, ÅKESSON, U, and SCHOUENBORG, B. (2008) *Experience from using the RILEM AAR-1 petrographic method among European petrographers – part of the PARTNER project*. In: M. BROEKMANS, and WIGUM, B., eds. 13th International Conference on Alkali-Aggregate Reaction in Concrete (ICAAR), Trondheim, 744-753.
- HEANEY, P (1994) *Structure and chemistry of the low-pressure silica polymorphs*. In: P. HEANEY, PREWITT, C., and GIBBS, G. (eds.) *Silica: physical behavior, geochemistry and materials applications*. Reviews in Mineralogy, 1-40.
- HEILBRONNER, R (1998) *Stripstar, public domain program for the calculation of 3-D grain size distributions from histograms of 2-D sections*. <http://pages.unibas.ch/earth/micro/index.html>; University of Basel.
- HEILBRONNER, R (1999) *Lazy Grain Boundaries, public domain macros for NIH Image*. <http://pages.unibas.ch/earth/micro/index.html>; University of Basel.
- HEILBRONNER, R (2000) *Automatic grain boundary detection and grain size analysis using polarization micrographs or orientation images*. *Journal of Structural Geology*, 22, 969-981.
- HEILBRONNER, R, and BRUHN, D (1998) *The influence of three-dimensional grain size distributions on the rheology of polyphase rocks*. *Journal of Structural Geology*, 20, 695-705.
- HELMUTH, RA, and STARK, D (1992) *Alkali silica reactivity mechanisms*. In: J. SKALNY (ed.) *Materials Science of Concrete III*. Westerville, OH, USA: American Ceramic Society, 131-208.
- HOBBS, DW (1988) *Alkali-silica reaction in concrete*, London, Thomas Telford Ltd.
- HUMPHRIES, DW (1992) *The preparation of thin sections of rocks, minerals and ceramics*, Royal Microscopical Society, Oxford Science Publications.
- ICHIKAWA, T (2009) *Alkali-silica reaction, pessimum effects and pozzolanic effect*. *Cement and Concrete Research*, 39, 716-726.
- ICHIKAWA, T, and MIURA, M (2007) *Modified model of alkali-silica reaction*. *Cement and Concrete Research*, 37, 1291-1297.
- IDEKER, J, FOLLIARD, K, FOURNIER, B, and THOMAS, M (2006) *the role of "non-reactive" aggregates in the accelerated (60°C) concrete prism test*. In: B. FOURNIER (ed.) *Marc-André Bérubé Symposium on Alkali-Aggregate Reactivity in Concrete*. Montreal, Canada, 45-70.
- IDEKER, JH, EAST, BL, FOLLIARD, KJ, THOMAS, MDA, and FOURNIER, B (2010) *The current state of the accelerated concrete prism test*. *Cement and Concrete Research*, 40, 550-555.

- ISO-9276-6 (2008) *Representation of results of particle size analysis - Parte 6: descriptive and quantitative representation of particles shape and morphology.*, 23.
- JENSEN, J (2006) *PARTNER Report No. 3.2. Experience from testing of the alkali reactivity of European aggregates according to the RILEM AAR-2 method.* SINTEF Report SBF52 A06020 / ISBN 82-14-04080-9 / 978-82-14-04080-9, 43 + appendices.
- JENSEN, V. (2012) *Reclassification of alkali aggregate reaction.* In: T. DRIMALAS, J.H. IDEKER, and FOURNIER, B., eds. 14th International Conference on Alkali-Aggregate Reactions in Concrete, Austin, Texas, USA, 10.
- KATAYAMA, T (2010) *The so-called alkali-carbonate reaction (ACR) - Its mineralogical and geochemical details, with special reference to ASR.* Cement and Concrete Research, 40, 643-675.
- KATAYAMA, T. (2012) *Rim-forming dolimitic aggregates in concrete structures in Saudi Arabia - is dedolomitization equal to the so-called alkali-carbonate reaction?* In: T. DRIMALAS, J.H. IDEKER, and FOURNIER, B., eds. 14th International Conference on Alkali-Aggregate Reactions in Concrete, Austin, Texas, USA, 10.
- KATAYAMA, T, and SOMMER, H. (2008) *Further investigations of the mechanisms of so-called alkali-carbonate reaction based on modern petrography techniques.* In: M. A. T. M. BROEKMANS, and WIGUM, B., eds. 13th International Conference on Alkali-Aggregate Reactions in Concrete, Trondheim, Norway, 850-861.
- KERRICK, DM, and HOOTON, RD (1992) *ASR of Concrete Aggregate Quarried from a Fault Zone - Results and Petrographic Interpretation of Accelerated Mortar Bar Tests.* Cement and Concrete Research, 22, 949-960.
- KLUG, HP, and ALEXANDER, LE (1974) *X-ray diffraction procedures for polycrystalline and amorphous materials*, John Wiley & Sons, 966.
- KRONENBERG, A (1994) *Hydrogen speciation and chemical weakening of quartz.* In: P. HEANEY, PREWITT, C., and GIBBS, G. (eds.) *Silica: physical behavior, geochemistry and materials applications.* Reviews in Mineralogy, 123-176.
- LARIVE, C, LAPLAUD, A, and COUSSY, O. (2000) *The role of water in alkali-silica reaction.* In: M. A. BÉRUBÉ, FOURNIER, B., DURAND, B., ed. 11th International Conference on Alkali-Aggregate Reactions in Concrete, Quebec, Canada, 61-69.
- LCPC (1994) *Recommandations pour la prevention des desordres dus a l'alkali-reaction.* Paris: Laboratoire Central des Ponts et Chaussées, 51.
- LINDGÅRD, J (2011) *RILEM TC 219-ACP: Literature survey on performance testing.* In: S. C. P. R. 27 (ed.). 85+appendices.
- LINDGÅRD, J, ANDIC-CAKIR, O, FERNANDES, I, RONNING, TF, and THOMAS, MDA (2012) *Alkali-silica reactions (ASR): Literature review on parameters influencing laboratory performance testing.* Cement and Concrete Research, 42, 223-243.
- LINDGÅRD, J, and HAUGEN, M (2006) *PARTNER report 3.1 - Experience from using petrographic analysis according to the RILEM AAR-1 method to assess alkali reactions in European aggregates.* SINTEF Report SBF52 A06019 / ISBN 82-14- 04079-5/978-82-14-04079-5.
- LINDGÅRD, J, NIXON, PJ, BORCHERS, I, SCHOUBORG, B, WIGUM, BJ, HAUGEN, M, and AKESSON, U (2010) *The EU "PARTNER" Project - European standard tests to prevent alkali reactions in aggregates: Final results and recommendations.* Cement and Concrete Research, 40, 611-635.
- LINDGÅRD, J, and WIGUM, B (2003) *Alkalireaksjoner i betong - feltefaringer.* SINTEF report, 129.
- LÓPEZ-BUENDÍA, A, CLIMENT, V, URQUIOLA, M, and BASTIDA, J. (2008) *Influence of dolomite stability on alkali-carbonate reaction.* In: M. A. T. M. BROEKMANS, and WIGUM, B. J., eds. 13th International Conference on Alkali-Aggregate Reactions in Concrete, Trondheim, Norway, 254-263.

- LU, D, FOURNIER, B, and GRATAN-BELLEW, P (2006) *Effect of aggregate particle size on determining alkali-silica reactivity by accelerated tests*. Journal ASTM International, 3, 11.
- MCGOWAN, JK, and VIVIAN, HE (1952) *Studies in cement-aggregate reaction: correlation between crack development and expansion of mortars*. Australian Journal of Applied Science, 3, 228-232.
- MIELLENZ, R (1946) *Petrographic examination of concrete aggregates*. Geological Society of America Bulletin, 57, 309-318.
- NB-21 (2008) *Durable concrete with Alkali Reactive Aggregates*. Norwegian Concrete Association, 15.
- NB-32 (2005) *Alkali-aggregate reactions in concrete, Test methods and Requirements to Test Laboratories*. Norwegian Concrete Association, 39.
- NIXON, P, HAWTHORN, F, and SIMS, I. (2004) *Developing an international specification to combat AAR proposals of RILEM TC 191-ARP*. In: M. TANG, and DENG, M., eds. 12th International Conference on Alkali-Aggregate Reaction in Concrete, Beijing, China, 8-16.
- NIXON, P, and LANE, S (2006) *PARTNER Report No. 3.3. Experience from testing of the alkali reactivity of European aggregates according to several concrete prism test methods*. SINTEF Report SBF52 A06021 / ISBN 82-14-04081-7 / 978- 82-14-04081-7, 35 + appendices.
- NIXON, P, LINDGÅRD, J, BORCHERS, I, WIGUM, B, and SCHOUENBORG, B. (2008) *The EU "PARTNER" project – European standard tests to prevent alkali reactions in aggregates - final results and recommendations*. In: M. BROEKMANS, and WIGUM, B., eds. 13th International Conference on Alkali-Aggregate Reaction in Concrete (ICAAR), Trondheim, 300-309.
- OBERHOLSTER, RE, and DAVIES, G (1986) *An Accelerated Method for Testing the Potential Alkali Reactivity of Siliceous Aggregates*. Cement and Concrete Research, 16, 181-189.
- PASSCHIER, CW, and TROUW, RAJ (2005) *Microtectonics*, Springer.
- PIKE, R (1967) *Pressures developed in cement pastes and mortars by the alkali-aggregate reaction* HRB Bull 172, 34-36.
- POOLE, AB (1992) *Introduction to alkali-aggregate reaction in concrete*. In: R. N. SWAMY (ed.) *The alkali-silica reaction in concrete*. London: Blackie and Son Ltd., 1-29.
- POWERS, T, and STEINOUR, H (1955a) *An interpretation of some published researches on the alkali-aggregate reaction. Part 1 – The chemical reactions and mechanisms of expansion*. Journal of American Concrete Institute, 51-26, 497-516.
- POWERS, T, and STEINOUR, H (1955b) *An interpretation of some published researches on the alkali-aggregate reaction. Part 2 – A hypothesis concerning safe and unsafe reactions with reactive silica in concrete*. Journal of American Concrete Institute, 51-40, 758-811.
- PREZZI, M, MONTEIRO, PJM, and SPOSITO, G (1997) *The alkali-silica reaction .I. Use of the double-layer theory to explain the behavior of reaction-product gels*. Aci Materials Journal, 94, 10-17.
- PRINCE, W, CASTANIER, G, and GIAFFERI, JL (2001) *Similarity between alkali-aggregate reaction and the natural alteration of rocks*. Cement and Concrete Research, 31, 271-276.
- RANDLE, V (1992) *Microtexture determination and its applications*, Great Britain, Bourne Press.
- RANDLE, V (2009) *Electron backscatter diffraction: Strategies for reliable data acquisition and processing*. Materials Characterization, 60, 913-922.
- RILEM-AAR-1 (2003) *Detection of potential alkali-reactivity of aggregates - Petrographic method, TC 191-ARP: Alkali-reactivity and prevention – Assessment, specification and diagnosis of alkali-reactivity, prepared by: Sims, I, Nixon, P, .* Materials and Structures, 36, 480-496.
- RILEM-AAR-2 (2000) *Detection of potential alkali-reactivity of aggregates - the ultra accelerated mortar bar test*. Materials and Structures, 33, 283-293.

- RILEM-AAR-3 (2000) *Detection of potential alkali-reactivity of aggregates: method for aggregate combination using concrete prisms*. Materials and Structures, 33, 209-293.
- RILEM-AAR-4.1 (to be published) *Detection of potential alkali-reactivity of aggregates. 60°C accelerated method for aggregate combinations using concrete prisms*, Committee Document RILEM /TC ACS/11/06. in preparation for publication in Materials and Structures.
- ROBIE, RA, HEMINGWAY, BS, and FISCHER, R (1978) *Thermodynamic properties of minerals and related substances at 298.15K and 1bar (10<sup>5</sup> Pascals) and at higher pressures and higher temperatures*. United States Geological Survey Bulletin 1452, 456.
- RODRIGUES, FA, MONTEIRO, P, and SPOSITO, G (1999) *The alkali-silica reaction. The surface charge density of silica and its effect on expansive pressure*. Cement and Concrete Research, 29, 527-530.
- RYKART, R (1995) *Quartz-Monographie*, Ott Verlag, Thun.
- SCHOUBENBORG, B, ÅKESSON, U, and LIEDBERG, L. (2008) *Precision trials can improve test methods for alkali aggregate reaction (AAR) – part of the PARTNER project*. In: M. A. T. M. BROEKMANS, and WIGUM, B. J., eds. 13th International Conference on Alkali-Aggregate Reaction in Concrete, Trondheim, Norway, 9.
- SHAYAN, A (1993) *Alkali-Reactivity of Deformed Granitic-Rocks - a Case-Study*. Cement and Concrete Research, 23, 1229-1236.
- SHAYAN, A (2007) *Field evidence for inability of ASTM C 1260 limits to detect slowly reactive Australian aggregates*. Australian Journal of Civil Engineering, 3, 13-26.
- SHAYAN, A, XU, A, and MORRIS, H (2008) *Comparative study of the concrete prism test (CPT 60°C, 100% RH) and other accelerated tests*. In: M. A. T. M. BROEKMANS, and WIGUM, B. J. (eds.) 13th International Conference on Alkali-Aggregate Reactions in Concrete. Trondheim, Norway, 391-400.
- SIEBEL, E, BOKERN, J, and BORCHERS, I (2006) *PARTNER Report No. 3.5. Field site tests sites established in the PARTNER project for evaluating the correlation between laboratory tests and field performance*. SINTEF Report SBF52 A06023 / ISBN 82-14-04083-3 / 978- 82-14-04083-3, 20 + appendices.
- SIMS, I, and BROWN, JM (1998) *Concrete Aggregates*. In: P. HEWLETT (ed.) *Lea's Chemistry of Cement and Concrete*. 4th edition ed. london: Arnold, 903-1011.
- SIMS, I, and NIXON, P (2003) *RILEM Recommended Test Method AAR-0: Detection of Alkali-Reactivity Potential in Concrete - Outline guide to the use of RILEM methods in assessments of aggregates for potential alkali-reactivity*. Materials and Structures, 36, 472-479.
- STANTON, T (1940) *Expansion of concrete through reaction between cement and aggregates*. Proceedings of the American Society of Civil Engineerings 66, 1781-1811.
- TANG, M (1981) *Some remarks about alkali-silica reactions*. cement and Concrete Research, 33, 208-219.
- THOMAS, M, FOURNIER, B, FOLLIARD, K, IDEKER, J, and SHEHATA, M (2006) *Test methods for evaluating preventive measures for controlling expansion due to alkali-silica reaction in concrete*. Cement and Concrete Research, 36, 1842-1856.
- THOMSON, ML, and GRATAN-BELLEW, PE (1993) *Anatomy of a Porphyroblastic Schist - Alkali-Silica Reactivity*. Engineering Geology, 35, 81-91.
- THOMSON, ML, GRATAN-BELLEW, PE, and WHITE, JC. (1994) *Application of microscopy and XRD techniques to investigate alkali-silica reactivity potential of rocks and minerals*. In: G. R. GOUDA, NISPEROS, A., BAYLES, J., ed. 16th International Conference on Cement Microscopy, Texas: International Cement Microscopy Association, 19.
- TI-B51 (1978) *Accelerated Method for Detection of Alkali-Aggregate Reactivities of Aggregates*. Cement and Concrete Research, 8, 647-650.
- UNDERWOOD, E (1970) *Quantitative stereology*, Addison-Wesley Publishing Company.

- WANG, H, and GILLOTT, JE (1991) *Mechanism of Alkali-Silica Reaction and the Significance of Calcium Hydroxide*. Cement and Concrete Research, 21, 647-654.
- WEST, G (1994) *Undulatory extinction of quartz in some British granites in relation to age and potential reactivity*. Quarterly Journal of Engineering Geology and Hydrogeology, 27, 69-74.
- WEST, G (1996) *Alkali-aggregate reaction in concrete roads and bridges*, London, Thomas Telford Publications.
- WIGUM, B, PEDERSEN, L, GRELK, B, and LINDGÅRD, J (2006) *PARTNER Report No. 2.1. State-of-the art report: Key parameters influencing the alkali aggregate reaction*. SINTEF Report SBF52 A06018 / ISBN 82-14-04078-7 / 978-82-14-04078-7, 55+appendices.
- WIGUM, BJ (1995) *Examination of microstructural features of Norwegian cataclastic rocks and their use for predicting alkali-reactivity in concrete*. Engineering Geology, 40, 195-214.
- WIGUM, BJ, HAGELIA, P, HAUGEN, M, and BROEKMANS, MATM. (2000) *Alkali aggregate reactivity of Norwegian aggregates assessed by quantitative petrography*. In: M. A. BÉRUBÉ, FOURNIER, B., DURAND, B., ed. 11th International Conference on Alkali-Aggregate Reactions in Concrete, Québec, 533-542.
- ZHANG, X, BLACKWELL, BQ, and GROVES, GW (1990) *The Microstructure of Reactive Aggregates*. British Ceramic Transactions and Journal, 89, 89-92.
- AARDT, JHPV, and VISSER, S (1977) *Calcium Hydroxide Attack on Feldspars and Clays - Possible Relevance to Cement-Aggregate Reactions*. Cement and Concrete Research, 7, 643-648.

## **Section of Original Papers**



**Grain size analysis of quartz in potentially alkali-reactive aggregates for concrete: a comparison between image analysis and point-counting**

*Authors: Nélia Castro, Børge J Wigum*

The candidate carried out the experimental work and wrote the paper. Ideas and the final manuscript were discussed with the supervisor and co-author Børge J Wigum.

*The paper was published in the proceedings of the 10<sup>th</sup> International Conference on Applied Mineralogy, Trondheim, Norway, August 2011, Springer Verlag, Heidelberg/berlin (2012), pp. 103-110.*



Is not included due to copyright



**Assessment of individual ASR-aggregate particles by XRD**

*Authors: Nélia Castro, Bjørn E Sorensen, Maarten ATM Broekmans*

The candidate wrote the paper and performed the petrographic analysis. XRD analyses were performed at the Department of Geology and Mineral Resources Engineering at NTNU by the candidate and the co-supervisor and second author Bjørn E Sorensen. EPMA analyses were performed by the technician at the Department of Materials Science and Engineering at NTNU in cooperation with the candidate and the co-supervisor and second author Bjørn E Sorensen. The XRF analysis was performed by the technician at the Department of Geology and Minerals Resources Engineering at NTNU, having the candidate followed the entire process. The ICP-MS analysis was performed by the technicians at the Norwegian Geological Survey. Ideas and the final manuscript were discussed with the co-supervisors and co-authors Maarten ATM Broekmans and Bjørn E Sorensen.

*The paper was published in the proceedings of the 10<sup>th</sup> International Conference on Applied Mineralogy (ICAM), Trondheim, Norway, August 2011, Springer Verlag, Heidelberg/berlin (2012), pp. 95-102.*

Is not included due to copyright



**Deleterious alkali-silica reaction in concrete: preliminary petrographical and microstructural characterisation of reacted and virgin materials from PARTNER project**

*Authors: Nélia Castro, Børge J Wigum, Maarten ATM Broekmans*

The candidate performed the experimental work and wrote the paper. Ideas and the final manuscript were discussed with the supervisor and co-author Børge J Wigum and with the co-supervisor and co-author Maarten ATM Broekmans.

*The paper was published in the proceedings of the 13<sup>th</sup> Euroseminar on Microscopy Applied to Building Materials, Ljubljana, Slovenia, September 2011, pp. 10.*



## DELETERIOUS ALKALI-SILICA REACTION IN CONCRETE: PRELIMINARY PETROGRAPHICAL AND MICROSTRUCTURAL CHARACTERIZATION OF REACTED AND VIRGIN MATERIALS FROM THE PARTNER PROJECT

Nélia Castro<sup>a</sup>, Børge J. Wigum<sup>a</sup>, Maarten A.T.M. Broekmans<sup>b</sup>

<sup>a</sup> Norwegian University of Science and Technology (NTNU), Department of Geology and Mineral Resources Engineering,  
Sem Sælands vei 1, N-7491 Trondheim, Norway, [nelia.castro@ntnu.no](mailto:nelia.castro@ntnu.no), [borge.j.wigum@ntnu.no](mailto:borge.j.wigum@ntnu.no)

<sup>b</sup> Geological Survey of Norway (NGU), Department of Industrial Minerals & Metals, PO Box 6315 Sluppen, N-7491  
Trondheim, Norway, [maarten.broekmans@ngu.no](mailto:maarten.broekmans@ngu.no)

### Abstract

Test methods to assess the potential reactivity of aggregate for concrete have been under development for several decades. Different European test methods were evaluated for their suitability for use with the wide variety of aggregates found across Europe in the EU-funded PARTNER project in 2002-2006. It was concluded that the accelerated mortar bar test (RILEM AAR-2) and the accelerated concrete prism test (RILEM AAR-4) are the most effective and have the best precision. It was found that the petrographic test (RILEM AAR-1) can potentially provide effective and reliable results quicker than other method, but with some limitations.

A variety of aggregate materials from European resources have been expansion-tested in the PARTNER project. This study uses available post-mortem expansion-test specimen and virgin aggregate from PARTNER, to investigate a number of properties and qualities of silica minerals that can contribute to its dissolution in "Alkali Silica Reaction (ASR) environment". Results from detailed petrography and preliminary results from grain size analyses of quartz are reported in this paper.

**Keywords:** ASR, aggregates for concrete, petrography, image analysis

### Introduction

This paper presents results from petrography and preliminary results from grain size analyse of quartz in post-mortem expansion-test specimen and virgin aggregate from PARTNER project. This study is part of a project that rose from the interest of applying geology knowledge and techniques to the study of the properties and qualities of the silica minerals that contribute to the alkali-reactivity of the aggregates for concrete. The aim of the project is to study the relationship between aggregate petrological properties and expansion test results. Mineralogical, geochemical and microstructural characteristics of reactive quartz in aggregate, with focus on the properties and qualities of silica minerals that can contribute to its dissolution in "Alkali Silica Reaction (ASR) environment", will be investigated. Results from expansion testing will provide a better knowledge of aggregate properties and performance in concrete and consequently a better understanding of the ASR mechanism. Full theoretical understanding on this very complex field is beyond the scope of this project. However, the findings of the project are intended to provide suggestions to the introduction of quantitative parameters in the petrographic test method (RILEM AAR-1) which can improve its accuracy and reproducibility, and contribute to a better understanding of the expansion tests.

Though the exact mechanism of ASR is a matter of dispute, there is general consensus that at some point the mechanism involves silica dissolution. A range of properties and qualities are known to affect the dissolution of quartz under geological conditions, and some may apply to 'ASR conditions' at pH14 and ambient temperature. Some quartz properties are relatively easy to assess, others require more specialized instrumentation or equipment. A summary of some fundamental considerations with respect to the solubility of silica minerals under geological and under ASR conditions can be found in Broekmans (1999, and 2004).

Test methods to assess the ASR-potential of aggregate for use in concrete have been under development for several decades. However, none of the accepted current methods actually assess aggregate properties in terms of 'quartz solubility under ASR conditions'. In nearly all tests, aggregate is exposed to severe conditions (eg. 1N NaOH, 38-60-80°C and up) to provoke expansion within acceptable time (i.e. weeks) for the building and construction industry.



Different European test methods were evaluated for their suitability for use with the wide variety of aggregates found across Europe in the EU-funded PARTNER project in 2002-2006. The project had 24 partners from 14 countries and 22 different types of aggregates from 10 countries were tested. In total 413 tests were performed within PARTNER project. Final results are published in Nixon *et al.* (2008) and Lindgård *et al.* (2010), additional data are to found in Grelk (2006), Jensen (2006), Lindgård & Haugen (2006), Nixon & Lane (2006), Siebel *et al.* (2006), Wigum *et al.* (2006), GBS (2006), Haugen *et al.* (2008), Borchers & Müller (2008), and Schouenborg *et al.* (2008). The overall experience from the PARTNER project is that in most cases the RILEM tests could successfully identify the reactivity of the aggregates tested. They were most successful with normally reactive and non-reactive aggregates. With aggregates that react very slowly, an extended test period may be necessary for some of the RILEM methods. It was concluded that the accelerated mortar bar test (RILEM AAR-2) and the accelerated concrete prism test (RILEM AAR-4) are the most effective and have the best precision. It was found that the petrographic test (RILEM AAR-1) can potentially provide effective and reliable results quicker than other method, but with some limitations. In the petrographic test (RILEM AAR-1) the aggregates are classified as potentially reactive or potentially innocuous based on their nomenclature. This method does not attempt to quantify the actual amount of reactive constituents in an aggregate but rather identify/quantify rock types that have proven to be susceptible to ASR in practice. Precision trials to this method carried out by PARTNER project determined that the identification of the rocks and minerals is similar, but the classification of the degree of alkali silica reactivity varies a great deal, probably due to the regional experience (Schouenborg, 2008; Lindgård *et al.*, 2010). The results confirm that the accuracy and reproducibility of the petrographic method strongly depends of the experience and expertise of the petrographer.

The project that originated this paper uses available post-mortem expansion-test specimen and virgin aggregate from PARTNER, including “normally” reactive (those that react in a time scale of 5 to 20 years), “slowly” reactive (those that react in a time scale greater than 15-20 years), and non-reactive aggregates. This allows the systematic comparison between reactive and non-reactive aggregates, and reactive aggregate particles with their virgin counterparts, using a range of techniques for later correlation with expansion tests. A first assessment by detailed petrography was essential to identify reactive aggregate particles and select the properties and qualities of silica minerals that can contribute to it dissolution in “ASR-environment” relevant to investigate in the scope of the project. This paper reports results from petrography and discusses the importance that this first assessment represented in the development of the project. Additionally, preliminary results from grain size analysis of quartz are also reported.

## Materials

This study uses available post-mortem expansion-test specimen and virgin aggregate from PARTNER project, for mineralogical and chemical characterization of reactive constituents. A total of 22 post-mortem expansion-tests specimens and 3 virgin aggregate samples were used in the present work. These samples represent 14 different aggregate types from 8 different European countries (Table 1), including 6 “normally” reactive, 5 “slowly”, and 3 non-reactive aggregates. In total 13 combinations of aggregates were tested in the 22 concrete prisms: 3 combinations with the AAR-3 method, 12 combinations with the AAR-4 method and 7 combinations with the German method (Table 1). The 3 virgin aggregate investigated correspond to the aggregates F2, G1 and It2.

## Petrography

### Introduction

All post-mortem expansion-test specimen and virgin aggregate were investigated with petrography. Main focus was given to the identification of potentially reactive particles of aggregate that could be suitable to further characterization by analytical techniques of petrography and mineralogy.

### Methods for assessment and analysis

Two sections ~20 mm were cut off from each post-mortem expansion-test specimen. One section was impregnated with fluorescence epoxy and polished according to Danish standard DS 423.39 (2002) with minor adaptations, while the other remained unprepared. Both sections were observed in a stereomicroscope Wild Leitz Heerbrugg using incident normal and fluorescent illumination in order to identify signs of AAR and potentially reactive aggregate particles. Impregnated polished thin sections were prepared from the unprepared section using standard procedures (e.g. Humphries, 1992). Thus the thin-sections were analysed under a Nikon Eclipse E600 microscope using transmitted illumination in plane-polarized light (PPL), cross-polarized light (XPL), and incident fluorescent illumination (FL).

Virgin aggregate material was weighed and washed. The particles were counted and separated by lithology using a stereomicroscope Wild Leitz Heerbrugg. Polished thin sections of potentially alkali-reactive

lithologies as well as some unidentified particles were prepared using standard procedures (e.g. Humphries, 1992). Thus the thin-sections were analysed in a Nikon Eclipse E600 microscope using transmitted illumination in plane-polarized light (PPL) and cross-polarized light (XPL).

**Table 1:** List of the 14 aggregate samples and 13 combinations of aggregates represented by the 22 post-mortem expansion-test specimens used in this project and respective results in the expansion test method (adapted from Nixon *et al.*, 2008 and Lindgård *et al.* 2010).

Aggregate / country	Fraction / Combination	Expansion test method		
		AAR-3	AAR-4	German
<b>“Non-reactive” aggregates</b>				
F1 - France	C + NRF		NR	NR
F2 - France	C + RF		NR/MR?	
	C + F		NR	NR
F3 - France	C + F		NR	
N3 - Norway	NRF			
S1 - Sweden	C + F		MR	
<b>“Normally” reactive aggregates</b>				
B1 - Belgium	C + F	R	R	R
D1 - Denmark	C + F		NR	NR
D2 - Denmark	RF			
G1 - Germany	C + NRF		R	R
N1 - Norway	C + NRF	R	R	R
UK1 - United Kingdom	C + F			R
<b>“Slowly” reactive aggregates</b>				
It2 - Italy	C + F		R	
N4 - Norway	C + F		R	
N5 - Norway	C + F	MR	R	

F = fine aggregate; C = coarse aggregate

NRF = non-reactive fine aggregate (=N3F); RF = reactive fine aggregate (=D2)

R = reactive (according to the critical limits in the different testing methods); NR = non-reactive (according to the critical limits in the different testing methods); MR = marginally reactive (i.e. expansions just above the critical limits in the different testing methods)

## Results

Table 2A, 2B and 2C summarize petrography results to “Non-reactive” aggregates, “Normally” reactive aggregates and “Slowly” reactive aggregates respectively. The results reflect the observations made during petrography of post-mortem expansion-test specimen and virgin aggregate with focus to the identification of potentially reactive particles within each aggregate.

Petrography results show two different groups of potentially reactive rocks among the studied samples. One group composed by so-called “slowly-reactive” rock types, like gneiss, rhyolite, granite, cataclastite, greywacke, and quartzite, that correspond to the aggregates N3, S1, N1, UK1, It2, N4, and N5. One group composed of flint/chert and silicified limestone, rock types usually described as fast reactive, that correspond to the aggregates F1, F3, B1, D1, D2, and G1. No reactive particles were identified in the aggregate F2.

**Table 2A:** Summary of petrography results for “Non-reactive” aggregates with focus to the identification of potentially reactive particles within each aggregate. These results reflect the observations made in post-mortem expansion-test specimen and virgin aggregate.

Aggregate country	Brief description	Potentially reactive lithologies
<i>“Non-reactive” aggregates</i>		
F1 - France	Polymictic river gravel mainly composed by flint/chert. Other rock types observed include silicified limestone, mudstone, and greywacke. Alkali-silica gel observed in some thin-sections associated with flint/chert-flint/chert particles.	Flint/chert
F2 - France	This aggregate contains several types of limestones. These include: mudstone, wackestone, packstone and grainstone. Braquiopode and foraminifera fossils, ooids and peloids are frequently observed. No signs of AAR reaction were observed.	None
F3 - France	Polymictic gravel from Rhine valley. Rock types observed include: flint/chert, silicified limestone, granite, sandstone, greywacke, quartzite, rhyolite. Alkali-silica gel was found in 2 of 7 thin-sections associated with porous flint/chert particles.	Flint/chert (silicified limestone, greywacke, sandstone, quartzite, rhyolite)
N3 - Norway	Natural sand from a glaciofluvial deposit. Consists mainly of monomineralic particles of quartz and rock fragments of granite and gneiss. No alkali-silica gel was found associated with this aggregate.	Gneiss (granite)
S1 - Sweden	Polymictic glaciofluvial gravel and sand. Rock types identified include: rhyolite (meta-rhyolite), granite, ganodiorite, gabbro, basalt. Alkali-silica gel was found partly filling an air void in 1 of 3 thin-sections, apparently associated with a very altered fragment of rock (basalt ?).	Rhyolite (meta-rhyolite) Granite (strained quartz and sub-granulation)

**Table 2B:** Summary of petrography results for “Normally” reactive aggregates with focus to the identification of potentially reactive particles within each aggregate. These results reflect the observations made in post-mortem expansion-test specimen and virgin aggregate.

Aggregate country	Brief description	Potentially reactive lithologies
<i>“Normally” reactive aggregates</i>		
B1 - Belgium	This aggregate contains several types of silicified limestones (mudstones, wackestones and packstones) with fossils (foraminifera). Alkali-silica gel was found in all the thin-sections.	Silicified limestone
D1 - Denmark	Glaciofluvial sand/gravel containing: flint/chert (some particles are dense while others are partly porous), silicified limestone, greywacke, quartzite, granite, gneiss, and mafic rocks. Alkali-silica gel was found filling cracks and air voids almost always associated with flint/chert particles.	Flint/chert (silicified limestone, greywacke, quartzite, gneiss)
D2 - Denmark	Sea dredged, polymictic gravel originally derived from glaciofluvial sediments. This aggregate is mainly composed of monomineralic particles of quartz and feldspar. Among the rock types identified the most abundante is flint/chert. Other rock types identified include: quartzite, granite, sandstone, and gabbro. Alkali-silica gel is found frequently associated with flint/chert particles.	Flint/chert
G1 - Germany	Partly crushed polymictic river gravel from upper Rhine valley. This aggregate presents considerable variation in constituent lithologies. Observed rock types include: flint/chert, silicified limestone, quartzite, sandstone, greywacke, granite, and mafic rocks. Alkali-silica gel is frequently observed in cracks and air voids associated with several rock types but more frequently with flint/chert, silicified limestone and sandstone.	Flint/chert Silicified limestone Sandstone
N1 - Norway	This aggregate is mainly composed of cataclasite. Other rock types observed include: granite and mylonite. Alkali-silica gel is found frequently in cracks and air voids associated with cataclasite particles.	Cataclasite
UK1 - United Kingdom	This aggregate is mainly composed by greywacke. Other lithologies observed include: sandstone, siltstone, mudstone, and basalt. Alkali silica gel was found in cracks and air voids associated with greywackes in all the thin-sections.	Greywacke

**Table 2C:** Summary of petrography results for “Slowly” reactive aggregates with focus to the identification of potentially reactive particles within each aggregate. These results reflect the observations made in post-mortem expansion-test specimen and virgin aggregate.

Aggregate country	Brief description	Potentially reactive lithologies
<i>“Slowly” reactive aggregates</i>		
It2 - Italy	Polymictic river gravel mainly composed by quartzite. Other lithologies observed include: gneiss, granite, flint/chert, gabbro, and eclogite. Alkali-silica gel can be found in cracks and air voids mainly associated with quartzite and gneiss particles.	Quartzite Gneiss
N4 - Norway	Natural gravel/sand from a moraine deposit. Rock types observed in this aggregate include: sandstone, siltstone, cataclasite, quartzite, granite, gneiss, gabbro, basalt. Alkali-silica gel was observed in cracks and air voids associated with particles of cataclasite, sandstone and quartzite.	Cataclasite Sandstone Quartzite
N5 - Norway	Sand/gravel from a glaciofluvial deposit mainly composed by quartzite. Other rock types identified include: rhyolite, granite, gneiss, sandstone. Alkali-silica gel is found partly and/or totally filling cracks and air voids usually associated with quartzites and rhyolites.	Quartzite Rhyolite

### Discussion

The alkali-reactivity of crystalline-quartz bearing rock types such as gneiss, rhyolite, granite, cataclasite, greywacke, and quartzite, is usually associated with the presence of strained, microcrystalline or cryptocrystalline quartz. Igneous and metamorphic quartz-bearing rocks affected by deformation processes are used as aggregates for concrete in many countries due to regional geological settings. Kerrick & Hooton (1992) studied granitic rocks from Eastern United States. They concluded that not only the microcrystalline quartz, which was formed by recrystallisation, but also textural properties of the rocks, influence their alkali reactivity. Identical results were obtained by Shayan (1993) with granitic rocks from Western Australia. Extensive work with granitic aggregates was also developed in Portugal (e.g. Fernandes, 2005; Fernandes *et al.*, 2004, 2007; Castro, 2008; Castro *et al.*, 2009). Virgin aggregate material and concrete samples from real structures such as dams and bridges were used in these studies. The overall conclusion is that microstructural characteristics, such as development of subgrains and recrystallisation of quartz, rather than the petrographic classification determine the reactive behaviour of granitic aggregates for concrete in Portugal. A recent study of Locati *et al.* (2010) with orthogneisses, mylonites and cataclasites from Argentina consider the reactivity of mylonites increased by ~30% to ~97% with respect to the non-mylonitised sample due to increment of the strained quartz content and subgrain development, grain size reduction and formation of glassy material.

In the present study, igneous and metamorphic quartz-bearing rocks rock types such as quartzite, gneiss, cataclasite and rhyolite show different microstructural characteristics such as strained quartz, subgrain development (Fig. 1), microcrystalline or cryptocrystalline quartz (Fig. 2).

A number of methods have been suggested that correlate microstructural characteristics of the aggregate with the expansion observed in concrete. One of the first methods suggested was the undulatory extinction angle of strained quartz. Gogte (1973), Dolar-Mantuani (1981) and West (1991, 1994) have developed and used different versions of this method to establish a correlation between the undulatory extinction angle and mortar bar expansion tests. However, many other researchers (e.g. Grattan-Bellew, 1986, 1992; French, 1992) have questioned the method. Based on the concept that the free energy of quartz, which determines its solubility and hence its potential alkali reactivity, is related to its degree of crystallinity, some authors (e.g. Thomson & Grattan-Bellew, 1993; Thomson *et al.*, 1994; Wigum, 1995; Broekmans, 2004) tried to establish a correlation between the Crystallinity Index (Murata & Norman, 1976) and expansion in concrete. It was expected that higher Crystallinity Index values would be associated with lower expansion in concrete. Although the proposed method works in principle, no correlation has been established and therefore no conclusion on the reability of the method has been drawn. Wigum (1995) showed a direct relationship between the expansion after 14 days of some mylonites, granites and gneisses and: 1) the inverse of the mean grain size,  $d_{50}$ ; 2) the total grain boundary area of quartz. Wigum *et al.* (2000) analysed more samples including different rock types and observed the same trend.

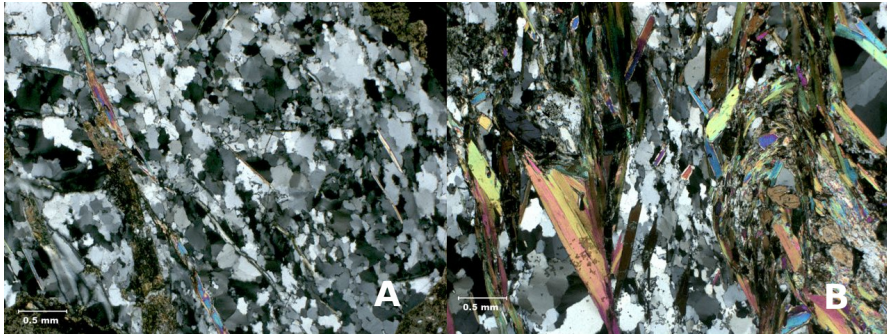


Figure 1: Example of strained quartz with subgrain development in: A) quartzite; B) gneiss. Both images are from It2 aggregate and were taken in cross-polarized light (XPL).

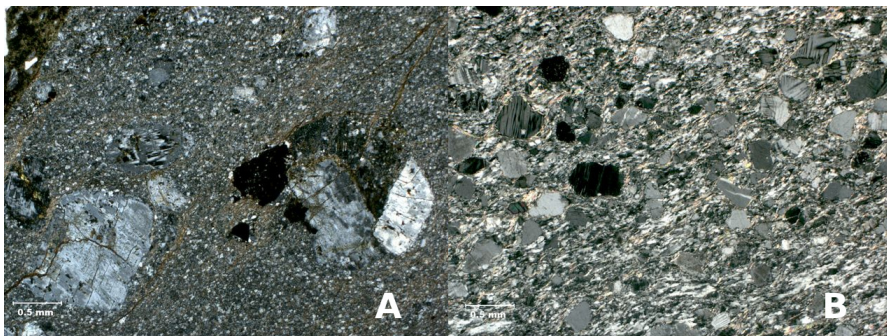


Figure 2: Example of microcrystalline and cryptocrystalline quartz in: A) rhyolite from S1 aggregate. B) cataclasite from N4 aggregate. Both images in cross-polarized light (XPL).

On the other hand, it is generally accepted that the alkali-reactivity of rock types such as flint/chert and silicified limestones is related to the presence of amorphous, disordered or poorly-crystalline forms of silica minerals. Petrography studies on altered flint/chert aggregate by Bulteel *et al.* (2004), showed an increase aggregate porosity and revealed internal degradation of the aggregate that created amorphous zones due to ASR. The appearance of amorphous zones and penetration of positive ions into the aggregate are correlated with the increase in the molar fraction of silanol groups (Bulteel *et al.* 2004; Verstraete *et al.*, 2004). This degradation is specific to the ASR. In the present study, as in Bulteel (2004) it was observed that flint/chert aggregates show heterogeneous behaviour towards the ASR. Different grains can have different alteration levels from dark spots to corroded appearance (Fig.3) and some grains remain unaltered (Fig. 4). It is a question worth to investigate if the heterogeneous behaviour of flint/chert aggregates towards the ASR can be justified by a different mineralogical composition of the particles. One of the prime issues pointed out in Broekmans (1999, 2004) is that different silica polymorphs have different dissolution rates. The polymorph in which silica occurs plays a dominant role in determining the potential alkali-reactivity of the aggregate, with disordered structures more reactive than structures containing cristobalite, which are in turn more reactive than structures containing quartz (Zhang, 1990). It is also important to investigate if this heterogeneous behaviour of flint/chert aggregates towards the ASR is due to differences in porosity between particles. As a general rule, aggregates with higher porosity show higher reactivity because the access to pore fluids is easier (e.g. Bulteel *et al.*, 2004).

Another interesting fact shown by petrography results is that flint/chert is not only found in the aggregates classified as “Normally” reactive in PARTNER project, but also in aggregates classified as non-reactive. This can be explained by the fact that pure reactive siliceous aggregates such as flint/chert have a “pessimum” effect, as defined by Hobbs (1988). For a given level of alkalis, the expansion of concrete increases with the reactive aggregate content to reach a “maximum” value. For aggregate content superior to the “maximum”, the expansion decreases due to an excess of reactive silica. Concretes based on both coarse and fine aggregate of reactive flint/chert usually do not swell.



A recent investigation by Garcia-Diaz *et al.* (2010) with siliceous limestones concluded that contrary to the pure siliceous aggregates, the content in reactive silica of siliceous limestones is too low to consume a maximum of alkalis in non-expansive adsorption process and to obtain non-expansive concretes.

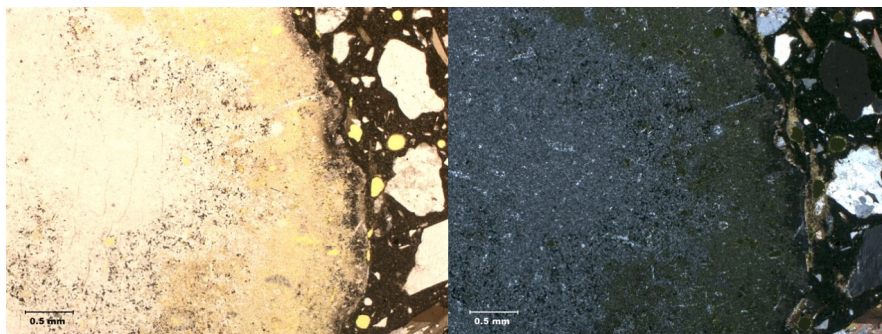


Figure 3: Example of flint/chert grain with corroded appearance from aggregate sample F1. Image on the left hand side in plane-polarized light (PPL), image on the right hand side on cross-polarized light (XPL).

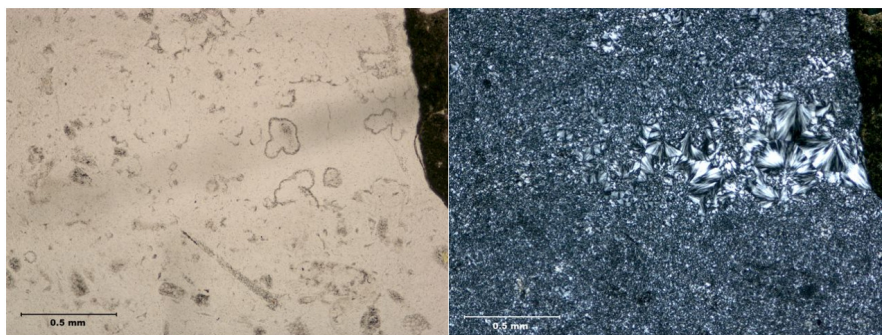


Figure 4: Example of flint/chert grain that remain unaltered from aggregate F1. Image on the left hand side in plane-polarized light (PPL), image on the right hand side on cross-polarized light (XPL).

Based on petrography observations, a number of properties and qualities of silica minerals that can contribute to its dissolution in “ASR-environment” raised the interest of the authors in the scope of the project:

- Grain size analysis of quartz
- Presence of different silica polymorphs
- Quality of the crystal lattice
- Presence of foreign species in the solid silica (e.g. trace elements)
- Presence of hydrous species in the solid silica

Petrography results show two different groups of potentially reactive rocks among the studied samples, one group composed by so-called “slowly-reactive” rock types, and one group composed by rock types usually described as fast reactive. The fact that the alkali reactivity of each group of potentially reactive rocks is explained by different mechanisms was taken into account in the selection of the properties and qualities of silica minerals to be investigated in each aggregate among the studied samples. Wigum (1995) and Wigum *et al.* (2000) showed a direct relationship between the expansion after 14 days of some “slowly-reactive” rock types and: 1) the inverse of the mean grain size,  $d_{50}$ ; 2) the total grain boundary area of quartz. Therefore, in the scope of this project, grain size analysis of quartz will be performed to the aggregates composed by so called “slowly-reactive” rock types, like gneiss, rhyolite, granite, cataclasite, greywacke, and quartzite in order to investigate if the same trend was observed. On the other hand, it is generally accepted that the alkali-reactivity of fast reactive rock types is related to the presence of amorphous, disordered or poorly-crystalline forms of silica minerals. Therefore, the presence of different silica polymorphs will be investigated in the aggregates containing fast reactive rock types such as flint/chert and silicified limestone.

## Grain size analysis of quartz

### Introduction

Quantitative petrographic examination of potentially alkali-reactive aggregates, based on grain size analysis by point-counting method, has shown that a relationship does exist between the total grain boundary of quartz and expansion results from accelerated mortar bar testing (Wigum 1995, Wigum *et al.*, 2000). In Wigum's method an automatic point-counter was used to measure quartz grains, including subgrains, along lines in the thin-section. Approximately 200 points for each thin-section were counted. In the case of foliated rocks with elongated quartz grains, the lines were measured 45° to the parallel foliation of the rock. As a measurement of the grain size, the length of a quartz grain laying at the line was used. Those measurements were then used to calculate the mean grain size of quartz and the total grain boundary of quartz.

In this paper the authors performed quantitative petrographic examination of potentially alkali-reactive aggregates, based on grain size analysis by image analysis, to a number of samples. In order to validate the method a comparative study between point-counting and image analysis results for the same samples was performed (Castro and Wigum, 2011). This comparative study revealed that image analysis can be more time efficient than point-counting without compromising the accuracy of the results.

### Methods for assessment and analysis

Aggregates N3, S1, N1, UK1, It2, N4, and N5 were selected for grain size analysis of quartz by thin-section petrography of post-mortem expansion-test specimen and virgin aggregate. Potentially reactive particles identified include gneiss, rhyolite, granite, cataclasite, greywacke, and quartzite.

The Lazy Grain Boundary (LGB) method (Heilbronner, 1999 and 2000), was used for creating grain boundary maps of the quartz contained in the selected aggregates. The LGB method is based on a set of macro commands programmed for Image SXM, a public domain image processing and analysing software. The procedure makes use of multiple input images. Sets of input images composed by six polarization micrographs: six images with crossed polarizers and  $\lambda$ -plate rotated 0°, 30°, 60°, 90°, 120°, 150°, were obtained in a Leica DM 2500P polarizing microscope with a Jenoptik ProgRes digital camera system (Figure 5). The number of input images needed to each sample depends upon the homogeneity/heterogeneity of the rock, the grain size of the rock and the number of grains that is necessary to analyse. Most of the sets were subjected to LGB procedure in a completely automatic way, but a few had to be subjected to an interactive process where the LGB procedure was not carried though in a fully automatic fashion (Figure 6). Instead, at some steps of the procedure, corrections were applied using the pencil tool or the block eraser. After segmentation, the grain boundary maps were saved, the particles analyzed and the resulting measurement files, listing the pixel values of the major and minor axis, the cross-sectional areas and perimeters of each grain, exported and saved.

A spread-sheet program was used to calculate the mean grain size of quartz and total grain boundary area of quartz, following the same assumptions and procedures as Wigum (1995) with minor changes. For measurement of the mean grain size of quartz, the  $d_{50}$  (mm) read from the cumulative particle size distribution curve was used. In order to estimate the total grain boundary area of quartz, each grain, including subgrains, was assumed to be cubic in shape. The average surface area and the number of grains that could be contained in 1 cm<sup>3</sup> were calculated to each fraction in the grading, using the average grain size of the respective fraction, and multiplied by the fraction frequency. This was done for all the fractions in the grading and all results summed up in order to obtain the grain boundary area for the entire grading. By multiplying this grain boundary area by the quartz amount in the rock, an estimate for the total grain boundary area of quartz (m<sup>2</sup>/cm<sup>3</sup>) in each sample was achieved.

### Discussion of the preliminary results

Only a limited number of results have at this stage been obtained for grain size analysis of quartz. Grain size maps and the respective grain size analysis have been performed to a number of samples with different grades of deformation. Rocks with higher grades of deformation, such as cataclasite, reveals a larger total grain boundary area of quartz than rocks with less deformation, such as granites. This is in agreement to the results of Wigum (1995) and Wigum *et al.* 2000. However, more samples need to be analysed to have a representative statistical study. In addition to the grain size analysis, the authors are attempting to perform shape analysis to the same samples. The deformation degree of the rock will be reflected in the shape of its quartz grains. As result of increasing deformation, the shape of quartz grains tends to be more irregular and elongated. Image analysis give us the unique opportunity of using the same sets of input images that are used to grain size analysis to subsequent investigation of grain shape. All the parameters will be compared against expansion test results in order to verify if there is a correlation between the different parameters and the reactivity of the aggregates.

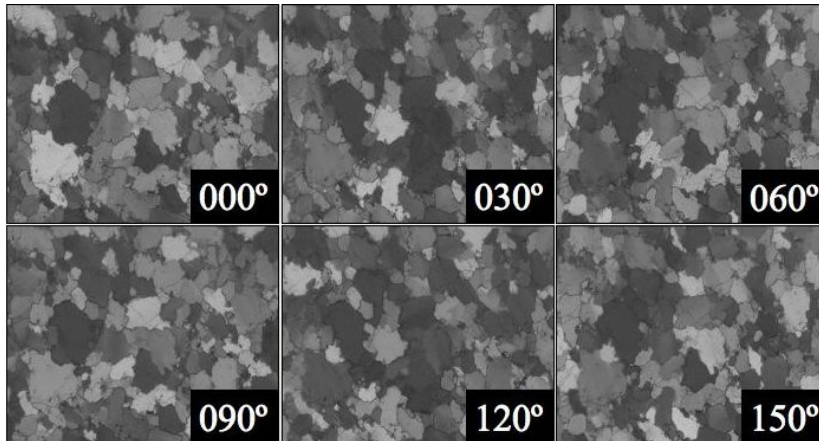


Figure 5: Example set of input images composed by six images with crossed polarizers and  $\lambda$ -plate rotated 0°, 30°, 60°, 90°, 120°, 150°.

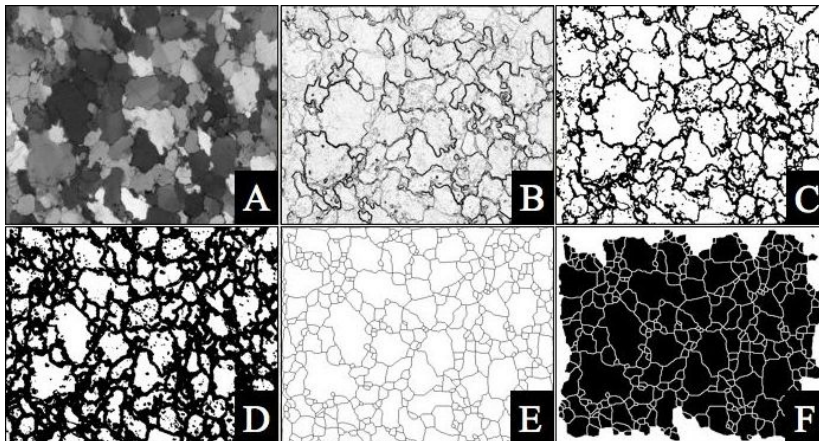


Figure 6: Schematic representation of automatic image segmentation using the LHB macro for Image SXM. (A) stack of input images (detail of last slice of stack), (B) images of the stack are segmented individually with an edge detection filter, (C) images of the stack are thresholded, (D) segmented images of the stack are combined into one image, (E) further segmentation and skeletonization is performed, (F) fully segmented grain boundary map.

### Future work

This paper presents results from petrography and preliminary results from grain size analysis of quartz in post-mortem expansion-test specimen and virgin aggregate from PARTNER project.

Petrography results show two different groups of potentially reactive rocks among the studied samples. One group composed by so-called “slowly-reactive” rock types, like gneiss, rhyolite, granite, cataclasite, greywacke, and quartzite. One group composed of flint/chert and silicified limestone, rock types usually described as fast reactive, that correspond to the aggregates. No reactive particles were identified in one of the aggregates. Based on petrography observations, a number of properties and qualities of silica minerals that can contribute to its dissolution in “ASR-environment” raised the interest of the authors.

Preliminary results of grain size analysis of quartz presented on this paper show that rocks with higher grades of deformation, such as cataclasite, reveals a larger total grain boundary area of quartz than rocks with less deformation, such as granites. This is in agreement with the results of Wigum (1995) and Wigum *et al.* 2000. Further work will be focus on the grain size analysis of quartz in more samples, including different rock types, and in the investigation of a correlation between other parameters, like grain shape, and the reactivity of the aggregates.



The presence of silica polymorphs will be investigated in aggregates containing fast reactive rock types such as flint/chert and silicified limestone. Zhang (1990) defend that the phase in which silica occurs plays the dominant role in determining the reactivity, with disordered structures more reactive than structures containing cristobalite, which are in turn more reactive than structures containing quartz. On the other hand, SiO<sub>2</sub> species like opal and chalcedony are of particular interest with respect to the AAR. Applying the appropriate nomenclature to fine grained silica varieties is complicated. For instance chert and chalcedony once were considered microcrystalline varieties of quartz, but it is now clear that these authigenic species represent nanoscale intergrowths of quartz and a metastable silica polymorph called moganite (Flörke *et al.*, 1991). The respective volume of quartz and moganite and the degree of misorientation between domains are thought to affect the dissolution of this type of silica and may also explain the variation in reference values for the solubility of chalcedony (Knauth, 1994). By investigating the presence of different silica polymorphs in samples of flint/chert and silicified limestone the authors aim to understand better the heterogeneous behaviour of these rock types towards the ASR.

Future work will also focus on the quality of the crystal lattice of quartz, the presence of foreign species in the solid silica, and the presence of hydrous species in the solid silica, since all these parameters can reflect a certain degree of deformation or distortion of the ideal crystallographic structure of quartz that will affect its solubility. As pointed out by Broekmans (2004), chemical impurities and foreign ions, including water and silanol groups, tend to associate with dislocations, vacancies and other structural irregularities in quartz, providing easy access for attack by chemical and/or physical forces. Within a dislocation (like a grain boundary or a crack) and in a small volume embedding the dislocation, the crystal lattice is distorted and deviates from the ideal quartz structure, which will facilitate the attack of the aggressive media. Thus, the solubility of quartz at dislocation arrays including grain boundaries is increased, which shows the importance of the investigation of the quality of the crystal lattice of quartz in the scope of this project.

Though the crystal lattice of quartz is very rigid and doesn't easily accommodate ions of deviating size, replacement is possible in minor amounts and specific locations. Most common replacements for Si<sup>4+</sup> are Al<sup>3+</sup> and Fe<sup>3+</sup>, leaving uncompensated charges in the structure. To maintain electrical balance, small monovalent cations like H<sup>+</sup>, Li<sup>+</sup>, Na<sup>+</sup> and/or K<sup>+</sup> enter the quartz structure in interstitial spaces (Kronenberg, 1994). The same author refers that one other way to replace silicium in quartz is by a silanol group. According to Dove and Rimstidt (1994), all kinds of impurities do have an enhancing effect upon the solubility of quartz. The same authors have also proved that quartz containing water has increased solubility.

A better knowledge of the properties and qualities of silica minerals that can contribute to its dissolution in "ASR-environment" is essential to improve the actual knowledge about the AAR mechanisms and the test methods used to evaluate the reactivity of the aggregates for concrete.

### Acknowledgements

The first author wishes to acknowledge financial support from Fundação para a Ciência e Tecnologia (FTC/Portugal) through doctoral grant reference SFRH/BD/41810/2007.

### References

- Borchers, I, Müller, C (2008): Field site tests established in the PARTNER project for evaluating the correlation between laboratory tests and field performance, in: Broekmans, MATM, Wigum, BJ (Editors), Proceedings of the 13<sup>th</sup> International Conference on Alkali-Aggregate Reaction in Concrete, Trondheim, CD-ROM, pp 10.
- Broekmans, MATM (1999): Classification of the alkali-silica reaction in geochemical terms of silica dissolution. In: Pietersen, H, Larbi, J, and Janssen, H (Editors): Proceedings of the 7th Euroseminar on Microscopy Applied to Building Materials, Delft: 155-170.
- Broekmans, MATM (2004): Structural properties of quartz and their potential role for ASR. *Materials Characterization* (53): 129-140.
- Bulteel, D., Rafai, N., Degrugilliers, P., Garcia-Diaz, E. (2004): Petrography study on altered flint aggregate by alkali-silica reaction, *Materials Characterization* (53): 141-154.
- Castro, N. (2008): Granitic aggregates for concrete. Attempt of correlation between the granite age and the potential reactivity to alkalis of concrete. Master thesis, Faculty of Sciences of University of Porto, Portugal, pp 122.

- Castro, N., Fernandes, I., Santos Silva, A. (2009): Alkali reactivity of granitic rocks in Portugal: a case study, In: Bernhard, M.; Just, A.; Klein, D.; Glaubitt, A.; Simon, J. (Editors), Proceedings of the 12<sup>th</sup> Euroseminar on Microscopy Applied to Building Materials Dortmund, Germany, pp 11.
- Castro, N., Wigum, B.J. (2011): Grain size analysis of quartz in potentially alkali-reactive aggregates for concrete: a comparison between image analysis and point-counting. In: Broekmans, MATM (Editor in chief) Proceeding of the 10<sup>th</sup> International Conference on Applied Mineralogy, Trondheim, Norway, 1-5 August 2011 (unpublished).
- Danish Standards Association (2002): Testing of concrete – Hardened concrete – Production of fluorescence impregnated plane sections (in Danish). DS 423.39.
- Dolar-Mantuani, L. (1981): Undulatory extinction in quartz used for identifying potentially alkali-reactive rocks, In: Oberholster, R.E. (Editor), Proceedings of the 5<sup>th</sup> International Conference on Alkali-aggregate Reaction in Concrete, Cape Town, National Building Research Institute Pretoria, paper S252/36.
- Dove, P.M., Rimstidt, J.D. (1994): Silica-water interactions. In: Heaney, P.J., Prewitt, C.T., and Gibbs, G.V. (editors), Silica: physical behaviour, geochemistry and materials applications. Reviews in Mineralogy (29): 259-308.
- Fernandes, I. (2005): Caracterização petrográfica, química e física de agregados graníticos em betões. Estudo de casos de obra., PhD Thesis, Faculdade de Ciências da Universidade do Porto, Portugal, pp 334.
- Fernandes, I., Noronha, F. e Teles, M. (2004): Microscopic analysis of alkali-aggregate reaction products in a 50-year-old concrete, Materials Characterization, Vol. 53, Issues 2-4, Elsevier: 295-306.
- Fernandes, I., Noronha, F. e Teles, M. (2007): Examination of the concrete from an old Portuguese dam. Texture and composition of alkali-silica gel, Materials Characterization, Vol. 58, Issues 11-12, Elsevier: 1160-1170.
- Flörke, O.W., Graetsch, H., Martin, B., Röller, K., and Wirth, R. (1991): Nomenclature of micro- and non-crystalline silica minerals, based on structure and microstructure. Neues Jahrbuch für Mineralogie, Abhandlungen (163): 19-42.
- French, W.J. (1992): The characterization of potentially reactive aggregates, In: Poole, A.B. (Editor), Proceedings of the 9<sup>th</sup> international Conference on Alkali-aggregate Reactions in Concrete, Concrete Society Publication (CS.104/1), London: 338-342.
- Garcia-Diaz, E., Bulteel, D., Monnin, Y., Degrugilliers, P., Fasseu, P. (2010): ASR pessimum behaviour of siliceous limestone aggregates, Cement and Concrete research (40): 546-549.
- Geological Survey of Belgium (2006): Petrographic Atlas of the Potentially Alkali-Reactive Rocks in Europe, G. Lorenzi, J. Jensen, B. Wigum, R. Sibbick, M. Haugen, S. Guédon, U. Åkesson, Professional paper 2006/1-N.302, Brussels ISSN 0378-0902, pp 63 + 192 photographs.
- Grattan-Bellew, P.E., (1986): Is high undulatory extinction in quartz indicative of alkali-expansivity of granitic aggregates?, In: Grattan-Bellew, P.E. (Editor), Proceedings of the 7th International Conference on Concrete Alkali-Aggregate Reaction. Ottawa, Canada. Noyes Publications, Park Ridge, New Jersey, USA: 434-439.
- Grattan-Bellew, P.E., (1992): Microcrystalline quartz, undulatory extinction and the alkali-silica reaction, In: Poole, A.B. (Editor), 9<sup>th</sup> International Conference on Alkali-Aggregate Reaction in Concrete, Concrete Society Publication CS.104 1, London: 383-394.
- Grelk, B (2006): PARTNER Report No. 3.4. Experience from testing of the alkali reactivity of European aggregates according to two Danish laboratory test methods; SINTEF Report SBF52 A06022 / ISBN 82-14-04082-5 / 978- 82-14-04082-5, pp 18 + appendices.
- Gogte, B.C. (1973): An evaluation of some common Indian rocks with special reference to alkali-aggregate reactions, Engineering Geology (7): 993-1004.
- Haugen, M, Lindgård, J, Åkesson, U, Schouenborg, B (2008): Experience from using the RILEM AAR-1 petrographic method among European petrographers – part of the PARTNER project, in: Broekmans, MATM, Wigum, BJ (Editors), Proceedings of the 13<sup>th</sup> International Conference on Alkali-Aggregate Reaction in Concrete, Trondheim, CD-ROM, pp 10.
- Heilbronner, R. (1999): Lazy grain boundaries, public domain macros for NIH Image, University of Basel. <http://www.unibas.ch/earth/GPI/micro/micro.html>.

- Heilbronner, R. (2000): Automatic grain boundary detection and grain size analysis using polarization micrographs or orientation images, *Journal of Structural Geology* (22): 969-981.
- Hobbs, D.W. (1988): Alkali-silica reaction in concrete, Thomas Telford Ltd. London, pp 183.
- Humphries, DW (1992): The preparation of thin sections of rocks, minerals and ceramics. Royal Microscopical Society, Oxford Science Publications, *Microscopy Handbooks* (24): pp 83.
- Image SXM*, S D Barrett (2008) <http://www.ImageSXM.org.uk>
- Jensen, J (2006): PARTNER Report No. 3.2. Experience from testing of the alkali reactivity of European aggregates according to the RILEM AAR-2 method; SINTEF Report SBF52 A06020 / ISBN 82-14-04080-9 / 978-82-14-04080-9, pp 43 + appendices.
- Kerrick, D., Hooton, R. (1992): ASR of concrete aggregate quarried from a fault zone: results and petrographic interpretation of accelerated mortar bar tests, *Cement and Concrete Research* (22): 949-960.
- Knauth, I.P. (1994): Petrogenesis of chert. In: Heaney, P.J., Prewitt, C.T., and Gibbs, G.V. (editors), *Silica: physical behaviour, geochemistry and materials applications. Reviews in Mineralogy* (29): 233-258.
- Kronenberg, A.K. (1994): Hydrogen speciation and chemical weakening of quartz. In: Heaney, P.J., Prewitt, C.T., and Gibbs, G.V. (editors), *Silica: physical behaviour, geochemistry and materials applications. Reviews in Mineralogy* (29): 123-176.
- Lindgård, J, Haugen, M (2006): PARTNER Report No. 3.1. Experience from using petrographic analysis according to the RILEM AAR-1 method to assess alkali reactions in European aggregates; SINTEF Report SBF52 A06019 / ISBN 82-14- 04079-5/978-82-14-04079-5, pp 19 + appendices.
- Lindgård, J, Nixon, PJ, Borchers, I, Schouenborg, B, Wigum, BJ, Haugen, M, and Åkesson, U (2010): The EU "PARTNER" Project — European standard tests to prevent alkali reactions in aggregates: Final results and recommendations. *Cement and Concrete Research*, 40-4: 611-635.
- Locati, F., Marfil, S., Baldo, E. (2010): Effect of ductile deformation of quartz-bearing rocks on the alkali-silica reaction, *Engineering Geology* (116): 117-128.
- Murata, K.J., Norman, M.B. (1976): An index of crystallinity for quartz, *American Journal of Science* (276): 1120-1130.
- Nixon, PJ, Lane, S (2006): PARTNER Report No. 3.3. Experience from testing of the alkali reactivity of European aggregates according to several concrete prism test methods; SINTEF Report SBF52 A06021 / ISBN 82-14-04081-7 / 978- 82-14-04081-7, pp 35 + appendices.
- Nixon, PJ, Lindgård, J, Borchers, I, Wigum, BJ, Schouenborg, B (2008): The EU "PARTNER" project – European standard tests to prevent alkali reactions in aggregates - final results and recommendations, in: Broekmans, MATM, Wigum, BJ (Editors), *Proceedings of the 13<sup>th</sup> International Conference on Alkali-Aggregate Reaction in Concrete*, Trondheim, CD-ROM, pp 10.
- RILEM AAR-1 (2003): Detection of potential alkali-reactivity of aggregates – Petrographic method, TC 191-ARP: Alkali-reactivity and prevention – Assessment, specification and diagnosis of alkali-reactivity, prepared by: Sims, I., Nixon, P., *Materials and Constructions*, (36): 480-496.
- RILEM AAR-2 (2000): Detection of potential alkali-reactivity of aggregates - the ultra accelerated mortar bar test. *Materials & Structures* (33): 283-289.
- RILEM AAR-4 (to be published): Detection of potential alkali-reactivity of aggregates: Accelerated (60oC) concrete prism test.
- Schouenborg, B, Åkesson, U, Liedberg, L (2008): Precision trials can improve test methods for alkali aggregate reaction (AAR) – part of the PARTNER project, in: Broekmans, MATM, Wigum, BJ (Editors), *Proceedings of the 13<sup>th</sup> International Conference on Alkali-Aggregate Reaction in Concrete*, Trondheim, CD-ROM, pp 9.
- Shayan, A. (1993): Alkali reactivity of deformed granitic rocks: a case study, *Cement and Concrete Research*, (23): 1229-1236.
- Siebel, E, Bokern, J, and Borchers, I (2006): PARTNER Report No. 3.5. Field site tests sites established in the PARTNER project for evaluating the correlation between laboratory tests and field performance; SINTEF Report SBF52 A06023 / ISBN 82-14-04083-3 / 978- 82-14-04083-3, pp 20 + appendices.

- Thomson, M.L., Grattan-Bellew, P.E. (1993): Anatomy of a porphyroblastic schist: Alkali-silica reactivity, *Engineering Geology*, 35, Elsevier Science Publishers B.V., Amsterdam: 81-91.
- Thomson, M.L., Grattan-Bellew, P.E., White, J.C. (1994): Application of microscopic and XRD techniques to investigate alkali-silica reactivity potential of rocks and minerals, In: Gouda, G.R., Nisperos, A., Bayles, J. (Editors), *Proceedings of the 16<sup>th</sup> International Conference on Cement Microscopy*, International Cement Microscopy Association, Texas, USA, pp 19.
- Verstraete, J., Khouchaf, L., Bulteel, D., Garcia-Diaz, E., Flank, A.M., Tuilier, M.H. (2004): Amorphisation mechanism of a flint aggregate during the alkali-silica reaction: X-ray diffraction and X-ray absorption XANES contributions, *Cement and Concrete Research* (34): 581-586.
- West, G. (1991): A note on undulatory extinction of quartz in granite, *Quarterly Journal of Geology and Hydrogeology* (24): 159-165.
- West, G. (1994): Undulatory extinction of quartz in some British granites in relation to age and potential reactivity, *Quarterly Journal of Engineering Geology and Hydrogeology* (27): 69-74.
- Wigum, B.J. (1995): Examination of microstructural features of Norwegian cataclastic rocks and their use for predicting alkali-reactivity in concrete, *Engineering Geology* (40): 195-214.
- Wigum, B.J., Hagelia, P., Haugen, M., Broekmans, M.A.T.M. (2000): Alkali aggregate reactivity of Norwegian aggregates assessed by quantitative petrography, In: Bérubé, M.A., Fournier, B., Durand, B. (Editors), *Proceedings of the 11<sup>th</sup> International Conference on Alkali-Aggregate Reaction in Concrete*, Québec: 533-542.
- Wigum, BJ, Pedersen, LT, Grelk, B, and Lindgård, J (2006): PARTNER Report No. 2.1. State-of-the art report: Key parameters influencing the alkali aggregate reaction; SINTEF Report SBF52 A06018 / ISBN 82-14-04078-7 / 978-82-14-04078-7, pp 55 + appendices.
- Zhang, X, Blackwell, BQ, Groves, GW (1990): The microstructures of reactive aggregates. *British Ceramic Transaction Journal* (89): 89-92.



**Deleterious alkali-aggregate reactions in concrete: relationship between mineralogical and microstructural characteristics of aggregates versus expansion tests**

*Authors: Nélia Castro, Børge J Wigum, Maarten ATM Broekmans*

The candidate performed the experimental work and wrote the paper. Ideas and the final manuscript were discussed with the supervisor and co-author Børge J Wigum and with the co-supervisor and co-author Maarten ATM Broekmans.

*The paper was published in the proceedings of the 14<sup>th</sup> International Conference on Alkali-Aggregate Reactions in Concrete, Austin, Texas, USA, May 2012, pp. 10.*



# DELETERIOUS ALKALI-AGGREGATE REACTION IN CONCRETE: RELATIONSHIP BETWEEN MINERALOGICAL AND MICROSTRUCTURAL CHARACTERISTICS OF AGGREGATES VERSUS EXPANSION TESTS

Nélia Castro<sup>1,\*</sup>, Børge J. Wigum<sup>1</sup>, Maarten A.T.M. Broekmans<sup>2</sup>

<sup>1</sup>Norwegian University of Science and Technology (NTNU),  
Department of Geology and Minerals Resources Engineering, TRONDHEIM, Norway

<sup>2</sup>Geological Survey of Norway, Dept. of Industrial Minerals and Metals,  
TRONDHEIM, Norway

## Abstract

A variety of aggregate materials from European sources have been studied in the EU-funded PARTNER project in 2002-2006 to evaluate the suitability of different European test methods. It was found that petrography can potentially provide effective and reliable results quickly than other method, but with some limitations [1].

This study uses available post-mortem expansion-test specimen and virgin aggregate from PARTNER, for mineralogical and microstructural characterization of reactive constituents. This contribution reports initial results from characterization of the silica minerals in different aggregate materials, using a range of techniques including optical petrography, image analysis, and XRD. When compared with expansion testing results, these findings will strengthen our understanding of the AAR mechanism. Ultimately, this contribution can provide the basis for a proposal to improve the reliability and accuracy of the petrographic test procedure and contribute to a better understanding of the expansion tests.

¶

**Keywords:** ASR, aggregates for concrete, petrography, image analysis, XRD

## 1 INTRODUCTION

This paper presents the initial results from microstructural and mineralogical characterization of concrete aggregates in post-mortem expansion test specimen and virgin aggregate from the PARTNER project [1]. This study is part of a project that rose from the interest of applying geology knowledge and techniques to the study of the properties and qualities of the silica minerals that contribute to the alkali-reactivity of the aggregates for concrete. The aim of the project is to study the relationship between aggregate petrological properties and expansion test results. Mineralogical, geochemical and microstructural characteristics of silica minerals in aggregate, with focus on the properties and qualities of silica minerals that can contribute to its dissolution under 'alkali silica reaction (ASR) conditions', will be investigated. Results from expansion testing will provide a better knowledge of aggregate properties and performance in concrete and consequently a better understanding of the ASR mechanism. Full theoretical understanding on this very complex field is beyond the scope of this project. However, the findings of the project are intended to provide suggestions to the introduction of quantitative parameters in the petrographic test method, which can

---

\* Correspondence to: [nelia.castro@ntnu.no](mailto:nelia.castro@ntnu.no)



improve the accuracy and reproducibility of the petrographic test procedure (RILEM AAR-1 [2]) and contribute to a better understanding of the expansion tests.

Though the exact mechanism of ASR is a matter of dispute, there is general consensus that at some point the mechanism involves silica dissolution. A range of properties and qualities are known to affect the dissolution of quartz under geological conditions, and some may apply to 'ASR conditions' at pH14 and ambient temperature. Some quartz properties are relatively easy to assess, others require more specialized instrumentation or equipment. A summary of some fundamental considerations with respect to the solubility of silica minerals under geological and under ASR conditions can be found in Broekmans [3, 4].

Test methods to assess the ASR-potential of aggregate for use in concrete have been under development for several decades. However, none of the accepted current methods actually assess aggregate properties in terms of 'quartz solubility under ASR conditions'. In nearly all tests, aggregate is exposed to severe conditions (eg. 1N NaOH, 38-60-80°C and up) to provoke expansion within acceptable time (i.e. weeks) for the building and construction industry.

Different European test methods were evaluated for their suitability for use with the wide variety of aggregates found across Europe in the EU-funded PARTNER project in 2002-2006. The project had 24 partners from 14 countries assessing 22 different types of aggregates from 10 countries in an overall total of 413 tests, comprising expansion testing and rock classification using thin section petrography. Final results have been published in [1, 5, 6], and references therein. The overall conclusion from PARTNER is that the RILEM AAR- 2 [7] and AAR-4 [8] test are able to reliably identify the reactivity of normally and non-reactive aggregates. However, slowly aggregates typically require an extended test period.

Petrographic assessment according to the protocol described in RILEM AAR-1 [2] classifies concrete aggregate as potentially reactive or innocuous based on rock nomenclature. This procedure does not assess the actual amount of individual potentially reactive mineral constituents in an aggregate particle, but rather quantifies rock types that have been identified as deleterious in field structures. On a worldwide basis, petrographers use essentially the same procedures for thin section preparation, and the same type of instrumentation to study them. However, different schools exist on the 'correct' application of rock nomenclature complicating use of uniform terminology (see eg. discussion in [9]). On top of that comes inter-operator variation due to variable levels of experience and skill. In addition, the alkali-reactivity potential of a given rock type is known to vary from one location (region, nation) to another, which has resulted in rather different rock classifications reflecting local experience [1, 10]. Together, above issues effectively prevent simple uniform classification of a given lithology as 'always alkali-reactive' or 'invariably innocuous', rendering petrographic assessment more complicated than desirable.

Here, we have investigated normally, slowly and non-reactive rock types in post-mortem concrete prisms and mortar bars previously tested for expansion in PARTNER, in addition to their untested virgin counterparts originally stocked for reference. This enables direct comparison of changes brought about by the reaction as well identification of certain properties/qualities that render the quartz in a given lithology alkali-reactive or innocuous. Materials were initially assessed by thin section petrography to identify actually alkali-reactive aggregate particles. Subsequently, selected particles investigated using digital image analysis and X-ray powder diffraction to assess mineral content.

## **2 MATERIALS AND METHODS**

### **2.1 Materials**

This study uses available post-mortem expansion-test specimen and virgin aggregate from the PARTNER project, for mineralogical and microstructural characterization of reactive constituents. In total, 22 post-mortem expansion test concrete prisms and 3 virgin aggregate samples were available for

characterization, representing 14 different aggregate types from 8 different European countries, including 6 normally, 3 slowly, and 5 non-reactive aggregates cf. RILEM AAR-1 [2] classification. In total, 13 combinations of aggregates were tested in the 22 prisms: 3 combinations with the AAR-3 method [11], 12 combinations with the AAR-4 method [8] and 7 combinations with the German method [12]. Further details are described in [13].

All post-mortem expansion-test specimen and virgin aggregate were investigated by petrography. The main focus was given to the identification of potentially reactive particles of aggregate that could be suitable to further characterization by analytical techniques of petrography and mineralogy.

Three aggregates (It2, N4, and N5) were selected for grain size analysis of quartz by thin section petrography of post-mortem expansion-test specimens and virgin aggregate, all initially classified as slowly reactive (Table 1). The alkali-reactivity of quartz bearing rock types is usually attributed to the presence of strained, microcrystalline or cryptocrystalline quartz. A number of methods have been suggested to correlate aggregate microstructure with the expansion observed in concrete. Wigum [14] found a correlation between expansion behavior of a number of mylonites, granite and gneiss rocks versus 1) the inverse of the mean grain size  $d_{50}$ , and 2) the total grain boundary area of quartz. Wigum *et al.* [15] analysed additional samples of different rock types confirming his earlier observations. In this study, the grain size analysis follows the same procedures developed by Wigum [14] but uses image analyses instead of point-counting.

It is generally accepted that the alkali-reactivity of flint/chert and silicified limestones is related to the presence of amorphous or poorly-crystalline forms of silica, eg. opal, chalcedony and possibly also moganite. Though different silica polymorphs do have different solubilities, the most relevant polymorph present in the vast majority of concrete aggregates is  $\alpha$ -SiO<sub>2</sub> or ordinary low-quartz, with subordinate quantities of chalcedony and/or opaline silica in certain lithologies [3, 4]. The lattice quality of the quartz plays an important role in determining its alkali-reactivity potential, a highly disordered structure being assumed more reactive than quartz-proper [16]. On the other hand, laboratory experiments investigating dissolution of natural quartzes with a broad range of dislocation densities were unable to reveal any measurable differences [17]. In this study, four aggregates (B1, D1, G1 – normally reactive, F1 – non-reactive; see Table 2) were assessed by X-ray diffraction (XRD) to identify silica polymorphs other than quartz.

## 2.2 Methods for assessment and analysis

### *Petrography*

All post-mortem expansion-test specimen and virgin aggregate were investigated by petrography. Two sections ~20mm thick were cut lengthwise from each concrete prism with a 3mm thick diamond blade. One section was impregnated with fluorescent epoxy and polished according to Danish standard DS 423.39 [18], the other section was left unprepared. Both sections were studied in a Leitz-Wild Heerbrugg stereomicroscope using incident plain or fluorescent illumination to identify AAR reaction products and reactive aggregate particles. Subsequently, fluorescence-impregnated polished thin sections comprising confirmed alkali-reactive particles were prepared from the unprepared section using the procedure outlined in Danish Standard DS 423.40 [19] with minor adaptations. Due to the thickness of the diamond blade, a >3mm mismatch exists between fluorescent versus unprepared plane sections, and the thin section prepared from latter, with possible consequences for intra-particle variation in mineral content and texture/fabric.

Virgin aggregate material was weighed and washed using ordinary tap water. Particles were counted and separated manually per lithology using a Leitz-Wild Heerbrugg stereomicroscope. Polished thin sections of potentially alkali-reactive lithologies as well as some unidentified particles were prepared using standard procedures (e.g. [20]). Thin sections were analysed in a Nikon Eclipse E600 microscope using transmitted

illumination in plane-polarized light (PPL), cross-polarized light (XPL), and incident fluorescent illumination (FL), as applicable.

#### *Grain size analysis of quartz*

Three aggregates (It2, N4, and N5 – all slowly reactive) were selected for grain size analysis of quartz by post-mortem thin section petrography of expansion test concrete prisms and matching virgin aggregate particles. Potentially reactive particles identified include gneiss, rhyolite, granite, cataclasite, greywacke, and quartzite (Table 1). The grain size analysis comprises the same type of assessment as described in [14], but uses automated image analysis instead of manual point counting. Re-assessment of the original thin sections from [14] by automated analysis produced results within analytical error, but significantly faster [21].

The Lazy Grain Boundary (LGB) method [22, 23] was used to create grain boundary maps of the quartz contained in the selected aggregates. The LGB method is based on a set of macro commands programmed for Image SXM [24]. The procedure makes use of multiple input images. Sets of input images composed of six micrographs with crossed polarizers and  $\lambda$ -plate rotated 0-150° at 30° increments were acquired in a Leica DM 2500P polarizing microscope with a Jenoptik ProgRes digital camera system. For reliable analysis, the image set must comprise a statistically sufficient number of grains, which is again a combined function of microscope magnification, grain size, and rock heterogeneity. The majority of the image sets were processed fully automated by the LGB method, a few required additional minor manual correction, eg. repairing discontinuous grain boundaries and/or erasing pending relics. After completed segmentation, grains were digitally analyzed for major and minor axis length, area and perimeter. Numerical data were collated in a spreadsheet for further processing.

The examination of a rock under a microscope gives a two-dimensional image and there are a number of measurements that can be made in order to characterize its grain size. In point-counting studies, usually the maximum grain length is measured and used as the diameter. In this case, it is considered that the grain is a sphere (equivalent) of this maximum dimension. When using image analysis, other quantities such as minimum length, volume or area can be used; however, will produce a different result for the grain size. Each answer will be correct, giving a true result for the property being measured. Independently of the method used to make the measurements (point-counting or image analysis) it is important to keep in mind a basic principle of stereology: a two-dimensional image will produce an overestimation of small grain sizes. Heilbronner and Bruhn [25] showed that the volume weighted distribution of radii of spheres,  $V(R)$ , conveys more physically relevant information than the numerical distribution of radii of sectional circles,  $h(r)$ , when it comes to grain size analysis. In other words, it corrects for the typical overestimation of small grains. In the present work, the areas of the grains measured by image analysis were used to calculate the equivalent circle diameter ( $d_A$ ), which means that the grain size is defined as the diameter of a circle having the same area. The equivalent circle diameters were then grouped into histograms of 20 classes, where the bins are delimited by their upper bound. The program StripStar [26] was used to calculate the parent distributions of spheres from the histograms of equivalent circle diameters; or in other words to calculate the equivalent spherical diameter ( $d_V$ ). In this case the grain size is defined as the diameter of a sphere having the same volume.

The mean grain size of quartz and the total grain boundary area of quartz, calculated using  $d_V$  as grain size, were used as size descriptors in this work. These descriptors were calculated following the same assumptions of Wigum [14] with minor changes. For determination of the mean grain size of quartz, the  $d_{50}$  (mm) read from the cumulative grain size distribution curve was used. In order to estimate the total grain boundary area of quartz, each grain, including subgrains, was assumed to be spherical in shape. The average grain size between two selected fractions was used to calculate the specific surface area ( $S_S$ ) for this specific part of the grading. The specific surface area obtained was multiplied by the amount of grains in that fraction

(j). This was done for all the selected fractions in the grading and all results summed up in order to obtain the grain boundary area for the entire grading. The total amount of quartz in the rock ( $Q_r$ ) was obtained by a visual estimation from the thin-section using volume % estimation diagrams. By multiplying the grain boundary area with the total amount of quartz in the rock an estimate for the total grain boundary area of quartz ( $m^2/cm^3$ ) in each sample was obtained. Additional details about the grain size analysis of quartz by image analysis are elaborated in [21].

#### *X-ray diffraction (XRD)*

Four aggregates (B1, D1, G1 – normally reactive, F1 – slowly reactive) were selected for mineralogical characterization by XRD. A total of 10 aggregate particles were analyzed with emphasis on identification and quantification of silica polymorphs. Potentially reactive lithologies identified by thin section petrography include flint/chert and siliceous limestone (Table 2).

Castro et al. [27] compared XRD analyses in polished and powdered specimen prepared from the same single aggregate particle and demonstrated that, for fine-grained rocks without preferred orientation like eg. chert, diffraction results are within analytical error. As an advantage, polished sections can also be used for petrography using reflected light (standard  $30\mu m$  thin sections are *not* recommended for XRD), and for subsequent in-situ chemical analysis by EMPA or SEM-EDS. Thus, this study uses polished specimens.

Ten aggregate particles were selected for XRD analysis by prior post-mortem thin section petrography on expansion test concrete prisms and matching virgin particles. The particles were cut from the unprepared counterparts, plane polished with  $0.25\mu m$  diamond, and mounted on a PMMA holder using pressure-sensitive adhesive. In the instrument, specimen height was carefully adjusted to the focal point of the goniometer to minimize offset and error in the apparent diffraction angle.

Operating conditions of the Bruker D8 Advance X-ray diffractometer were set to 40kV and 40mA, using Ni-filtered  $CuK\alpha$  radiation of wavelength  $\lambda=1.54178\text{\AA}$ . Specimen were analyzed spinning. Diffractograms were recorded from  $2-80^\circ 2\theta$ , in  $0.01^\circ 2\theta$  increments with 1s counting time per increment, with total scan time 2h10m. Phase quantification was performed using the Rietveld refinement software TOPAS 4.0 with the fundamental parameter approach. Resulting detection limits are on the order of  $\sim 1\text{vol}\%$ , depending on eg. bulk mineral modal content, intergrinding effects, (cryptic) preferred orientation, all as applicable.

### **3 RESULTS**

#### *Petrography*

Thin section petrography confirms the presence of two different groups of potentially alkali-reactive rocks in the materials studied. The first group comprises slowly-reactive rock types, like gneiss, rhyolite, granite, cataclasite, greywacke, and quartzite, which were further assessed by grain size analysis of quartz. The cataclastic rock of granitic composition in aggregate N4 shows extensive geo-tectonic deformation leading to faulting and post-tectonic compaction of debris and cementation by redeposition and recrystallization. In contrast, the quartzite of N5 and gneiss of It2 both show limited deformation and recrystallization only.

The second group comprises normally reactive flint/chert and silicified limestone, which were further investigated by XRD to identify and quantify silica polymorphs. Additional details from thin section petrography are elaborated in [13].

#### *Grain size analysis of quartz*

Results from image analysis and data post-processing are collated in Table 3. The number of individual quartz grains assessed by the LGB method ranges from 13061 to 27606, whereas traditional point-

counting petrography typically assesses ~200 grains. The time needed to process a single sample varied from 30 to 120 minutes, in contrast to non-automated assessment requiring up to a whole day for a single thin section.

Furthermore, the cataclaste of N4 has a greater inverse mean grain size  $1/d_{50}$  than the less deformed quartzite in N5 and gneiss in It2, and consequently a larger total grain boundary area than both other lithologies.

#### *X-ray diffraction (XRD)*

Initial results from the XRD analysis, for selected particles, are normalized to 100vol% and are presented in Table 4 together with rock names from petrographic assessment. Main rock-forming constituents are quartz and calcite. Dolomite content in BI-13, as well as calcite contents in F1-40, F1-41 and F1-43 are all very near the lower limit of detection at ~1vol%, hence are of indicative value only. Materials D1-01 and D1-05 consisting of opaline silica in a limestone host, appear to contain a substantial volume of light silica polymorphs cristobalite and tridymite, presumably representing opal-CT.

## **4 DISCUSSION**

A first assessment by detailed petrography was essential to identify reactive aggregate particles and select the properties and qualities of silica minerals that can contribute to its dissolution in “ASR-environment” relevant to investigate in the scope of the project. Original descriptions elaborated during the PARTNER project have been limited to a few lines in the final PARTNER report, and therefore important information essential to the present work was lacking.

The results of detailed petrography and grain size analysis of quartz by image analysis are consistent with each other. The sample with higher degree of deformation, like N4, have a larger total grain boundary area of quartz than rocks that enjoyed less extensive deformation, such as samples N5 and It2. With image analysis not only is it possible to analyse samples much faster than with point-counting, a much larger number of grains can be analysed. Furthermore, typical stereological problems such as the overestimation of the small grains produced by a two-dimension representation of a rock (thin-section) can be easily and efficiently overcome. The calculated values of the inverse of the mean grain size of quartz and the total grain boundary of quartz were compared with expansion tests results (Figure 1). The average results obtained during PARTNER project for the accelerated mortar bar test RILEM AAR-2 with long prisms (40×40×160mm) [28] were used. These first results show a correlation between the size descriptors and the expansion test results, in agreement with previous results of [14, 15]. Work in progress is focus on the grain size analysis of quartz in more samples, including different rock types, and in the investigation of a correlation between other parameters, like grain shape. The deformation degree of the rock will be reflected in the shape of its quartz grains. As result of increasing deformation, the shape of quartz grains tends to be more irregular and elongated. Image analysis give us the unique opportunity of using the same sets of input images that are used to grain size analysis to subsequent investigation of grain shape. All the parameters will be compared against expansion test results in order to verify if there is a correlation between the different parameters and the reactivity of the aggregates.

The results of detailed petrography and XRD are consistent with each other. The mineral characterization by XRD was especially useful in the identification and quantification of silica polymorphs other than quartz. Combined tridymite and cristobalite content in D1-01 and D1-05 determined by XRD are consistent with the opaline silica content determined by petrography. When evaluating the results of XRD analysis it was of interest to compare the wt% of the different silica minerals with expansion tests results. In the PARTNER test program, short (40x40x160 mm) and long bars (25x25x285 mm) were used in RILEM

AAR-2 to compare the effect in the results obtained. For those aggregates where both coarse and fine fractions existed, the results of testing the crushed coarse fraction were compared with those of the fine fraction. Table 5 summarizes the results obtained during PARTNER project for the accelerated mortar bar test RILEM AAR-2 for the aggregates B1, D1, F1, and G1 [28]. The aggregate F1 has the higher wt% of quartz but the lowest expansion value. This can be explained by the fact that pure reactive siliceous aggregates such as flint/chert have a pessimum effect, as defined by Hobbs [29]. For a given level of alkalis, the expansion of concrete increases with the reactive aggregate content to reach a maximum value. For aggregate content superior to the maximum, the expansion decreases due to an excess of reactive silica. Concretes based on both coarse and fine aggregate of reactive flint/chert usually do not swell. A recent investigation by Garcia-Diaz *et al.* [30] with siliceous limestones concluded that contrary to the pure siliceous aggregates, the content of reactive silica in siliceous limestones is too low to consume a maximum of alkalis in non-expansive adsorption process and to obtain non-expansive concretes. This is in agreement with the results obtained for the aggregates B1 and G1. Both have variable amounts of carbonates and higher reactivity than the aggregate F1. The presence of silica polymorphs other than quartz, notably cristobalite and tridymite was detected in the two specimens of the aggregate D1 that were analyzed. Zhang [16] defend that the phase in which silica occurs plays the dominant role in determining the reactivity, with disordered structures more reactive than structures containing cristobalite, which are in turn more reactive than structures containing quartz.

## 5 CONCLUSIONS

Initial results from microstructural characterization by grain size analysis of quartz of a number of aggregates showed that rocks with higher grades of deformation have a larger total grain boundary area of quartz than rocks with less deformation. This is in agreement with the results of [14, 15]. Work in progress is focus on the grain size analysis of quartz in more samples, including different rock types, and in the investigation of a correlation between other parameters, like grain shape, in an attempt to understand better the influence of the microstructure of the so called slowly-reactive rock types in its ASR-reactivity.

First results from mineralogical characterization by XRD of several aggregates have shown that the dominant silica polymorph in the aggregate plays indeed a dominant role in determining its reactivity as defended by [16]. By investigating the presence of different silica polymorphs in more samples of flint/chert and siliceous limestone, the authors aim to understand better the heterogeneous behaviour of these rock types towards the ASR.

Future work shall also focus on the quality of the crystal lattice of quartz, the presence of foreign species in the solid silica, and the presence of hydrous species in the solid silica, since all these parameters can reflect a certain degree of deformation or distortion of the ideal crystallographic structure of quartz that will affect its solubility. A better knowledge of the properties and qualities of silica minerals that can contribute to its dissolution in ASR-environment is essential to improve the actual knowledge about the ASR mechanisms and the test methods used to evaluate the reactivity of the aggregates for concrete.

## 6 ACKNOWLEDGEMENTS

First author NC acknowledges financial support from the Portuguese Fundação para a Ciência e Tecnologia (FCT) through doctoral grant reference SFRH/BD/41810/2007.

## 7 REFERENCES

- [1] Lindgard, J, Nixon, PJ, Borchers, I, Schouenborg, B, Wigum, BJ, Haugen, M, Akesson, U (2010): The EU "PARTNER" Project - European standard tests to prevent alkali reactions in aggregates: Final results and recommendations, *Cement Concrete Res*, 40 611-635.

- [2] AAR-1, R (2003): Detection of potential alkali-reactivity of aggregates - Petrographic method, TC 191-ARP: Alkali-reactivity and prevention – Assessment, specification and diagnosis of alkali-reactivity, prepared by: Sims, I, Nixon, P, , Mater Struct, 36 480-496.
- [3] Broekmans, MATM (2002): The alkali-silica reaction: mineralogical and geochemical aspects of some Dutch concretes and Norwegian mylonites, in, University of Utrecht, pp. pp144.
- [4] Broekmans, MATM (2004): Structural properties of quartz and their potential role for ASR, Mater Charact, 53 129-140.
- [5] Haugen, M, Lindgård, J, Åkesson, U, Schouenborg, B (2008): Experience from using the RILEM AAR-1 petrographic method among European petrographers – part of the PARTNER project, in: M. Broekmans, B. Wigum (Eds.) 13th International Conference on Alkali-Aggregate Reaction in Concrete (ICAAR), Trondheim, pp. 744-753.
- [6] Nixon, P, Lindgård, J, Borchers, I, Wigum, B, Schouenborg, B (2008): The EU "PARTNER" project – European standard tests to prevent alkali reactions in aggregates - final results and recommendations, in: M. Broekmans, B. Wigum (Eds.) 13th International Conference on Alkali-Aggregate Reaction in Concrete (ICAAR), Trondheim, pp. 300-309.
- [7] AAR-2, R (2000): Detection of potential alkali-reactivity of aggregates - the ultra accelerated mortar bar test, Mater Struct, 33 283-283.
- [8] AAR-4.1, R (2011): Detection of potential alkali-reactivity of aggregates. 60°C accelerated method for aggregate combinations using concrete prisms, Committee Document RILEM /TC ACS/11/06, in preparation for publication in Materials and Structures.
- [9] Broekmans, M, Fernandes, I, Nixon, P (2009): A global petrographic atlas of alkali-silica reactive rock types: a brief review, in: B. Middendorf, A. Just, D. Klein, A. Glaubitt, J. Simon (Eds.) 12th Euroseminar on Microscopy Applied to Building Materials, Dortmund, pp. 39-50.
- [10] Schouenborg, B, Åkesson, U., Lieberg, L. (2008): Precision trials can improve test methods for alkali aggregate reactions (AAR) - part of the PARTNER project, in: M.A.T.M. Broekmans, Wigum, B.J. (Ed.) 13th International Conference on Alkali-Aggregate Reactions in Concrete, Trondheim, pp. 1186-1195.
- [11] AAR-3, R (2000): Detection of potential alkali-reactivity of aggregates: method for aggregate combination using concrete prisms, Mater Struct, 33 209-293.
- [12] Deutscher Ausschuss für Stahlbeton, D (2001): Vorbeugende Maßnahmen gegen schädigende Alkalireaktion im Beton : Alkali-Richtlinie, in, Beuth, Berlin, (DAFStb-Richtlinie).
- [13] Castro, N, Wigum, BJ, Broekmans, MATM (2011): Deleterious alkali-silica reaction in concrete: preliminary petrographical and microstructural characterisation of reacted and virgin materials from PARTNER project, in: A. Mauko, A. Kosec, T. Tinkara, N. Gartner (Eds.) 13th Euroseminar on Microscopy Applied to Building Materials, Ljubljana, pp. 10.
- [14] Wigum, BJ (1995): Examination of microstructural features of Norwegian cataclastic rocks and their use for predicting alkali-reactivity in concrete, Eng Geol, 40 195-214.
- [15] Wigum, BJ, Hagelia, P, Haugen, M, Broekmans, MATM (2000): Alkali aggregate reactivity of Norwegian aggregates assessed by quantitative petrography, in: M.A. Bérubé, Fournier, B., Durand, B. (Ed.) 11th International Conference on Alkali-Aggregate Reactions in Concrete, Québec, pp. 533-542.
- [16] Zhang, X, Blackwell, BQ, Groves, GW (1990): The Microstructure of Reactive Aggregates, Brit Ceram Trans J, 89 89-92.
- [17] Blum, AE, Yund, RA, Lasaga, AC (1990): The Effect of Dislocation Density on the Dissolution Rate of Quartz, Geochim Cosmochim Ac, 54 283-297.
- [18] Association, DS (2002): Concrete testing - hardened concrete - production of fluorescence impregnated plane sections (in Danish). DS 423.39, in, pp. 8.
- [19] Association, DS (2002): Concrete testing - hardened concrete - production of fluorescence-impregnated thin sections (in Danish) DS 423.40, in, pp. 12.
- [20] Humphries, DW (1992): The preparation of thin sections of rocks, minerals and ceramics, Royal Microscopical Society, Oxford Science Publications.
- [21] Castro, N, Wigum, BJ (2011): Grain size analysis of quartz in potentially alkali-reactive aggregates for concrete: a comparison between image analysis and point-counting, in: M.A.T.M. Broekmans (Ed.) 10th International Conference on Applied Mineralogy, Trondheim, pp. 103-110.

- [22] Heilbronner, R (1999): Lazy Grain Boundaries, public domain macros for NIH Image, in, University of Basel, <http://pages.unibas.ch/earth/micro/index.html>.
- [23] Heilbronner, R (2000): Automatic grain boundary detection and grain size analysis using polarization micrographs or orientation images, J Struct Geol, 22 969-981.
- [24] Barrett, SD (2008): Image SXM, in, <http://www.ImageSXM.org.uk>.
- [25] Heilbronner, R, Bruhn, D (1998): The influence of three-dimensional grain size distributions on the rheology of polyphase rocks, J Struct Geol, 20 695-705.
- [26] Heilbronner, R (1998): Stripstar, public domain program for the calculation of 3-D grain size distributions from histograms of 2-D sections, in, University of Basel, <http://pages.unibas.ch/earth/micro/index.html>.
- [27] Castro, N, Sorensen, BE, Broekmans, MATM (2011): Assessment of individual ASR-aggregate particles by XRD, in: M.A.T.M. Broekmans (Ed.) 10th International Conference on Applied Mineralogy (ICAM), Trondheim, pp. 95-102.
- [28] Jensen, J (2006): PARTNER report No. 3.2 Experience from testing of the alkali reactivity of European aggregates according to the RILEM AAR-2 method, SINTEF.
- [29] Hobbs, DW (1988): Alkali-silica reaction in concrete, Thomas Telford Ltd., London.
- [30] Garcia-Diaz, E, Bulteel, D, Monnin, Y, Degrugilliers, P, Fasseu, P (2010): ASR pessimum behaviour of siliceous limestone aggregates, Cement Concrete Res, 40 546-549.
- [31] Whitney, DL, Evans, BW (2010): Abbreviations for names of rock-forming minerals, Am Mineral, 95 185-187.

**Table 1:** Compositions of selected slowly reactive bulk aggregate materials from PARTNER, by optical petrography on post-mortem concrete prisms and/or matching virgin coarse aggregate. These materials have been assessed by automated image analysis in a separate procedure. Further explanation in text. Table adapted from [13].

sample	brief lithological description	observed ASR reactive
It2	polymict rounded river gravel, main constituent quartzite, minor gneiss and granite, traces of flint/chert, gabbro, eclogite	quartzite, gneiss
N4	polymict rounded moraine gravel/sand containing sand-/siltstone, cataclasite, quartzite, granite, gneiss, gabbro, basalt	cataclasite, sandstone, quartzite
N5	polymict rounded glaciofluvial gravel/sand, main constituent quartzite, minor rhyolite, granite, gneiss, sandstone	quartzite, rhyolite

material provenance: It=Italy, N=Norway

**Table 2:** Compositions of selected normally reactive (F1: non-reactive) bulk aggregate materials from PARTNER, by optical petrography on post-mortem concrete prisms and/or matching virgin coarse aggregate. These materials have been assessed by XRD in a separate procedure. Further explanation in text. Table adapted from [13].

sample	brief lithological description	observed ASR reactive
B1	angular fragments of various types of siliceous limestone (mud-, wacke-, packstones) containing foraminifera.	siliceous limestone
D1	sub-rounded glaciofluvial gravel/sand, main constituents flint/chert and opaline limestone, minor greywacke, quartzite, granite, gneiss, and mafic rocks.	flint/chert, opaline limestone
G1	partly crushed, partly naturally rounded polymict river gravel, main constituents flint/chert and siliceous limestone, minor quartzite, sandstone, greywacke, granite, and mafic rocks.	flint/chert, siliceous limestone, sandstone
F1	polymict rounded river gravel, main constituent flint/chert, minor siliceous limestone, mudstone, and greywacke.	flint/chert

material provenance: B=Belgium, D=Denmark, F=France, G=Germany



**Table 3:** Results from automated image analysis of quartz in selected PARTNER lithologies, with alkali-reactivity confirmed by post-mortem optical petrography on concrete prisms. Further explanation in text.

sample	total number of quartz grains analyzed	mean grain size, $d_{50}$ (mm)	total grain boundary area ( $m^2 \cdot cm^{-3}$ )
It2	14095	0.10	0.031
N4	13061	0.22	0.015
N5	27606	0.16	0.017

**Table 4:** Mineral modal compositions of selected PARTNER aggregate lithologies with confirmed alkali-reactivity, by XRD on polished sections, in vol% (normalized). Mineral acronyms cf. [31]. Further explanation in text.

sample	lithology	mineral					
		Qz	Cal	Dol	Crns	Trd	SUM
B1-12	siliceous limestone	15	85	1	<LLD	<LLD	100
B1-13	siliceous limestone	16	81	3	<LLD	<LLD	100
D1-01	opaline limestone	36	43	<LLD	12	8	100
D1-05	opaline limestone	51	29	1	12	6	100
G1-26	flint/chert	77	21	<LLD	<LLD	<LLD	100
G1-29	siliceous limestone	79	20	<LLD	<LLD	<LLD	100
G1-31	flint/chert	69	31	<LLD	<LLD	<LLD	100
F1-40	flint/chert	99	1	<LLD	<LLD	<LLD	100
F1-41	flint/chert	96	1	1	<LLD	1	100
F1-43	flint/chert	97	1	1	<LLD	1	100

**Table 5:** Selected 14-day expansion data on bulk aggregate from PARTNER, cf. RILEM AAR-2 with short prisms, in %. Further explanation in text. Table adapted from [28].

sample	fraction	results (14 days)		S/L ratio	reported reactivity in the field
		short (40×40×160 mm)	long (25×25×285 mm)		
B1	F	0.20-0.28	0.42	0.47-0.67	high
	C	0.25	0.18	1.39	very high
D1	F	0.23	-	-	very high (pessimum effect)
G1	C	0.27-0.41	0.46	0.59-0.89	high
F1	C	0.03	0.01-0.06	0.5-3	low-moderate (pessimum)

C = coarse fraction (> 4mm); F = fine fraction (< 4mm)

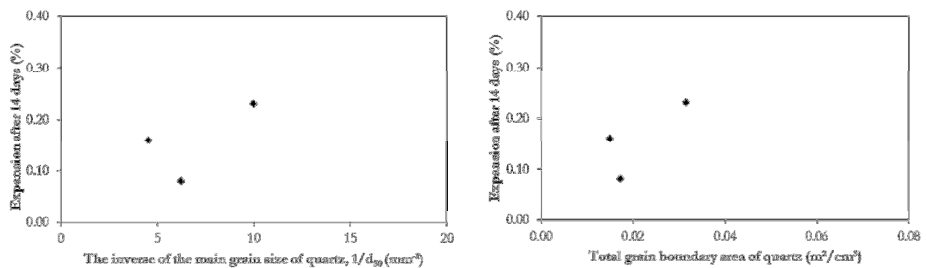


**Figure 1:** Correlation of average values of expansion data from PARTNER cf. RILEM AAR 2 on long prisms (%) [28], versus reciprocal quartz mean grain size  $1/d_{50}$  (in  $mm^{-1}$ ) at left, and versus total grain boundary area of quartz (in  $m^2/cm^3$ ) at right.

**Assessment of the potential alkali-reactivity of aggregates for concrete by images analysis petrography**

*Authors: Nélia Castro, Børge J Wigum*

The candidate carried out the experimental work and wrote the paper. Ideas and the final manuscript were discussed with the supervisor and co-author Børge J Wigum.

*The paper was published in Cement and Concrete Research 42 (2012): 1635-1644.*





## Assessment of the potential alkali-reactivity of aggregates for concrete by image analysis petrography

Nélia Castro<sup>\*</sup>, Børge J. Wigum

Norwegian University of Science and Technology (NTNU), Department of Geology and Minerals Resources Engineering, Sem Sælands vei 1, N-7491 Trondheim, Norway

### ARTICLE INFO

#### Article history:

Received 27 January 2012

Accepted 9 August 2012

Available online xxxx

#### Keywords:

Image analysis (B)

Petrography (B)

Crystal size (B)

Crystal shape

Alkali-Aggregate Reactions (C)

### ABSTRACT

The petrographic method RILEM AAR-1 has proven to be very effective, reliable and time efficient in assessing the potential alkali-reactivity of aggregates for concrete when performed by experienced petrographers. However, on a global scale, some challenges in the assessment of so-called “slowly” reactive aggregates have been reported.

This paper uses image analysis petrography to assess quantitatively the microstructure of aggregates for concrete. Grain size and grain shape descriptors were calculated for 11 aggregate samples from 3 countries (Italy, Norway and Portugal), including reactive and non-reactive rock types. Results from image analysis petrography were critically reviewed against expansion data and reported experience in structures. It was concluded that image analysis petrography can be used as a supplementary technique to overcome some of the limitations of the traditional petrographic method RILEM AAR-1 reported in the literature and improve its value as a tool to evaluate the potential reactivity of aggregates for concrete.

© 2012 Elsevier Ltd. All rights reserved.

### 1. Introduction

Alkali-Aggregate Reactions (AAR) cause severe damage in concrete structures worldwide. The most widespread type of AAR is Alkali-Silica Reactions (ASR) in which silica *sensu lato* in the aggregate react with available alkali from the cement paste forming a hygroscopic gel. The alkali gel expands upon hydration and may introduce cracking in the surrounding concrete, thereby reducing structure service-life and increasing cost for society. The incubation time needed before ASR damage starts ranges from a few months to several decades, much depending on aggregate type, binder type, and exposure climate.

There are two generalised classes of siliceous aggregates known to be potentially reactive with alkalis in concrete [1]: the normally reactive aggregates (those that react in a time scale of 5 to 20 years) and the slowly reactive aggregates (those that react in a time scale greater than 15–20 years). Normally reactive aggregates are characterized by the presence of very fine grained quartz and disordered forms of silica (e.g. opal, chalcedony). Slowly reactive aggregates are typically crystalline quartz-bearing rock types (e.g. mylonite, granite, gneiss, quartzite, greywacke, phyllite, and argillite). In many of these rocks strained, microcrystalline or cryptocrystalline quartz is believed to be the reactive component.

Test methods to assess the ASR-potential of aggregates for concrete have been under development for several decades. To meet

the needs of the building and construction industry these test methods are required to provide an accurate and precise result in the shortest time possible using the least resources possible. The petrographic method shall always be the first step in the assessment of the potential alkali-reactivity of aggregates for concrete [2]. The RILEM petrographic method AAR-1 [3] comprises two techniques: macroscopic petrography, and thin-section petrography. Macroscopic petrography is used in coarse aggregate fractions >4 mm. Thin-section petrography is applied to all fine aggregate fractions <4 mm (point-counting method), as well as to any coarse constituent that could not be unequivocally identified by macroscopic petrography (whole rock petrography). The objective is to identify the mineral and rock constituents of the aggregate accordingly to acknowledge nomenclature and classify the alkali-reactivity potential of each mineral and rock type identified as: I – Very unlikely to be alkali-reactive; II – Alkali-reactivity uncertain; and III – Very likely to be alkali-reactive. When all samples have been studied, the modal content in volume percent for each identified lithology is calculated and the data used to classify the alkali-reactivity potential of the bulk aggregate material, applying criteria based on local (national, regional) experiences, recommendations and specifications. Different countries use different standards and methodologies to perform the petrographic method (e.g. [3–5]) and have their own criteria for classification of the potential alkali-reactivity of the aggregates. However, all classification systems are based in the application of mineral and rock nomenclature. Therefore, it is very important that the petrographic analysis is carried out by a qualified geologist or petrographer with experience of materials used for

<sup>\*</sup> Corresponding author. Tel.: +47 73 59 48 41; fax: +47 73 59 48 14.  
E-mail address: [nelia.castro@ntnu.no](mailto:nelia.castro@ntnu.no) (N. Castro).

concrete and good local knowledge of alkali-reactive aggregates and minerals.

The petrographic examination shall be followed by accelerated laboratory tests to confirm the results obtained [2]. Mortar or concrete prisms are exposed to elevated conditions of temperature and alkalinity to provoke expansion within days, weeks or years, depending of the method. Several accelerated laboratory tests have been used worldwide for more than 15 years, but none of the methods have proven to be reliable for use with all aggregate types and all types of binders [1].

Different European test methods were evaluated for their suitability for use with the wide variety of aggregates found across Europe in the EU-funded PARTNER project in 2002–2006. The overall experience from the PARTNER project is that in most cases the RILEM tests could successfully identify the reactivity of the aggregates tested [1]. It was concluded that the accelerated mortar bar test RILEM AAR-2 [6] and the accelerated concrete prism test RILEM AAR-4 [7] (60 °C) are the most effective and have the best precision. Recent studies developed in North America have reported that a significant reduction in expansion was observed when known reactive aggregates were tested in the accelerated concrete prism test (60 °C) and compared to the standard concrete prism test (38 °C) [8]. The RILEM concrete prism methods evaluated in the PARTNER project were most successful with normally reactive and non-reactive aggregates. With aggregates that react very slowly, an extended test period may be necessary for some of the RILEM methods [1]. It was also found that the RILEM petrographic method [3] can potentially provide effective and reliable results quicker than other methods, but with some limitations. Precision trials to RILEM petrographic method [3] carried out by PARTNER project determined that the identification of the rocks and minerals is similar among different laboratories, but the classification of the potential alkali-reactivity of the aggregates (i.e. class I, II, or III) varies a great deal, probably due to the regional experience [1,9,10]. The spread between the four most experienced laboratories was rather low, though. The results show that the precision and reproducibility of the petrographic method strongly depends on the experience and expertise of the petrographer.

In summary, the petrographic method has proven to be a very effective, reliable and time efficient method when performed by petrographers experienced both with the method and the local aggregates. In Norway, after more than 20 years of experience, the petrographic method [5] is regarded as a very reliable tool to assess the alkali reactivity of the Norwegian aggregates [10]. However, when assessing so-called “slowly” reactive aggregates some challenges in the application of the petrographic method have been reported on a global scale. Some rock types have been identified as non-reactive in one place (country, region) and as reactive elsewhere. Granitic aggregates for example are considered non-reactive in several countries [3], but ASR damage associated with granitic aggregates in large structures has been reported by several authors worldwide (e.g. [11–14]). Another problem often reported in the literature is that rock types that have shown significant variation in reactivity by expansion tests or field experience were given the same classification of the degree of alkali-reactivity by the petrographic method (class I, II, III). For example, in Norway, a local criteria of 20 vol.% is used [5]. This means that if the aggregate contains 20 vol.% or more of rock types considered reactive the aggregate is classified as potentially reactive. The construction industry shall therefore use this information to take additional measures to avoid deterioration by ASR if this aggregate is to be used in construction. However, all rock types are counted the same, even though it is known that for example a mylonite is more reactive than a phyllite.

Alkali-reactivity of so-called “slowly” reactive rock types has been associated with the presence of strained, microcrystalline or cryptocrystalline quartz by several authors (e.g. [11,13–16]). Therefore, the degree of reactivity of certain rock types is dependent upon the microstructural

features of the rock type, rather than the mineralogical composition and petrographic nomenclature. Rock nomenclature has special meaning for geologists/petrographers. A mineral, textural, structural, genetic meaning is contained in each rock name. But, sometimes, rock nomenclature is not consensual worldwide among geologists/petrographers. Taking again granite as example, some geologists/petrographers consider that a granite can have a certain degree of deformation (strained quartz, subgranulation), whilst for others the definition of granite is more strict and if the rock exhibits deformation then it is no longer designated by granite but by gneiss or mylonite, depending on the extent of deformation that the rock has suffered. If the petrographic method RILEM AAR-1 aims to be a reference method to assess the alkali reactivity of aggregates both within Europe and worldwide, the quantification of microstructural features within the aggregates may be an essential complement to the traditional application of nomenclature when evaluating the potential reactivity of “slowly” reactive aggregates.

Experience within some regions and with particular materials (i.e. highly metamorphic rocks) has shown that determining the quartz grain size is important in the assessment of the potential reactivity of an aggregate [10]. Wigum [17] demonstrated by theoretical approach and experimental work that the alkali reactivity of cataclastic rocks is clearly related to the total grain boundary area of quartz. The study showed a direct relationship between the quartz grain size and the potential reactivity of the aggregate, using the inverse of the  $d_{50}$  (mm), the total grain boundary of quartz ( $m^2/cm^3$ ) and the accelerated mortar bar expansion after 14 days of some mylonites, granites and gneisses. Wigum et al. [18] analysed more samples including more rock types and observed the same trend. Alaejos and Lanza [19] studied the effect on the reactivity of aggregates containing different quartz crystal sizes (0–10  $\mu m$ ; 10–60  $\mu m$ ; 60–130  $\mu m$ ), measured with point-counting, proposing a unique limit for all of them applied to their weighted sum (Equivalent Reactive Quartz). Although the method seems to tackle the problem in an interesting way, more research is needed to overcome some limitations of the method and confirm the proposed limits. Both authors [17,19] referred that image analysis procedure could help to establish standard/automatized procedures, hence making the grain size analysis more repeatable and reproducible.

In the present work, image analysis was used to quantify microstructural parameters of rock types such as granite, mylonite, cataclastite, and quartzite. Grain size and shape parameters were calculated. Size descriptors similar to those used by Wigum [17] and Wigum et al. [18] were critically reviewed against results from expansion data and experience in structures to assess the aggregate potential reactivity and evaluate the influence of grain size and shape in the potential reactivity of the aggregate. The overall objective is to investigate if/how quantitative petrographic image analysis can be used to overcome some limitations of the traditional petrographic method RILEM AAR-1 improving its value as a tool to evaluate the potential reactivity of aggregates for concrete.

## 2. Material and methods

### 2.1. Material

This study uses selected samples of virgin aggregate and post-mortem expansion test prisms previously applied in three different projects [1,15,17,20]. Rock types usually regarded as “slowly reactive” were selected. It was also important that results of laboratory tests (i.e. petrographic method, expansion data) were available to use as assessment of their potential reactivity. When available, reported experience in structures was also taken into account. The final list contained 11 aggregate samples from 3 countries (Italy, Norway and Portugal), including reactive and non-reactive rock types (Table 1) [21].

**Table 1**  
Aggregate description.

Aggregate country	Brief petrographic description	Sample	Reported field experience	Reference
A Norway	Porphyritic granite from North Norway. Most of the quartz grains exhibit strong undulatory extinction, and many of them contain parallel strain lamellae indicating some ductile deformation. The occurrence of myrmekite could also be observed in some of the feldspars.	Virgin aggregate	–	[17] (Note: original designation of these aggregates was 1.4, 3.3 and 5.1, respectively)
B Norway	Mylonite from the Southeastern Precambrian region in Norway. Elongated quartz grains show sutured grain boundaries and the beginning of subgrain development, whilst some areas are granulated into small subgrains of quartz. It also contains a relatively high content of finely distributed micas and chlorite.	Virgin aggregate	–	
C Norway	Mylonite from the Southwest part of Norway. It was classified as a mylonite with significant subgrain development.	Virgin aggregate	–	
D Portugal	Granite from a Pre-orogenic pluton, North Portugal. The quartz crystals show extensive sub-granulation at grain boundaries of strained quartz. Strain has caused the quartz crystal to deform into domains with high undulatory extinction angles.	Virgin aggregate	–	[15,20] (Note: original designation of these aggregates was Belver, Bemposta, S. Tomé de Castelo, Alpendurada, and Vila Flor, respectively)
E Portugal	Granite from a Syn-orogenic, Syn-D3 pluton, North Portugal. Undulatory extinction in strained boundaries, sub-granulation and microcrystalline quartz was observed. It was verified that the phyllosilicate minerals are oriented. Deformation is also visible in feldspars and in the cleavage plans of muscovite and biotite crystals.	Virgin aggregate	Aggregate has caused damage in a dam over Douro river, Portugal.	
F Portugal	Granite from a Syn-orogenic, Late-D3 pluton, North Portugal. Quartz crystals are frequently strained, exhibiting undulatory extinction. Areas with sub-granulation and recrystallisation of quartz with gottular shape in strained quartz and plagioclase crystals were also observed.	Virgin aggregate	Aggregate has caused damage in a bridge over Douro river, Portugal.	
G Portugal	Granite from a Syn-orogenic, Late-D3 pluton, North Portugal. Strained quartz crystals with undulatory extinction. Sub-granulated quartz can also be found in small areas in the limits of some strained quartz crystals.	Virgin aggregate	–	
H Portugal	Granite from a Late to Post-orogenic pluton, Centre Portugal. The quartz crystals exhibit undulatory extinction but no other signs of deformation were found.	Virgin aggregate	The aggregate was used in the construction of a dam over Tagus river in Portugal but no deterioration was reported.	
I Italy	Polymictic river gravel mainly composed by quartzite. Other lithologies observed include: gneiss, granite, flint/chert, gabbro, and eclogite. ASR was associated with the presence of quartzite and gneiss particles. Undulatory extinction in strained boundaries, sub-granulation and microcrystalline quartz was observed both in quartzite and gneiss particles. In some particles of gneiss the cleavage plans of muscovite crystals are also deformed.	Concrete prism (tested with RILEM AAR-4 [4])	Damage has been reported for example in a 50 year old water construction.	[1] (Note: original designation of these aggregates was It2, N4, and N5, respectively)
J Norway	Natural gravel/sand from a moraine deposit. Rock types observed in this aggregate include: sandstone, siltstone, cataclasite, quartzite, granite, gneiss, gabbro, and basalt. ASR was associated with the presence of cataclasite and quartzite particles. Subgranulation and areas with microcrystalline quartz were observed in the cataclasite particles. In the quartzite particles the quartz grains show undulatory extinction, sutured grain boundaries and subgrain development.	Concrete prisms (tested with RILEM AAR-3 [6] and RILEM AAR-4 [4])	Moderate damage reported if the humidity and alkali content are high (eg. 20–25 year old constructions, mainly bridges).	
K Norway	Sand/gravel from a glaciofluvial deposit mainly composed by quartzite. Other rock types identified include: rhyolite, granite, gneiss, and sandstone. ASR was associated with the presence of quartzite and rhyolite particles. The quartzite particles are characterized by quartz grains with undulatory extinction, sutured grain boundaries and subgrain development. A relatively high content of finely distributed micas was observed in some particles. Strong subgranulation and areas with microcrystalline quartz were observed in the rhyolite particles. The occurrence of myrmekite could also be observed in some of the feldspars.	Concrete prisms (tested with RILEM AAR-3 [6] and RILEM AAR-4 [4])	Moderate damage reported if the humidity and alkali content are high (eg. 20–25 year old constructions, mainly bridges).	

## 2.2. Methods for assessment and analysis

### 2.2.1. Quantitative assessment of the aggregates microstructure by image analysis

Image analysis allows the extraction of useful information from an image, e.g. the quantification of the aggregate microstructure (quartz grain size and shape) on microscopic scale (thin-sections). The segmentation of images obtained from thin-sections can be accomplished through several edge detection algorithms (e.g. [22,23]). In this study the Lazy Grain Boundary (LGB) method [24,25] was used for creating grain boundary maps of the quartz contained in the

aggregates. The LGB method is based on a set of macro commands programmed for Image SXM [26], a public domain image processing and analysing software. The procedure makes use of multiple input images. Sets of input images (stacks) composed of six polarization micrographs were acquired with crossed polarizers and  $\lambda$ -plate rotated  $0^\circ$ – $150^\circ$  at  $30^\circ$  increments in a Leica DM 2500P polarizing microscope with a Jenoptik ProgRes digital camera system. For reliable analysis, the image set must comprise a statistically sufficient number of grains, which is a combined function of microscope magnification, grain size, and rock heterogeneity. The preparation of the input images included the elimination by gradient filtering of all minerals

present in the sample except quartz. In the studied samples this procedure was effective to filter even feldspars due to the fact that sets of multiple input images acquired with crossed polarizers and  $\lambda$ -plate rotated at different angles were used. The majority of the image sets were processed fully automated by the LGB method. A few sets required additional minor manual corrections (e.g. repairing discontinuous grain boundaries and/or erasing pending relics). After segmentation, the quartz grains were analysed for major and minor axis length of the best fit ellipse, cross-sectional area and perimeter. A spread-sheet programme was used to calculate grain size and grain shape descriptors since both are very important in the characterization of the microstructure of rocks. However, there is no single definition of grain size and grain shape.

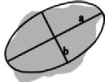
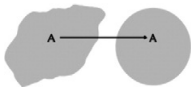
A number of measurements can be made in order to characterize the size of a grain. In point-counting studies, usually the maximum grain length is measured and used as the diameter. In this case, it is considered that the grain is a sphere (equivalent) of this maximum dimension. When using image analysis, other quantities such as minimum length, volume or area can be used; however, this will produce a different result for the grain size. Each answer will be correct, giving a valid result for the property being measured. Independent of the method used to make the measurements (point-counting or image analysis) it is important to keep in mind that a two dimensional image (like the one obtained from the examination of a rock under the microscope) will produce an overestimation of small grain sizes. To obtain a more accurate estimation of the grain size one uses stereology (the extrapolation from two- to three-dimensional space). Numerous analytical procedures are available for determining grain size distribution of spheres from section size distributions [27]. In other words, stereology is used to correct the typical overestimation of small grains obtained from measurements in a plane (thin-section), which in turn leads to a more accurate estimation of the grain size distribution.

In the present work three different measurements were used to calculate the grain size (Table 2):

- (1) *The length of the major axis of the best fit ellipse ( $d_E$ ):* In order to mirror the results obtained by Wigum [17] and Wigum et al. [18] with point counting, the  $d_E$  was used as diameter of the particle. In this case it is considered that the grain is a sphere (equivalent) of this maximum dimension.
- (2) *The equivalent circle diameter ( $d_A$ ):* The areas of the grains measured by image analysis were used to calculate the  $d_A$ , which means that the grain size is defined as the diameter of a circle having the same area.
- (3) *The equivalent spherical diameter ( $d_V$ ):* The equivalent circle diameters were then grouped into histograms of 20 classes, where the bins are delimited by their upper bound. The programme StripStar [28] was used to calculate the parent distributions of spheres from the histograms of equivalent circle diameters; or in other words to calculate the  $d_V$ . In this case the grain size is defined as the diameter of a sphere having the same volume, which represents a more accurate estimation of the grain size distribution than the previous two measurements (see Section 4.1).

A granular structure is better characterized by the distribution of grain sizes (e.g. the grain size distribution cumulative curve). However, for practical reasons a system of grains is often represented by numerical parameters that will define the distribution curve. The mean grain size of quartz and the total grain boundary area of quartz were used as size descriptors in this work (Table 3). These descriptors were calculated following the same assumptions of Wigum [17] with minor changes. For determination of the mean grain size of quartz, the  $d_{50}$  (mm) read from the cumulative grain size distribution curve was used. In order to estimate the total grain boundary area of quartz, each grain, including subgrains, was assumed to be spherical in shape.

**Table 2**  
Grain size measurement.

Name	Definition	Observations
Equivalent major axis of the best fit ellipse diameter	$d_E = a$	
Equivalent circle diameter	$d_A = 2\sqrt{A\pi}$	
Equivalent spherical diameter	$d_V$	Calculated with the programme Stripstar [29]

Notation: a = best fit ellipse major diameter; b = best fit ellipse minor diameter; A = area; V = volume.

The average grain size between two selected fractions was used to calculate the specific surface area (SS) for this specific part of the grading. The specific surface area obtained was multiplied by the amount of grains in that fraction ( $f$ ). This was done for all the selected fractions in the grading and all results summed up in order to obtain the grain boundary area for the entire grading. The total amount of quartz in the rock ( $Qz_r$ ) was obtained by a visual estimation from the thin-section using volume % estimation diagrams. By multiplying the grain boundary area with the total amount of quartz in the rock an estimate for the total grain boundary area of quartz ( $m^2/cm^3$ ) in each sample was achieved.

Intuitively, the shape of an object can be described by comparison with another one. Thus, in image analysis, shape is commonly characterized by quantifying the difference between a given object and a reference shape. A number of shape factors have been described in the literature (e.g. [27,29,30]). Shape factors are dimensionless parameters derived from the basic geometrical measurements (e.g. best fit ellipse, cross sectional area, perimeter) and generally vary between 0 and 1, the maximum value corresponding to perfect geometric shapes and the minimum corresponding to irregular shapes. In the present work, axial ratio and circularity were employed for shape characterization according to ISO 9276-6 [29] (Table 4). Axial ratio is defined as the ratio between the minor diameter of the best fit ellipse ( $b$ ) and the major diameter of the best fit ellipse ( $a$ ). This shape descriptor is sensible to the elongation of the grains. Circularity is the ratio between the perimeter equivalent ( $P_{equ}$ ), that corresponds to the perimeter of a circle with the same area as the analysed grain, and the perimeter of the particle ( $P$ ), measured by image analysis. This descriptor is sensible to the irregularities of the contour of the grain. Note that the names and definitions of these parameters may vary in the literature.

**Table 3**  
Size descriptors used in the present study.  
Adapted from [17].

Name	Definition	Unit	Observation
Mean grain size	$d_{50}$	mm	50% of the analysed grains have diameters smaller than this value
Total grain boundary of quartz	$TGBA = \left( \sum_{i=1}^n SS_i \times f_i \right) \times Qz_r$	$m^2/cm^3$	$n$ = number of fractions $SS = \frac{SA}{V} = \frac{4\pi r^2}{\frac{4}{3}\pi r^3} = \frac{3}{r}$

Notation: SS = specific surface area (surface area per unit of volume); SA = surface area; V = volume;  $f$  = amount of grain in this fraction (in percentage);  $Qz_r$  = amount of quartz in the rock.

**Table 4**  
Shape descriptors used in the present study.  
Adapted from [29].

Name	Definition	Sensitivity
Axial ratio	$E = \frac{b}{a}$	Elongation
Circularity	$C = \sqrt{\frac{4\pi A}{P^2}} = \frac{P_{eq}}{P}$	Circular shape and contour irregularities

Notation: A = area; P = perimeter;  $P_{eq}$  = perimeter equivalent (perimeter of a circle with the same area as the analysed grain); a = best fit ellipse major diameter; b = best fit ellipse minor diameter.

2.2.2. Test procedures to determine potential alkali-reactivity

The samples used in this study were previously applied in three different projects [1,15,17,20] where the aggregate reactivity was assessed

using several laboratory test methods and experience in structures. However, not necessarily the same methods were used in all samples. A brief outline of each test method can be found in Table 5.

All aggregates were submitted to the petrographic method according to RILEM AAR-1 [3]. All 11 aggregates were also tested with an accelerated mortar bar test (AMBT). However, different projects used different AMBT procedures: NBRI modified [31], ASTM C 1260 [32], and RILEM AAR-2 [6]. Differences in the mortar bars' size, curing time and conditions, and storage time before zero reading are found when comparing the three different test procedures [6,31,32] as summarized in Table 5. Additionally, the aggregates previously applied in PARTNER project (I, J, and K) were tested with a range of other tests, namely the concrete prism method RILEM AAR-3 [21], the accelerated concrete prism method RILEM AAR-4

**Table 5**  
Brief outline of laboratory test methods.

Test method	Brief outline of the method	Reference	Distinctive characteristics
Petrographic method	The petrographic method comprises two techniques: macroscopic petrography, and thin-section petrography. Macroscopic petrography is used in coarse aggregate fractions > 4 mm. Thin-section petrography is applied to all fine aggregate fractions < 4 mm (point-counting method), as well as to any coarse constituent that could not be unequivocally identified by macroscopic petrography (whole rock petrography). The objective is to identify the mineral and rock constituents of the aggregate according to acknowledge nomenclature and classify the alkali-reactivity potential of each mineral and rock type identified. At the end of the test an aggregate should be classified as: I – Very unlikely to be alkali-reactive; II – Alkali-reactivity uncertain; III – Very likely to be alkali-reactive.	RILEM AAR-1 [3]	
Accelerated mortar bar method	Test duration of 14 days. Mortar bars made with the aggregate and a reference high alkali cement are stored in 1 M NaOH at 80 °C. Results of less than 0.10% are likely to indicate non-expansive materials, whilst results exceeding 0.20% are likely to indicate expansive materials. Results between 0.10% and 0.20% are difficult to interpret and in the absence of additional local experience shall be regarded as potentially expansive. These critical limits are still under discussion for RILEM AAR-2.	NBRI modified [32] ASTM C 1260 [33] RILEM AAR-2 [6]	Mortar bars dimension: 40 × 40 × 160 mm. Curing: 48 h Storage before zero reading: 48 h immersed in water at 80 °C Mortar bars dimension: 25 × 25 × 285 mm. Curing: 24 h at 23 °C and RH 95% Storage before zero reading: 24 h immersed in water at 80 ± 2 °C Mortar bars dimension: 40 × 40 × 160 mm and 25 × 25 × 285 mm Curing: 24 h at 20 ± 1 °C and RH > 90% Storage before zero reading: 24 h immersed in water at 80 ± 2 °C
Concrete prism method	Test duration of 12 months. Wrapped concrete prisms (dimensions ranging between 250 ± 50 mm and 75 ± 5 mm) made with the aggregate and a reference high alkali cement are stored in individual containers within a constant temperature room at 38 °C and measured at 20 °C. The aggregate is considered reactive if expansion is higher than 0.05% in the end of the test.	RILEM AAR-3 [21]	
Accelerated concrete prism method	Test duration of 20 weeks. Concrete prisms (dimensions ranging between 250 ± 50 mm and 75 ± 5 mm) made with the aggregate and a reference high alkali cement are stored in individual containers within a reactor at 60 °C and measured at 20 °C. The aggregate is considered reactive if expansion is higher than 0.03% in the end of the test.	RILEM AAR-4 [7] RILEM AAR-4 Alt. [7]	Unwrapped concrete prisms Wrapped concrete prisms
The Danish mortar bar test	Test duration of 52 weeks. Mortar prisms (40 × 40 × 160 mm) made with the aggregate are stored in saturated NaCl solution at 50 °C. The aggregate is considered non-reactive if expansion is less than 0.04% after 20 weeks; late slow reactive if expansion is lower than 1.0% after 20 weeks and higher than 1.0% after 52 weeks; and fast highly reactive if expansion is higher than 1.0% after 20 weeks.	TI-B51 [34]	
The Danish Chatterji method	The degree of reaction between silica in the aggregate and KCl is determined by measuring the alkalinity after 24 h reaction to a non-reactive standard.	[35]	
German concrete prism method	Test duration of 9 months. Three concrete prisms (100 × 100 × 500 mm) and one cube (300 × 300 × 300 mm) are stored in a fog chamber at 40 °C with measurements taken immediately with no cooling down period. The aggregate is considered reactive if expansion is higher than 0.06% in the end of the test.	[36]	
Norwegian concrete prism method	Test duration of 12 months. Three concrete prisms (100 × 100 × 450 mm) made with the aggregate and a reference high alkali cement are stored in individual containers within a constant temperature room at 38 °C and 100% relative humidity and measured at 20 °C. The aggregate is considered reactive if expansion is higher than 0.04% in the end of the test.	[37]	



[7], the alternative version of the accelerated concrete prism method RILEM AAR-4 alt. [7], and the Danish mortar bar test TI-B51 [33], the Danish Chatterji method [34], the German concrete prism method [35] and the Norwegian concrete prism method [36].

Field site test with concrete cubes (300 mm lateral length) was performed for aggregates I and J [1,37]. Experience with real structures is known to aggregates E, F, H, I, J, and K (Table 1).

**3. Results**

**3.1. Quantitative assessment of the aggregates microstructure by image analysis**

Results from the size descriptors (mean grain size of quartz and total grain boundary area of quartz) and the shape descriptors (axial ratio and circularity) are summarized in Table 6. In this study between 2 and 40 image sets (stacks) were needed to obtain the reported results. The number of individual quartz grains assessed by the LGB method ranges from 186 to 27,606, whereas the point-counting method suggested by Wigum [17] typically assesses ~200 grains. A considerably higher number of grains were analysed in the aggregate samples I, J and K, when compared with the other aggregate samples, because these aggregate samples are polymictic, which means that a statistically representative number of grains had to be analysed for each rock type present in the aggregate sample. Total segmentation time for single samples was approximately 10–120 min, in contrast to non-automated assessment requiring several hours for a single thin section.

As expected the use of different measurements ( $d_E$ ,  $d_A$ ,  $d_V$ ) lead to different values for the size descriptors (see Section 2.2.1 for details). In the samples included in this paper, due to the normal distribution of the cumulative grain size distribution curves, good linear correlation is found between the two size descriptors for all samples (Fig. 1).

**3.2. Test procedures to determine potential alkali-reactivity**

As referred before, this study uses selected aggregate samples previously applied in three different projects [1,15,17,20], hence the summary of results presented in Table 7 were compiled from those projects.

Detailed expansion results after 14 days obtained from the AMBT were compiled in Table 8. Aggregates A, B, and C were tested with short bars (40×40×160 mm). Aggregates D, E, F, G, and H, were tested with long bars (25×25×285 mm). Aggregates I, J, and K were tested with both short and long bars. At the standard 14 day test age, the long and short bars give different results, with the long bars having the highest expansion. At 14 days, therefore, the short bars would need a different (smaller) limiting requirement to differentiate between reactive

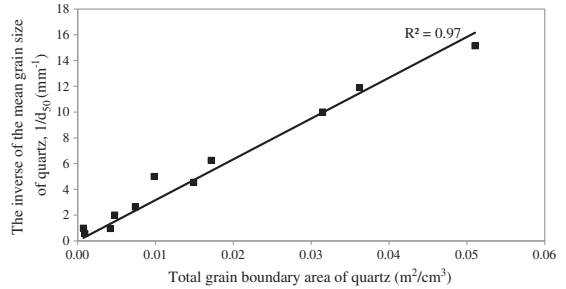


**Fig. 1.** Correlation between the total grain boundary area of quartz and the inverse of the mean grain size of quartz.

and non-reactive aggregates [1]. A correlation between long and short bars has been discussed in the literature, although no consensus has been achieved. For example, RILEM AAR-2 [6] proposes a correlation factor of 0.54, but data collected in PARTNER project points to a mean correlation factor of 0.75 [1]. For this reason, the acceptance criteria for interpretation of the results of RILEM AAR-2 [6] are still under discussion [1]. However, for long mortar bars, it is common to consider that results of less than 0.10% are likely to indicate non-expansive materials, whilst results exceeding 0.20% are likely to indicate expansive materials. Results between 0.10% and 0.20% are difficult to interpret and in the absence of additional local experience shall be regarded as potentially expansive [6,32]. In this work, to further correlate with grain size and grain shape descriptors obtained by image analysis petrography, it was decided to use results obtained with long bars. The PARTNER correlation factor was applied to recalculate the original data for short bars of aggregates A, B and C. Original data for long bars was used for aggregates D, E, F, G, and H. Regarding aggregates I, J and K, results from more than one laboratory were available. A critical evaluation of the results reported by each laboratory during PARTNER project lead to the decision of using average values reported only by the laboratories that have proven to be familiar with the method and that have reported reliable results for all the aggregates.

**4. Discussion**

**4.1. Quantitative assessment of the aggregate microstructure by image analysis**

Wigum [17] was one of the first researchers to investigate the quantitative assessment of the microstructure in aggregates for concrete. The point-counting method proposed by the author would take several

**Table 6**  
Results of calculations of size and shape descriptors.

Aggregate	Number of grains analysed	Size descriptors						Shape descriptors					
		Equivalent major axis of the best fit ellipse diameter ( $d_E$ )		Equivalent circle diameter ( $d_A$ )		Equivalent spherical diameter ( $d_V$ )		Axial ratio (b/a)			Circularity ( $P_{equ}/P$ )		
		$d_{50}$ (mm)	TGBA ( $m^2/cm^3$ )	$d_{50}$ (mm)	TGBA ( $m^2/cm^3$ )	$d_{50}$ (mm)	TGBA ( $m^2/cm^3$ )	min	max	avg.( $\mu$ )	min	max	avg.( $\mu$ )
A	186	0.30	0.003	0.20	0.004	1.02	0.001	0.13	0.96	0.62	0.36	0.95	0.80
B	1119	0.03	0.060	0.03	0.074	0.07	0.051	0.27	1.00	0.69	0.47	1.00	0.88
C	877	0.05	0.076	0.04	0.091	0.08	0.036	0.18	1.00	0.68	0.53	1.00	0.86
D	853	0.14	0.010	0.12	0.022	0.50	0.005	0.15	1.00	0.68	0.47	1.00	0.84
E	4556	0.09	0.019	0.07	0.031	0.20	0.010	0.12	1.00	0.71	0.44	1.00	0.87
F	2101	0.13	0.019	0.10	0.023	0.38	0.007	0.22	1.00	0.70	0.50	0.99	0.86
G	1071	0.24	0.012	0.19	0.028	1.04	0.004	0.20	1.00	0.68	0.38	1.00	0.83
H	207	0.40	0.012	0.29	0.010	1.74	0.001	0.21	0.98	0.63	0.51	1.00	0.79
I	14,095	0.06	0.069	0.05	0.102	0.10	0.031	0.12	1.00	0.67	0.29	1.00	0.86
J	13,061	0.09	0.035	0.08	0.043	0.22	0.015	0.14	1.00	0.67	0.43	1.00	0.86
K	27,606	0.10	0.045	0.08	0.045	0.16	0.017	0.20	1.00	0.69	0.51	1.00	0.86

**Table 7**

Summary of results of laboratory test methods, field site test and experience in structures.  
Adapted from [1,15,17,20,37].

Aggregate	AAR-1	AMBT <sup>a</sup>	AAR-3	AAR-4/AAR-4 alt.	TI-B51/Chatterji	German/Norwegian	Field site test after 7 years <sup>b</sup>	Reported reactivity in structures?
A	NR	R						
B	R	R						
C	R	R						
D	R	NR						
E	R	NR						Yes, > 40 years.
F	R	NR						Yes, > 10 years.
G	R	NR						
H	NR	NR						No, > 30 years.
I	R	R	NR	R/R	NR/-		n.r	Yes, 50 years.
J	R	R	MR	R/-	R/R	MR/MR		Yes, 20–25 years.
K	R	R	MR	R/-	R/R	MR/MR		Yes, 20–25 years.

R = reactive; NR = non-reactive; MR = marginally reactive; n.r = no rating yet possible.

<sup>a</sup> See Table 8 for details.

<sup>b</sup> The evaluation of the preliminary results from field sites is based on measurements of crack widths after about 7 years of exposure and expansion during the last 6 years (the expansion measurements were re-started in 2005 due to a problem with the zero measurement at some field sites).

<sup>c</sup> First indications of a reaction on at least one field site.

hours to assess ~200 quartz grains. With the image analysis method used in this study between 10 and 120 min was used to assess up to 27,606 quartz grains. As demonstrated by Castro and Wigum [38], and confirmed by the present study, petrographic image analysis allows the assessment of a higher number of quartz grains in a shorter time without compromising the precision of the results.

Furthermore, by calculating the size descriptors from the equivalent spherical diameter it was possible to achieve more accurate results (close to the real values). As discussed in Section 2.2.1 and shown in Table 6, different values are obtained when different measurements of grain size ( $d_E$ ,  $d_A$  or  $d_V$ ) are used. The values obtained with  $d_E$  and  $d_A$  will be similar if the grains have higher circularity and increasingly different with the increase of the irregularity of the grains. However, the calculation of these diameters does not take into account the overestimation of small grains produced by a two-dimensional planar section of a rock (thin-section). The equivalent spherical diameter  $d_V$ , being calculated with base on the volume weighted distribution of radii of spheres, represents a more accurate estimation of the grain size distribution [39]. Therefore, the size descriptors calculated from this measurement are also more accurate. Yet another advantage of petrographic image analysis is the possibility of doing grain shape analysis.

Even though both size descriptors are calculated using the cumulative grain size distribution curve obtained from the thin section examination by image analysis, only the total grain boundary area of quartz takes into account the shape of the cumulative curve. When comparing two rocks with the same mean grain size, the sample with a higher amount of quartz and a higher proportion of microcrystalline quartz will give a higher available total surface area [17]. Hence, the total grain boundary area of quartz gives a better

relationship with the reactivity of the aggregate than the mean grain size of quartz. Therefore, further correlations (Section 4.3) use the total grain boundary area of quartz calculated with  $d_V$ .

#### 4.2. Test procedures to determine potential alkali-reactivity

Based on local experience and criteria limits, all aggregates were classified as reactive by the petrographic method RILEM AAR-1 [3], except aggregates A and H that were considered non-reactive. This is in agreement with the reported reactivity in the structures for all the 6 aggregates to which field experience in structures is known.

There is good agreement between the ranking of the expansion of the aggregates after 14 days with the AMBT long bars (Tables 7 and 8) and their known reactivity in structures (Tables 1 and 7) for 4 samples, based upon acceptance criteria discussed in Section 3.2 and in Table 6. However, two aggregates reported to exhibit field reactivity (aggregates E and F) show low expansion. The agreement between the expansion of the aggregates after 14 days with the AMBT (Tables 7 and 8) and their potential reactivity by RILEM AAR-1 [3] (Table 7) is good for 6 samples. However, four aggregates reported to be potentially reactive by the petrographic method (aggregates D, E, F, and G) show low expansions by AMBT, and aggregate A reported to be non-reactive by the petrographic method shows an unexpected high expansion by AMBT. RILEM AAR-2 [6] claims that the AMBT may be especially useful for aggregates that react slowly (e.g. granite, rhyolite, gneiss, quartzite). However, several authors have shown that the limits usually applied are unable to detect some “slowly” reactive aggregates (e.g. [15,17,40]). The results from several studies (e.g. [11,12,15,20,41]) lead to the conclusion that these tests were considered inappropriate to evaluate the alkali reactivity of the Portuguese granitic aggregates [41], which may

**Table 8**

Detailed results of the accelerated mortar bar tests after 14 days.  
Adapted from [1,15,17,20].

Aggregate	AMBT	Original data		Data used for correlation with image analysis	
		Short bars	Long bars	Long bars	Observations
A	NBRI modified	0.10	–	0.13	Data calculated with PARTNER correlation factor (0.75)
B		0.17	–	0.23	
C		0.16	–	0.21	
D	ASTM C 1260-94	–	0.06	0.06	Original data
E		–	0.08	0.08	
F		–	0.03	0.03	
G		–	0.02	0.02	
H	–	0.01	0.01		
I	RILEM AAR-2	0.12	0.14–0.32	0.23	Average values of original data
J		0.14–0.25	0.10–0.21	0.21	
K		0.05–0.13	0.05–0.16	0.16	

explain some of the discrepancies found between the AMBT, the RILEM AAR-1 and the experience reported in structures to some of the Portuguese granites included in this study. The authors acknowledge that the results would be stronger if all AMBT have been performed using the same method and by the same laboratory.

From the additional laboratory tests performed to aggregates I, J and K during PARTNER project the accelerated concrete prism RILEM AAR-4 [7] gives the best correlation with the reported reactivity in structures for the aggregates. These results are also in agreement with the results for the petrographic method RILEM AAR-1 [3] and the AMBT RILEM AAR-2 [6]. The results from the concrete prism test RILEM AAR-3 [21] and the Danish mortar bar TI-B51 [33] do not correlate with the other test method results and experience with structures, especially for aggregate I. Despite the studies showing a significant reduction in expansion observed when known reactive aggregates were tested in the accelerated concrete prism test (60 °C) and compared to the concrete prism test (38 °C) [8], PARTNER conclusion was that for the studied aggregates the AMBT RILEM AAR-2 [6] and the accelerated concrete prism test RILEM AAR-4 [7] were the most effective and reliable [1]. The field site test after 7 years of experience [37] was not able to rate aggregate I yet, whilst aggregate J was classified as reactive, which means that more time is needed to get reliable results for these aggregates with this method.

#### 4.3. Correlation between the aggregate microstructure and test methods to determine potential reactivity

Samples with lower mean grain size and higher total grain boundary area correspond indeed to the rock types that exhibit higher deformation features in their microstructure (Table 6). Overall there is good agreement between the size descriptors (Table 6), the potential reactivity of the aggregate by RILEM AAR-1 [3], and the field experience reported in structures to 6 aggregates (Tables 1 and 7). The aggregates A and H, both classified non-reactive by the petrographic method RILEM AAR-1 [3] are the ones with lower total grain boundary area of quartz. Experience in structures is not known to aggregate A but aggregate H was used in at least one dam in Portugal and no damage in the structure has been reported after more than 30 years [15,20].

Fig. 2 shows the correlations between the total grain boundary area of quartz and the results obtained with the AMBT at 14 days. A reasonable logarithmic correlation was found ( $R^2 = 0.79$ ). The best fit line follows the same trend as the ones obtained by Wigum [17] and Wigum et al. [18] even if the rock types included in the present study have a more limited range of grain sizes. These results confirm that the reactivity of the “slow reactive” aggregates is related to the total grain boundary of quartz, which is strongly influenced by sub-grain development. These results can also be interpreted as evidence that grain size analyses by petrographic image analyses has similar precision to grain size analysis by the traditional point-counting method. It is a strong belief of the

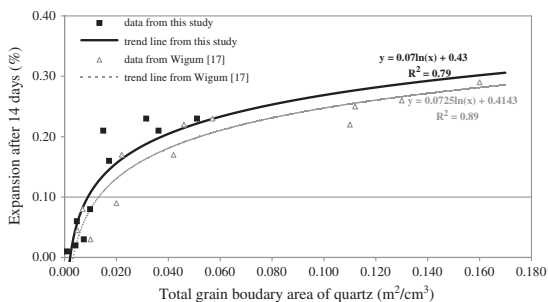


Fig. 2. Total grain boundary area of quartz versus accelerated mortar bar expansion results.

authors that if all AMBT have been performed using the same method and by the same laboratory better correlation would be achieved.

Aggregate sample A was regarded as outlier and was not included in the statistical model. The anomalous behaviour found for sample A was explained by Wigum [17]. Sample A is a porphyritic granite that contains relatively coarse quartz grains. The total grain boundary area of quartz is small; however, a relatively high expansion was registered by the AMBT. This might be due to the occurrence of strain lamellae which are observed in some of the quartz crystals. If these lamellae were regarded as subgrain boundaries, then the proportion of microcrystalline quartz would increase, and consequently the total grain boundary area would increase too which would lead to a better agreement with the model. On the other hand, the occurrence of myrmekite with thin rods of quartz in feldspar might also contribute to an enhanced solubility of the porphyritic granite. The role of strain lamellae and myrmekite must be investigated further before such types of granite are included into the model. The determination of error-free edges for a thin section is a complex task. Automated methods yield mistakes in classification whilst manual editing is tedious, prone to subjective judgments and human error. Fortunately, many scientists focus their research in the improvement of the efficiency of the edge detection algorithms.

The results of the concrete prism test RILEM AAR-3 [21] and the Danish mortar bar TI-B51 [33] do not correlate well with the total grain boundary area of quartz. Aggregate I, classified as non-reactive by both methods, have higher total grain boundary area of quartz when compared with aggregates J and K, which should mean that is the one with the higher potential to exhibit reactive behaviour. However, aggregates J and K have higher expansion results than aggregate I in both tests.

At this point, the authors consider that more research is needed to establish criteria limits on the total grain boundary area of quartz that determines an aggregate reactivity. Future research should focus on the investigation of more rock types and on the use of precise and reliable expansion tests. If the method to assess the aggregate reactivity is more accurate, the correlation with grain size and shape will be stronger.

The averaging of shape descriptors over all grains in a sample has shown to be an ineffective approach with no correlation with the expansion tests. Fig. 3 shows an example of the correlation between the average values of axial factor and circularity versus the results obtained with the AMBT at 14 days. Distributions of other characteristics were attempted, for example grain size distribution. Fig. 4 shows a typical example of the axial factor versus grain size distribution for the aggregates studied. Again no correlation is observed. A better correlation is visible when comparing circularity with grain size distribution (Fig. 5). It was observed that smaller grains tend to be more regular than bigger grains. This can be explained by the fact that smaller grains result from recrystallization whilst bigger grains have suffered ductile strain effects and deformation. Even though that is not evident from the data obtained with the studied samples, the grain shape can enhance the aggregate

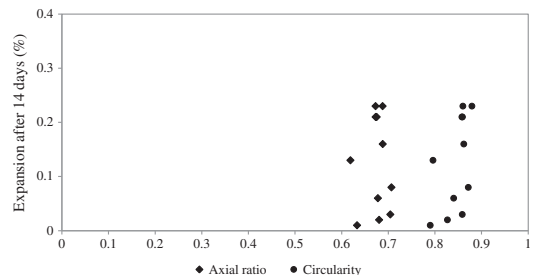


Fig. 3. Average axial factor versus accelerated mortar bar expansion results and average circularity versus accelerated mortar bar expansion results.

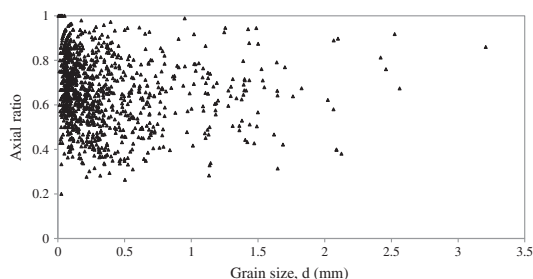


Fig. 4. Typical distribution of axial factor according to grain size distribution for the studied aggregates.

reactivity by increasing the surface area of the grain and therefore, future work shall not neglect the investigation of the influence of quartz grain shape in the aggregate reactivity.

## 5. Conclusions

In the current study image analysis has proven to be a precise and accurate method for grain size and grain shape analysis of aggregates for concrete:

- Not only is it possible to analyse samples much faster than with point-counting, a much larger number of grains can be analysed.
- Typical stereological problems such as the overestimation of the small grains produced by a two-dimension representation of a rock (thin-section) can be easily and efficiently overcome.
- Very good correlation was found between the grain size descriptors and the petrographic method RILEM AAR-1 [3] and the reported reactivity in structures.
- The correlations found between grain size descriptors and the AMBT follow the same trends by Wigum [17] and Wigum et al. [18], confirming that the reactivity of the “slow reactive” aggregates is related to the total grain boundary of quartz, which is strongly influenced by subgrain development.
- Good correlation was also found with the results of the accelerated concrete prism test RILEM AAR-4 [7] although only three results are available.
- No correlation was found between the average values of the grain shape descriptors and the laboratory tests to assess the potential reactivity of the aggregates or reported reactivity in structures, but it was observed that overall the small grains are more regular than bigger grains.

Hence we consider the image analysis approach presented above to be a real improvement over point-counting procedure suggested by Wigum [17] to perform grain size analysis of quartz. The method is

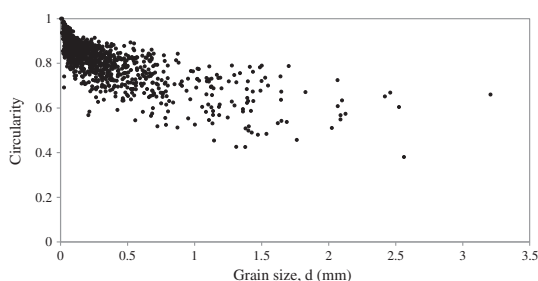


Fig. 5. Typical distribution of circularity according to grain size distribution for the studied aggregates.

currently limited to rock types with grain sizes resolvable under the optical microscope and quartz grains without high degree of strain. The grain size limitation can be easily overcome by adapting the method to input images obtained with other microscopes with higher resolution (for example a scanning electron microscope). The analysis of rock types with high degrees of strain may be possible in the future if further investigation is focussed in the improvement of the edge detection algorithms used to segment the images and build the grain boundary maps. The application of image analysis petrography is not restricted to the assessment of aggregates for concrete. This method bears great potential to be adapted to the assessment of deterioration in real structures (concrete thin-sections can also be analysed). Used as a supplement to the petrographic method RILEM AAR-1 [3], petrographic image analysis can help to overcome some of the limitations of the traditional petrographic method that have been reported in the literature and improve its value as a tool to evaluate the potential reactivity of aggregates for concrete.

## Acknowledgement

The first author wishes to acknowledge Fundação para a Ciência e Tecnologia ([www.fct.pt](http://www.fct.pt)) for the financial support through the doctoral grant SFRH/BD/41810/2007.

## References

- [1] J. Lindgård, P.J. Nixon, I. Borchers, B. Schouenborg, B.J. Wigum, M. Haugen, U. Åkesson, The EU “PARTNER” Project – European standard tests to prevent alkali reactions in aggregates: final results and recommendations, *Cem. Concr. Res.* 40 (2010) 611–635.
- [2] I. Sims, P. Nixon, RILEM recommended test method AAR-0: detection of alkali-reactivity potential in concrete – outline guide to the use of RILEM methods in assessments of aggregates for potential alkali-reactivity, *Mater. Struct.* 36 (2003) 472–479.
- [3] RILEM Recommended Test Method AAR-1, Detection of potential alkali-reactivity of aggregates – petrographic method, TC 191-ARP: ALKALI-reactivity and prevention – assessment, specification and diagnosis of alkali-reactivity, prepared by: Sims, I, Nixon, P, Mater. Struct. 36 (2003) 480–496.
- [4] ASTM C 295-98, in: Standard Guide for Petrographic Examination of Aggregates for Concrete, The American Society for Testing and Materials, 2007, p. 8.
- [5] Norsk Betongforening, Durable concrete with alkali reactive aggregates, *Norsk Betongforening* 2 (1) (2008) 15.
- [6] RILEM Recommended Test Method AAR-2, Detection of potential alkali-reactivity of aggregates – the ultra accelerated mortar bar test, *Mater. Struct.* 33 (2000) 283–283.
- [7] RILEM Recommended Test Method AAR-4.1, Detection of potential alkali-reactivity of aggregates. 60 °C accelerated method for aggregate combinations using concrete prisms, (in preparation).
- [8] J.H. Ideker, B.L. East, K.J. Folliard, M.D.A. Thomas, B. Fournier, The current state of the accelerated concrete prism test, *Cem. Concr. Res.* 40 (2010) 550–555.
- [9] B. Schouenborg, U. Åkesson, L. Lieberg, Precision trials can improve test methods for alkali aggregate reactions (AAR) – part of the PARTNER project, in: M.A.T.M. Broekmans, B.J. Wigum (Eds.), 13th International Conference on Alkali-Aggregate Reactions in Concrete, Trondheim, 2008, p. 9.
- [10] M. Haugen, J. Lindgård, U. Åkesson, B. Schouenborg, Experience from using the RILEM AAR-1 petrographic method among European petrographers – part of the PARTNER project, in: M. Broekmans, B.J. Wigum (Eds.), 13th International Conference on Alkali-Aggregate Reaction in Concrete (ICAAR), Trondheim, 2008, pp. 744–753.
- [11] I. Fernandes, F. Noronha, M. Teles, Microscopic analysis of alkali-aggregate reaction products in a 50-year-old concrete, *Mater. Charact.* 53 (2004) 295–306.
- [12] I. Fernandes, F. Noronha, M. Teles, Examination of the concrete from an old Portuguese dam: texture and composition of alkali-silica gel, *Mater. Charact.* 58 (2007) 1160–1170.
- [13] D.M. Kerrick, R.D. Hooton, ASR of concrete aggregate quarried from a fault zone – results and petrographic interpretation of accelerated mortar bar tests, *Cem. Concr. Res.* 22 (1992) 949–960.
- [14] A. Shayan, Alkali-reactivity of deformed granitic-rocks – a case-study, *Cem. Concr. Res.* 23 (1993) 1229–1236.
- [15] N. Castro, I. Fernandes, A. Santos Silva, Alkali reactivity of granitic rocks in Portugal: a case study, in: M. Bernhard, A. Just, D. Klein, A. Claubitt, J. Simon (Eds.), 12th Euroseminar on Microscopy Applied to Building Materials, Dortmund, 2009, p. 11.
- [16] F. Locati, S. Marfil, E. Baldo, Effect of ductile deformation of quartz-bearing rocks on the alkali-silica reaction, *Eng. Geol.* 116 (2010) 117–128.
- [17] B.J. Wigum, Examination of microstructural features of Norwegian cataclastic rocks and their use for predicting alkali-reactivity in concrete, *Eng. Geol.* 40 (1995) 195–214.
- [18] B.J. Wigum, P. Hagelia, M. Haugen, M.A.T.M. Broekmans, Alkali aggregate reactivity of Norwegian aggregates assessed by quantitative petrography, in: M.A. Bérubé, B.

- Fournier, B. Durand (Eds.), 11th International Conference on Alkali-Aggregate Reactions in Concrete, Québec, 2000, pp. 533–542.
- [19] P. Alaejos, V. Lanza, Influence of equivalent reactive quartz content on expansion due to alkali silica reaction, *Cem. Concr. Res.* 42 (2011) 99–104.
- [20] N. Castro, Granitic aggregates for concrete. Attempt of correlation between the granite age and the potential reactivity to alkalis of concrete, Master thesis, Faculdade de Ciências da Universidade do Porto, Portugal, 2008, pp. 122.
- [21] RILEM Recommended Method AAR-3, Detection of potential alkali-reactivity of aggregates: method for aggregate combination using concrete prisms, *Mater. Struct.* 33 (2000) 209–293.
- [22] J.S. Goodchild, F. Fueten, Edge detection in petrographic images using the rotating polarizer stage, *Comput. Geosci.* 24 (1998) 745–751.
- [23] J. Starkey, A.K. Samantary, Edge detection in petrographic images, *J. Microsc.* 172 (1993) 263–266.
- [24] R. Heilbronner, Lazy Grain Boundaries, Public Domain Macros for NIH Image, University of Basel, 1999. <http://pages.unibas.ch/earth/micro/index.html>.
- [25] R. Heilbronner, Automatic grain boundary detection and grain size analysis using polarization micrographs or orientation images, *J. Struct. Geol.* 22 (2000) 969–981.
- [26] S.D. Barrett, Image SXM, <http://www.ImageSXM.org.uk2008>.
- [27] E. Underwood, Quantitative Stereology, Addison-Wesley Publishing Company, 1970.
- [28] R. Heilbronner, Stripstar, Public Domain Program for the Calculation of 3-D Grain Size Distributions from Histograms of 2-D Sections, University of Basel, 1998. <http://pages.unibas.ch/earth/micro/index.html>.
- [29] ISO 9276-6, in: Representation of Results of Particle Size Analysis – Parte 6: Descriptive and Quantitative Representation of Particles Shape and Morphology, 2008, p. 23.
- [30] M. Takahashi, Fractal analysis of experimentally, dynamically recrystallized quartz grains and its possible application as a strain rate meter, *J. Struct. Geol.* 20 (1998) 269–275.
- [31] R.E. Oberholster, G. Davies, An accelerated method for testing the potential alkali reactivity of siliceous aggregates, *Cem. Concr. Res.* 16 (1986) 181–189.
- [32] ASTM C 1260-94, in: Standard Test Method for Potential Alkali-Aggregates (Mortar Bar Method), The American Society for testing and Materials, Philadelphia, 2007, p. 4.
- [33] TI-B51, Accelerated method for detection of alkali-aggregate reactivities of aggregates, *Cem. Concr. Res.* 8 (1978) 647–650.
- [34] S. Chatterji, A.D. Jensen, A simple chemical-test method for the detection of alkali-silica reactivity of aggregates, *Cem. Concr. Res.* 18 (1988) 654–656.
- [35] Deutscher Ausschuss für Stahlbeton, in: Vorbeugende Maßnahmen gegen schädigende Alkalireaktion im Beton : Alkali-Richtlinie, Beuth, Berlin, (DAFStb-Richtlinie), 2007.
- [36] Norwegian Concrete Association, Alkali-aggregate reactions in concrete, test methods and requirements to test laboratories, in: NB Publication No 32, 2005, p. 39, (in Norwegian).
- [37] I. Borchers, C. Müller, Seven years of field tests to assess the reliability of different laboratory test methods for evaluating the alkali-reactivity potential of aggregates, in: T. Drimalas, J.H. Ideker, B. Fournier (Eds.), 14th International Conference on Alkali-Aggregate Reactions in Concrete, Astin, Texas, USA, 2012, p. 10.
- [38] N. Castro, B.J. Wigum, Grain size analysis of quartz in potentially alkali-reactive aggregates for concrete: a comparison between image analysis and point-counting, in: M.A.T.M. Broekmans (Ed.), Proceedings of the 10th International Conference on Applied Mineralogy (ICAM), Springer Verlag, Heidelberg/Berlin, Trondheim, 2012, p. 8.
- [39] R. Heilbronner, D. Bruhn, The influence of three-dimensional grain size distributions on the rheology of polyphase rocks, *J. Struct. Geol.* 20 (1998) 695–705.
- [40] A. Shayan, Field evidence for inability of ASTM C 1260 limits to detect slowly reactive Australian aggregates, *Aust. J. Civ. Eng.* 3 (2007) 13–26.
- [41] A. Silva, A. Gonçalves, Appendix A – Portugal, in: B.J. Wigum, L.T. Pedersen, B. Grelk, J. Lindgård (Eds.), State-of-the-Art Report: Key Parameters Influencing the Alkali Aggregate Reaction, SINTEF, Trondheim, 2006, pp. 57–61.

**Quantitative assessment of alkali-reactive particles mineral content through XRD using polished sections as a supplementary tool to RILEM AAR-1 (Petrographic Method)**

*Authors: Nélia Castro, Bjørn E Sorensen, Maarten ATM Broekmans*

The candidate wrote the paper and performed the petrographic analysis. XRD analyses were performed at the Department of Geology and Mineral Resources Engineering at NTNU by the candidate and the co-supervisor and second author Bjørn E Sorensen. EPMA-CL analyses were performed by the technician at the Department of Materials Science and Engineering at NTNU in cooperation with the candidate and the co-supervisor and second author Bjørn E Sorensen. Ideas and the final manuscript were discussed with the co-supervisors and co-authors Maarten ATM Broekmans and Bjørn E Sorensen.

*The paper was published in Cement and Concrete Research 42 (2012): 1428-1437.*





## Quantitative assessment of alkali-reactive aggregate mineral content through XRD using polished sections as a supplementary tool to RILEM AAR-1 (petrographic method)

Nélia Castro <sup>a,\*</sup>, Bjørn E. Sorensen <sup>a</sup>, Maarten A.T.M. Broekmans <sup>b</sup>

<sup>a</sup> Norwegian University of Science and Technology (NTNU), Department of Geology and Mineral Resources Engineering, Sem Sælands vei 1, N-7491 Trondheim, Norway

<sup>b</sup> Geological Survey of Norway, Department of Industrial Minerals and Metals, PO Box 6315 Sluppen, N-7491 Trondheim, Norway

### ARTICLE INFO

#### Article history:

Received 22 June 2012

Accepted 9 August 2012

#### Keywords:

Alkali-aggregate reaction (C)

Aggregate (D)

X-ray diffraction (B)

Petrography (B)

Opaline silica

### ABSTRACT

The mineral content of 5 aggregate samples from 4 different countries, including reactive and non-reactive aggregate types, was assessed quantitatively by X-ray diffraction (XRD) using polished sections. Additionally, electron probe microanalyzer (EPMA) mapping and cathodoluminescence (CL) were used to characterize the opal-CT identified in one of the aggregate samples. Critical review of results from polished sections against traditionally powdered specimen has demonstrated that for fine-grained rocks without preferred orientation the assessment of mineral content by XRD using polished sections may represent an advantage over traditional powder specimens. Comparison of data on mineral content and silica speciation with expansion data from PARTNER project confirmed that the presence of opal-CT plays an important role in the reactivity of one of the studied aggregates. Used as a complementary tool to RILEM AAR-1, the methodology suggested in this paper has the potential to improve the strength of the petrographic method.

© 2012 Elsevier Ltd. All rights reserved.

### 1. Introduction

Alkali-aggregate reactions (AAR) cause severe damage in concrete structures worldwide. The most widespread type of AAR is the alkali-silica reaction (ASR), in which alkali-reactive silica *sensu lato* in the aggregate forms a hygroscopic and hydraulic gel with alkali inherited from the cement paste. The alkali gel expands upon hydration and cracks up the surrounding concrete, thereby reducing structure service-life and increasing cost for society. The incubation time needed before ASR damage starts ranges from a few months to several decades, much depending on aggregate type, binder type, and exposure climate.

There are two generalized classes of siliceous aggregates known to be potentially reactive with alkalis in concrete [1]: the normally reactive aggregates (those that react in a time scale of 5 to 20 years) and the slowly reactive aggregates (those that react in a time scale greater than 15–20 years). Normally reactive aggregates are characterized by the presence of very fine grained quartz and disorder forms of silica (e.g. opal, chalcedony). Slowly reactive aggregates are typically crystalline quartz-bearing rock types (e.g. mylonite, granite, gneiss, quartzite, greywacke, phyllite, and argillite).

Though the exact mechanism of AAR is a matter of dispute, there is general consensus that AAR at some point involves silica dissolution. Silica dissolves at extreme pH values in strongly acidic or strongly

alkaline conditions, and less around neutral pH. For this reason it is designated as an amphoteric material. Extreme values of pH are not very often found in geological ambient. However, the pore solution of concrete is an extreme alkaline environment (pH > 13), which will be a driving factor on the dissolution of silica minerals within the aggregates. A summary of a number of fundamental considerations related to the solubility of silica minerals under geological versus ASR conditions can be found in [2–4]. One of the key issues pointed out by [3,4] is that different silica species have different dissolution rates. Thus, the predominant silica species largely governs the alkali-reactivity potential of the aggregate, a disordered silica structure being more reactive than cristobalite, which in turn is more reactive than 'orderly quartz' [5].

Test methods to assess the ASR-potential of aggregate for concrete have been under development for several decades. To meet the needs of the building and construction industry these test methods are required to provide an accurate and precise result in the shortest time possible using the least resources possible. The petrographic method is used as a "first step" to assess the potential alkali-reactivity of aggregates for concrete followed by accelerated laboratory tests to confirm the results obtained. Mortar or concrete prisms are exposed to severe conditions of temperature and alkalinity to provoke expansion within days, weeks or years, depending on the method. Different European test methods were evaluated for their suitability for use with the wide variety of aggregates found across Europe in the EU-funded PARTNER project. The overall experience from the PARTNER project is that in most cases the RILEM tests could successfully identify the

\* Corresponding author. Tel.: +47 73 59 48 41; fax: +47 73 59 48 14.  
E-mail address: [nelia.castro@ntnu.no](mailto:nelia.castro@ntnu.no) (N. Castro).



reactivity of the aggregates tested [1]. It was concluded that the accelerated mortar bar test RILEM AAR-2 [6] and the accelerated concrete prism test RILEM AAR-4 [7] are the most effective and have the best precision. It was also found that the petrographic test RILEM AAR-1 [8] can potentially provide effective and reliable results quicker than other method, but has some limitations. Petrographic assessment according to the protocol described in RILEM AAR-1 classifies concrete aggregate as potentially reactive or innocuous based on rock nomenclature. It has been verified that this approach is not always reliable. On a worldwide basis, petrographers use essentially the same procedures for thin section preparation, and the same type of instrumentation to study them. However, different schools exist on the correct application of rock nomenclature complicating use of uniform terminology (see e.g. discussion in [9]). International trials using the RILEM AAR-1 method [8] carried out for the PARTNER project have shown that the precision and reproducibility of the petrographic method strongly depend on the experience and expertise of the petrographer. In addition, the alkali-reactivity potential of a given rock type is known to vary from one location (region, nation) to another, which has resulted in rather different rock classifications reflecting local experience [1,10]. Together, the above issues effectively prevent simple uniform classification of a given lithology as always alkali-reactive or invariably innocuous using solely rock nomenclature. It seems evident that the reactivity of certain rock types is dependent upon the microstructural features of the rock, rather than only the rock nomenclature.

As discussed previously, characterization of the predominant crystal structures is essential to assess the effect on the alkali-reactivity potential of aggregates for concrete, especially in rock types usually characterized as normally reactive. Major texts on XRD analysis [11–14] generally discourage the use of material without prior comminution and/or disaggregation for a range of reasons, primarily (too coarse) particle size, (poor) particle count statistics, (preferred) orientation issues, among many others. However, in materials like e.g. polymictic virgin aggregate, field concrete, and post-mortem mortar bars and concrete prisms, traditional sample preparation by pulverization can present a real challenge, for various reasons. Reliable mineralogical analysis of bulk (concrete, aggregate) material is compromised by limited sample size and hence unsatisfying representativeness (e.g. [15]), whereas analysis of individual particles as identified in thin section petrography is challenged by preparation issues and access to limited amounts of material too, albeit on a different size scale. On the other hand, sample and specimen preparation both do introduce artifacts affecting diffraction by attributing lattice deformation, contamination from equipment wear, etc. Thus, minimizing material treatment before analysis bears a strong potential to improve the result, especially for intrinsically fine-grained lithologies without (optically discernible) preferred orientation, e.g. chert, siltstone, rhyolite, siliceous limestone. In concrete petrography, use of polished solid samples offers several advantages. Rather than extracting fragile and often already cracked material (problematic in hardened concrete) and subsequent comminution, the chert particle of interest is cut in situ and polished with diamond paste. Thus prepared polished sections can be assessed in a petrographic microscope using incident illumination, SEM, and XRD, whereas the unpolished counterpart can be sacrificed for additional analysis by destructive methods. Castro et al. [16] compared XRD analyses on polished and powdered specimens prepared from the same single aggregate particle and demonstrated that diffraction results for both methods are indistinguishable.

In this paper, we have investigated normally and non-reactive rock types in post-mortem concrete prisms previously tested for expansion in PARTNER, in addition to virgin aggregate originally stocked for reference. This enables direct comparison of changes brought about by the reaction as well as identification of certain properties/qualities that render the quartz in a given lithology alkali-reactive or innocuous. Materials were initially assessed by thin section petrography to actually

identify alkali-reactive aggregate particles. Subsequently, selected particles were investigated using X-ray diffraction (XRD) on powdered sample as well as on polished sections, electron probe micro-analyzer (EPMA) and cathodoluminescence (CL) to assess mineral content and silica speciation. Results from XRD on polished sections are critically reviewed against results from traditionally powdered specimen. Finally, data on mineral content and silica speciation were compared with expansion data from PARTNER to identify the possible correlation.

## 2. Materials and methods

### 2.1. Materials

This study uses selected samples of virgin aggregate and post-mortem expansion test specimens previously applied in the PARTNER project [1]. Five aggregate samples (F1, F3 – non-reactive; B1, D1, G1 – normally reactive) from 4 different countries (France, Belgium, Denmark, and Germany) were selected for mineralogical and chemical characterizations of reactive constituents. After initial petrographic assessment, 25 individual particles were selected for further characterization by XRD.

### 2.2. Methods for assessment and analysis

#### 2.2.1. Thin section petrography

Two sections ~20 mm thick were cut lengthwise from each concrete prism with a 3 mm thick diamond blade. One section was impregnated with fluorescent epoxy and polished according to DS 423.39 [17], the other section was left unprepared. Both sections were studied in a Leitz-Wild Heerbrugg stereomicroscope using incident plain or fluorescent illumination to identify AAR reaction products and reactive aggregate particles. Subsequently, fluorescence-impregnated polished thin sections comprising confirmed alkali-reactive particles were prepared from the unprepared section using the procedure outlined in DS 423.40 [18] with minor adaptations. Due to the thickness of the diamond blade, a ~3 mm mismatch exists between fluorescent versus unprepared plane sections and a thin section prepared from latter, with possible consequences for intra-particle variation in mineral content and texture/fabric.

Virgin aggregate material was weighed and washed using ordinary tap water. Particles were counted and separated manually per lithology according to the RILEM AAR-1 [8] list, using a Leitz-Wild Heerbrugg stereomicroscope. Polished thin sections of potentially alkali-reactive lithologies as well as some unidentified particles were prepared using standard procedures (e.g. [19]).

Thin sections were analyzed in a Nikon Eclipse E600 microscope using transmitted illumination in plane-polarized light (PPL), cross-polarized light (XPL), and incident fluorescent illumination (FL), as applicable.

#### 2.2.2. X-ray diffraction (XRD)

A number of virgin aggregate particles were prepared for XRD analysis by powdering. These particles were pre-crushed using a percussion mortar to pass a 400  $\mu\text{m}$  sieve, and charged to a McCrone Micronizer with corundum grinding elements, adding 10 ml of ethanol as a grinding agent. All samples were ground for 5 min, extracted from the grinding jar, rinsed with ethanol, and subsequently dried overnight at 50 °C in a covered Petri dish. Pulverized sample material was put in a polymethyl methacrylate (PMMA) specimen holder following standard procedures described in [12] with minor adaptations. The powder surface was finished with a carrier glass for microscopy to ensure planarity and flatness.

In addition, this study uses polished specimens. Selected (potentially) alkali-reactive particles were liberated from the unprepared ex-PARTNER counterparts, manually plane polished in several steps and finished with 0.25  $\mu\text{m}$  diamond paste. Planarity and flatness of the polished surface were verified by putting a carrier glass for microscopy on the surface and observing the presence/absence of an

optical interference pattern. Fig. 1 shows a specimen prepared according to this procedure. Next, the polished aggregate particle was mounted on a PMMA holder using plasticine, similar to as common for observation of polished ore specimen for reflected light petrography. After manually charging the sample holder containing the polished specimen to the instrument, specimen height was carefully adjusted to the focal point of the goniometer to minimize offset and error in the apparent diffraction angle (Fig. 1C).

All specimens were analyzed spinning at 60 rpm in a Bruker D8 Advance X-ray diffractometer at the Department of Geology and Mineral Resources Engineering at NTNU. On both specimen types (i.e. powdered or polished), the projected primary beam had a diameter maximum of 12 mm, never exceeding the perimeter of the prepared specimen. Operating conditions were set to 40 kV and 40 mA, using CuK $\alpha$  radiation of wavelength  $\lambda = 1.54178 \text{ \AA}$ . Radiation was applied without monochromator, but K $\beta$  was removed by a Ni-foil filter in the incident/primary beam. Diffractograms were recorded using a Lynxeye CCD linear detector from 2 to 80° 2 $\theta$ , in 0.01° 2 $\theta$  increments with 1 s counting time per increment, with total scan time ~2 h and 17 min. Phase quantification was performed using the Rietveld refinement software TOPAS 4.2 with the fundamental parameter approach, using as few parameters as possible to fit the data in order to get better precision in the quantification.

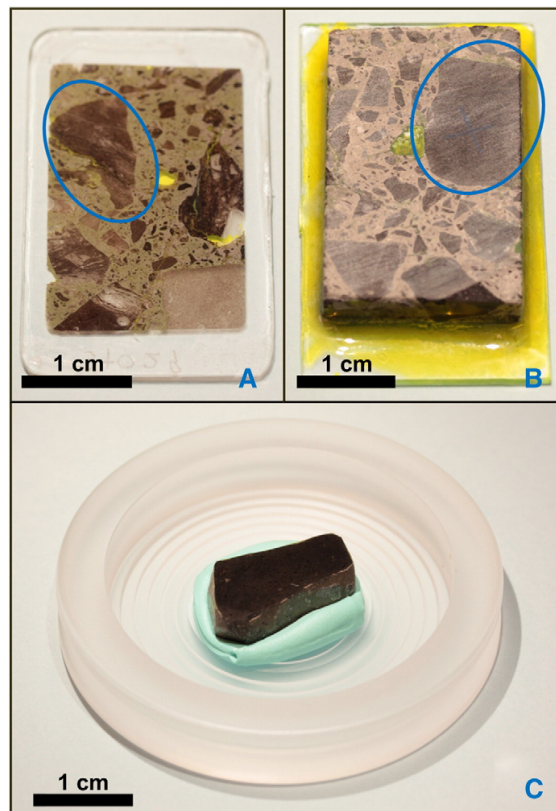


**Fig. 1.** Schematic representation of the steps needed to prepare the polished specimens to XRD analysis: (A) thin-section used to select the particle of interest; (B) unprepared thin-section counterpart; (C) particle liberated from the unprepared thin-section counterpart, manually plane polished and mounted on a PMMA holder using plasticine. Note that due to the thickness of the diamond blade, a ~3 mm mismatch exists between thin-section versus unprepared counterpart which explains the particle shape variation indicated by the blue ellipsoids.

### 2.2.3. Electron probe micro-analyzer – cathodoluminescence (EPMA-CL)

For element mapping by EPMA, a 30  $\mu\text{m}$  thick polished thin section was prepared from the unimpregnated counterpart of the ex-PARTNER prism containing particle D1-01, and sputter coated with ~270  $\text{\AA}$  carbon. Coated section was loaded in a JEOL JXA-8500F thermal field emission electron probe micro-analyzer at the Department of Materials Science and Engineering at NTNU. The instrument is equipped with five WDS (LIF, TAP, PET) spectrometers and one EDS spectrometer, allowing simultaneous acquisition of 5 + 16 elements Be–U, in addition to BE and SE imaging modes. The instrument also includes a WDS-based cathodoluminescence (CL) detector by XCLent, enabling simultaneous per-pixel analysis of CL spectrum and intensity as well as element composition.

The instrument was operated at  $10^{-5}$  Torr or better, 15.0 kV accelerating voltage, 20 nA beam current, and 250 ms dwell time, with an effective beam diameter of ~1  $\mu\text{m}$  (i.e. current density > 25 nA  $\mu\text{m}^2$ ). To obtain sufficient data for statistical assessment, a total of 3 maps acquired were distributed over the particle. Each area was scanned only once to preserve the luminescent properties of quartz, which often change with extended beam exposure (see e.g. [20]). Two element maps were acquired at  $400 \times 400$  pixel resolution (1 pixel = 2.5  $\mu\text{m}$ ) for Si, Ca, Fe, and Mg. Total acquisition time was 12 h and 22 min per map. One element map was acquired at  $512 \times 512$  pixel resolution (1 pixel = 1  $\mu\text{m}$ ) for Si, Ca, Fe, and Mg, with total acquisition time ~20 h and 12 min.

## 3. Results

### 3.1. Thin section petrography

Petrographic analysis of aggregate samples reveals that the aggregate material contains considerable variation in constituent lithologies. Fig. 2 presents some examples of the random textures typical of the rock types included in this study. Aggregate sample B1 contains angular fragments of various types of siliceous limestone (mud-, wacke-, packstones) containing calcareous foraminifera. Five particles of micritic limestone, containing predominantly calcite and minor quartz were selected for XRD analysis. Aggregate sample D1 contains sub-rounded glacio-fluvial gravel/sand, main constituent flint/chert and opaline limestone, minor greywacke, quartzite, granite, gneiss, and mafic rocks. Six particles were selected for XRD analysis: 2 particles of chert/flint containing predominantly quartz and minor carbonates; 2 particle of micritic limestone containing similar amounts of quartz and calcite and presumably minor opal; 2 particles of micritic limestone containing predominantly quartz and minor calcite. A reliable quantification of the tiny spherical aggregates (so-called lepispheres) of presumably opal observed in two of the particles of this aggregate was not possible due to the very fine grained nature of the samples. Aggregate sample G1 contains partly crushed, partly naturally rounded polymict river gravel, main constituent flint/chert and siliceous limestone, minor quartzite, sandstone, greywacke, granite and mafic rocks. Seven particles were selected for XRD analysis: 4 particles of micritic mudstone containing predominantly quartz and minor (relic) carbonate (note that numbers G1-75 and G1-76 apply to two separate parts of one and the same particle); 1 particle of micritic limestone containing predominantly calcite and minor quartz; 2 particles of chert/flint containing predominantly quartz and calcite veins crossing the particle. Aggregate sample F1 contains rounded polymict river gravel, main constituent flint/chert, minor siliceous limestone, mudstone, and greywacke. Six particles of chert/flint containing predominantly quartz and minor amounts of carbonates were selected for XRD analysis. Aggregate sample F3 contains sub-rounded polymictic gravel from Rhine valley, main constituents flint/chert and siliceous limestone, minor granite, sandstone, greywacke, quartzite, and rhyolite. One particle

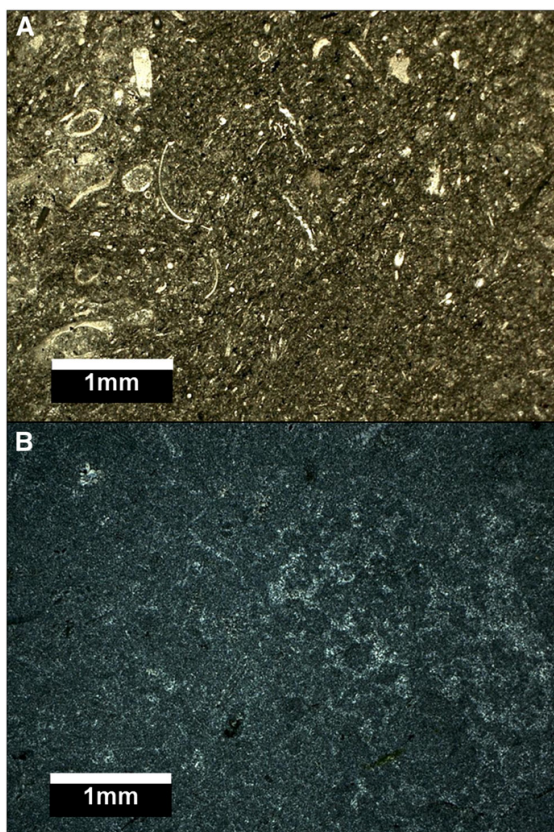


**Fig. 2.** Example of the random textures typical of the rock types studied in this paper: (A) microphotograph in plane-polarized light of a micritic limestone particle (aggregate sample B1) containing predominantly calcite and minor amounts of quartz and several examples of calcareous foraminifera; (B) microphotograph in crossed-polarized light of a chert particle (aggregate sample F1) containing predominantly quartz and minor amounts of carbonates.

of micritic limestone containing predominantly quartz and minor calcite was selected for XRD analysis.

### 3.2. X-ray diffraction (XRD)

Results from the XRD analysis, normalized to 100 wt.%, are collated in **Table 1**. Main rock forming constituents include quartz and calcite. The corundum identified in some of the powder sample material was regarded as contamination from the comminution process. Materials D1-01 and D1-05 appear to contain a substantial volume of light silica polymorphs cristobalite and tridymite, presumably representing fine-grained intergrowths in opal-CT (**Fig. 3**).

### 3.3. Electron probe micro-analyzer – cathodoluminescence (EPMA-CL)

Element maps for Si, Ca, Mg, and Fe, for each of the 3 areas in particle D1-01 were combined into a single map revealing the presence of quartz (Si only), and calcite (Ca only). Mg and Fe are not present in this sample or its amounts are below the detection limit of the EPMA equipment. A typical example of element maps for Si, Ca, and Fe is given in **Fig. 4**. Areas seemingly containing Si + Ca were regarded as overlap artifacts from the threshold method applied to segment single element images due to the porosity of the sample because

**Table 1**

Mineral modal composition of polished sections and powdered material by XRD quantitative Rietveld, in wt.% (LLD < 1). Mineral acronyms cf. [34].

Sample	Specimen type	Qz	Cal	Dol	Crs	Trd	Crn	SUM
LLD (in wt.%) <sup>a</sup>		1	1	1	1	1	1	–
B1-11	Polished section	1	97	1	<LLD	<LLD	<LLD	100
B1-12	Polished section	15	85	1	<LLD	<LLD	<LLD	100
B1-13	Polished section	16	81	3	<LLD	<LLD	<LLD	100
B1-14	Polished section	5	90	4	<LLD	<LLD	<LLD	100
B1-15	Polished section	6	91	2	<LLD	<LLD	<LLD	100
D1-00	Polished section	95	2	2	<LLD	1	<LLD	100
D1-01	Polished section	36	43	<LLD	12	8	<LLD	100
D1-02	Polished section	85	15	<LLD	<LLD	<LLD	<LLD	100
D1-03	Polished section	96	2	1	<LLD	1	<LLD	100
D1-04	Polished section	84	15	<LLD	<LLD	<LLD	<LLD	100
D1-05	Polished section	51	29	1	12	6	<LLD	100
F1-40	Polished section	99	1	<LLD	<LLD	<LLD	<LLD	100
F1-41	Polished section	96	1	1	<LLD	1	<LLD	100
F1-42	Polished section	95	2	1	<LLD	1	<LLD	100
F1-43	Polished section	97	1	1	<LLD	1	<LLD	100
F1-44	Polished section	97	1	1	<LLD	1	<LLD	100
F1-45	Polished section	96	1	2	<LLD	1	<LLD	100
F3-77	Polished section	82	18	<LLD	<LLD	<LLD	<LLD	100
G1-75	Polished section	65	33	1	<LLD	<LLD	<LLD	100
G1-76	Pulverized material	55	36	1	<LLD	<LLD	8	100
G1-26	Pulverized material	77	21	<LLD	<LLD	<LLD	1	100
G1-27	Pulverized material	46	27	26	<LLD	<LLD	<LLD	100
G1-28	Pulverized material	63	37	<LLD	<LLD	<LLD	<LLD	100
G1-29	Polished section	79	20	<LLD	<LLD	<LLD	<LLD	100
G1-30	Polished section	37	62	1	<LLD	<LLD	<LLD	100
G1-31	Polished section	69	31	<LLD	<LLD	<LLD	<LLD	100

<sup>a</sup> Lower detection limits stated by the equipment manufacturer for a single phase in a multiphase mixture and supported by major XRD books (e.g. [12,13]). Calibrated methods can achieve lower detection limits [23].

such phases are not expected in a low temperature rock type as the studied sample and all the areas with Si + Ca are in the boundary between Si and Ca grains. **Table 2** collates the results for combined multi-element maps for the 3 areas analyzed.

The acquired element maps contain at least  $400 \times 400 = 16,000$  data points for each of the 4 species analyzed. Corollary, one single data point (= pixel) represents 1/16,000 or 0.00625% part of the entire data set comprised in a single-element map. Thus, data can be reliably reported with 4 significant digits equalling  $1:10^4$  precision, or 0.01%.

Respective weight percentages of (assumedly) stoichiometrically pure quartz ( $\alpha$ -SiO<sub>2</sub>) and calcite (CaCO<sub>3</sub>) in the bulk sample material were calculated from relative surface areas in the Si + Ca multi-element maps and normalized using mineral densities: 2.65 g/cm<sup>3</sup> for quartz (ignoring polymorphism) and 2.71 g/cm<sup>3</sup> for calcite [21]. Average amounts of quartz and calcite in the sample are 64 wt.% and 36 wt.% respectively.

The visible CL-color can be expressed as a composite of the RGB-values for each pixel of the CL-image. The correlation of spectral regions with RGB-values for siliceous grains in the sample is shown in **Fig. 5**, where red covers the wavelengths from 730 to 580 nm, green from 580 to 500 nm, and blue from 500 to 360 nm. **Fig. 5**, spectrum B represents the CL-characteristics of the quartz in the sample. The investigation of the CL-properties of opal-CT in the studied chert particle did not yield results because of its very fine grain size, and intimate intergrowth with other minerals, especially quartz and calcite. Higher resolution CL images are required to better discriminate (supposed) opal-CT grains showing a characteristic CL-spectrum with a strong broad band at 540 nm and a weaker one at 650 nm [20,22] from the host. Now, the acquired CL spectrum may be affected by that from ordinary quartz at 650 nm and perhaps also from calcite at wavelength lower than 540 nm (**Fig. 5**, spectrum A). Therefore, reliable quantification of the relative modal amounts of quartz and opal-CT based on CL data was not possible here.



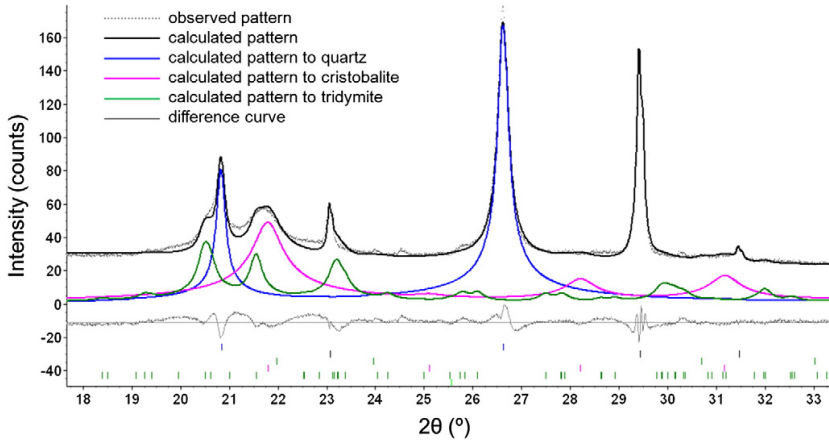


Fig. 3. Example of XRD fit for aggregate particle with opal.

4. Discussion

4.1. Thin section petrography

A first assessment by detailed petrography was essential to identify reactive aggregate particles relevant to investigate further in the scope of this paper. Original descriptions elaborated during the PARTNER project have been limited to a few lines in the final PARTNER report [23], and therefore important information essential to the present work was lacking. Overall there is good agreement

between the descriptions reported by PARTNER and the detailed petrographic assessment made in the scope of this study. The reactivity of the studied aggregates is indeed related with rock types such as flint/chert and silicified limestone being the siliceous limestone particles of aggregate D1 that present stronger signs of reaction such as dissolution, cracks and alkali-silica gel. For the micro- and cryptocrystalline rock types investigated here, reliable assessment of mineral modal content by thin section petrography is at least challenging and often impracticable, defining the demand for an operator-independent instrumental method.

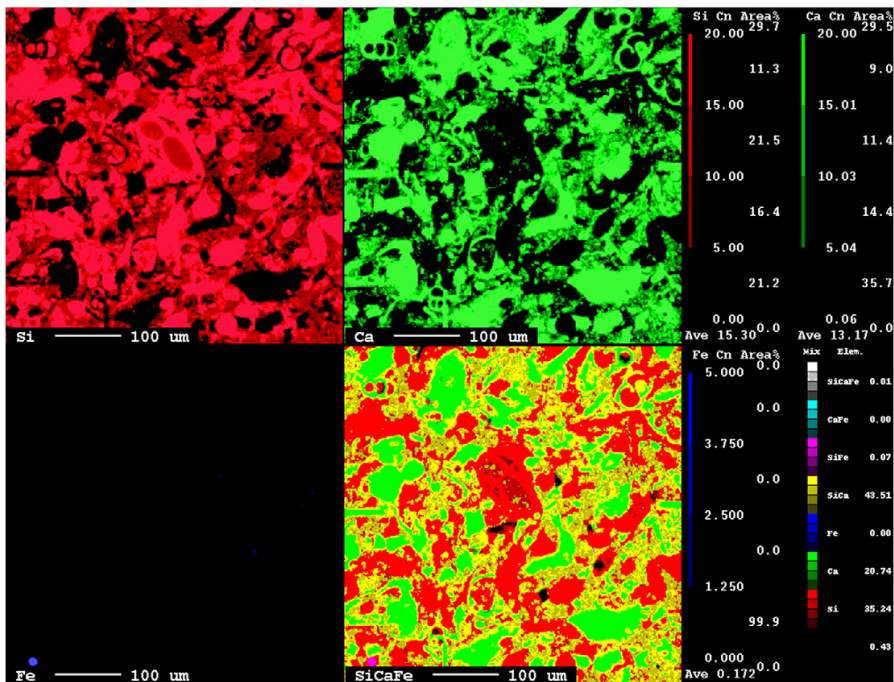


Fig. 4. Example of EPMA combined elemental map for Si, Ca and Fe, in area%. This image shows the typical distribution of these elements, but variation is observed from map to map (see Table 2). Note that the 20–100 μm areas consist of a multitude of randomly oriented grains up to 5 μm.

**Table 2**  
Relative surface areas per main element (combination) in sample D1-01 by EPMA, in area%.

Main element/ combination	Si	Ca	SiCa	Others	SUM total
Phase	SiO <sub>2</sub> polymorphs	Calcite	Porosity		
Map number #1	36.71	21.63	41.08	0.58	100
#2	39.07	18.97	41.52	0.44	100
#3	35.31	20.74	43.52	0.43	100
Avg. ( $\mu$ )	37.03	20.45	42.04	0.48	100
SD ( $\sigma$ )	1.90	1.35	1.30	0.08	

#### 4.2. X-ray diffraction (XRD)

After an optical petrographic microscope using polarized light, an XRD is arguably among the most widely available analytical instruments suitable for identification of crystalline substances, hereunder minerals. Moreover, data collections of confirmed quality on natural minerals and numerous synthetic crystalline substances are publicly available from an independent body, the International Center for Diffraction Data ([www.ICDD.com](http://www.ICDD.com)). Both optical properties and XRD data enable unequivocal identification of mineral species, as demonstrated by the fact that both are essential parts in the approval of new-identified mineral species. Finally, XRD analysis can be automated to a large extent. Here, we discuss a number of issues related to pulverization of sample material and powder mounts for XRD, compared to polishing of a cut surface.

##### 4.2.1. Particle count statistics

In traditional XRD analysis, sample materials are comminuted to fine powder (“flour”) as an adequately powdered sample comprises an infinite number of particles, thus enhancing signal count statistics for each recorded diffraction peak. According to Smith [24], the effective volume for SiO<sub>2</sub> (regardless of speciation) analyzed in a typical XRD instrumental setup using CuK $\alpha$  is on the order of 20 mm<sup>3</sup>. For 2–5  $\mu$ m powder, assuming 15 vol.% packing interspace in a particulate material, this comprises approximately 0.25–4 billion particles.

According to optical petrography in transmitted light (thin sections) and incident light (polished sections), the grain size of the chert/flint and siliceous limestone analyzed using polished sections is ~5  $\mu$ m maximum, their average size being estimated around 3  $\mu$ m. Thus, assuming a uniform 3  $\mu$ m grain size, and the sum volume of internal porosity (15 vol.%) and non-silica minerals (e.g. carbonate at 30 vol.%) the total number of grains of silica in diffraction is in the order of ~0.5 billion, i.e. well within the range of 0.25–4 billion grains as specified in Smith [24]. Note that the 20–100  $\mu$ m contiguous areas of Si in Figs. 2, 4 and 5 in fact consist of a multitude of randomly oriented silica grains up to 5  $\mu$ m, which element mapping is unable to resolve. Attempts to determine average grain size and size distribution of the silica in chert/flint using SEM and Electron Backscatter Diffraction (EBSD) mapping were unsuccessful, presumably attributable to specimen preparation issues.

##### 4.2.2. Particle size and distribution

Optimum particle size for quartz (or silica in general) is 2–5  $\mu$ m [11–14,24,25]. Undersized particles show peak height reduction and broadening, whereas oversized particles may exaggerate peak intensity when fulfilling the Bragg condition [14]. As discussed above, the samples investigated here with polished sections have an estimated mean grain size of ~3  $\mu$ m and maximum grain size of ~5  $\mu$ m, i.e. well within the range considered optimal for XRD analysis. Debris and relic abrasive from the polished section preparation may be nearly completely removed from voids and pores in the sample by ultrasonication, and will therefore not affect diffraction. Samples with grain size >5  $\mu$ m were comminuted to fine powder. It is important to prepare a powder with both optimum particle size and a narrow size distribution. This is readily achievable and reproducible with the micronizing equipment used [11,12]. Some powdered samples were found to contain traces of corundum  $\alpha$ -Al<sub>2</sub>O<sub>3</sub> most probably inherited from the corundum grinding elements in the micronizer.

##### 4.2.3. Surface amorphization

As results of the powdering process, an amorphous layer known as the Beilby–Bowden layer (after Beilby [26], and Bowden and Hughes [27]) of ~0.03  $\mu$ m = 30 nm forms at the particle surface, attenuating

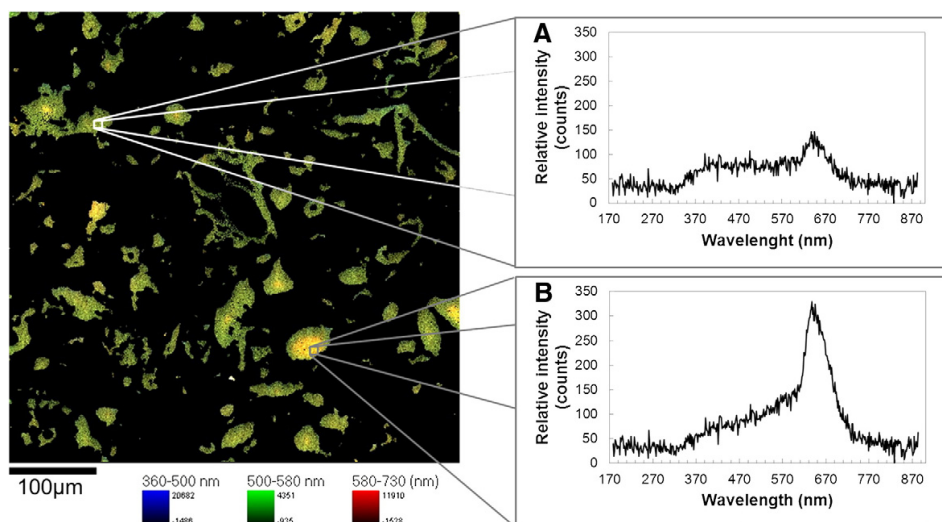


**Fig. 5.** CL-image and -spectra from siliceous material from particle D1-01: (A) spectra containing finely intergrowth grains of presumably opal-CT, quartz and calcite; (B) quartz. Note that the 20–100  $\mu$ m areas consist of a multitude of randomly oriented silica grains up to 5  $\mu$ m.

both incident and diffracted X-rays and deteriorating the signal with efficacy increasing for smaller particles. Amorphization as a preparation artifact is considerably less in a micronizer than for e.g. a ball mill, due to the cooling action of the liquid grinding medium, as well as the tension–yield predominated comminution (i.e. rubbing, as opposed to ball-pummeling). Furthermore, wide grain size distribution including both excessively amorphized undersized particles as well as oversized particles, typical of milled products, is nearly absent in micronized products. Polished sections are of course not only subject to surface amorphization (see e.g. [28]), but also the silica grains in the surface that are in direct contact with the polishing lap, representing a small percentage of the total number. The underlying grains are left unaffected by the polishing, so that the total volume of amorphized material is considerably less than in comminuted material, arguably on par with mortared or even micronized material. Light etching as usual for EBSD mapping might be able to remove the Beilby–Bowen layer. In conclusion, whereas in powder diffraction, comminuted grains smaller than  $\sim 1 \mu\text{m}$  are detrimental to the diffracted signal due to excessive amorphization (see following section), polished sections are not subject to comminution, and hence grains of that small size may be expected to contribute to the diffraction.

#### 4.2.4. Specimen mounting

Powdered materials are usually mounted in a sample well of a glass, aluminum or plastic specimen holder, as described here in Section 2.2.2. When charging the sample material to the holder, care must be taken to avoid preferred orientation of minerals with one or more pronounced cleavages, e.g. carbonates, mica or clay minerals, leading to relative overexposure of certain XRD reflections and rendering the analysis unfit for quantitative assessment of modal phase content. However, preferred orientation can be used to identify (not quantify) even small amounts of clay minerals that would remain unnoticed in randomly oriented specimen (e.g. [29]). Any clay minerals possibly present in the samples investigated here are below the XRD detection limit, as none have been identified.

The quartz grains in chert/flint and siliceous limestone analyzed with polished sections might potentially have a cryptic preferred orientation. As the fine grain size prevents assessment using a universal stage on an optical microscope, the presence/absence of a preferred orientation can be assessed by EBSD mapping in an SEM instrument (unsuccessful here, as mentioned above), or by assessment of selected reflections in the XRD diffractogram using the TOPAS software application. The latter did not reveal the presence of preferred orientation, so this can be ruled out for the samples investigated here.

#### 4.2.5. Summary

For the chert/flint and siliceous limestone investigated here, possible effects from sample/specimen preparation as discussed above for powdered mounts versus polished sections seem to balance out rather evenly. However, sample materials of different origins may have a very different grain size and size distribution, thus polished sections may not be suitable for all materials.

#### 4.2.6. Nature of tridymite and cristobalite

Aggregate sample D1 (D1-01 and D1-05) in two particles identified lightweighted silica polymorphs tridymite and cristobalite that were interpreted as fine intergrowths as opal-CT. Opal-CT is a paracrystalline form of hydrated silica containing ordered domains that mimic stacked sequences of cristobalite and tridymite sheets [24,25]. There is considerable stacking disorder in the ordered domains. However, the disordered regions contribute a weak, broad diffraction “scattering” peak in the XRD pattern onto which diffraction patterns of the ordered domains are superimposed. As defined by Smith [25], the XRD pattern is distinguished by the presence of a well-defined broad hump in the  $22^\circ$   $2\theta$  region with a satellite peak on the low-angle side and possible shoulder on the high angle. Some authors have developed methodologies to a

reliable quantification of different opals by XRD (e.g. [30]). Those methodologies are complex and difficult to apply to rock types where opal-CT represents only a small portion of the sample. Therefore, this study did not attempt to model opal-CT but rather the constituent polymorphs and assume that the combined amount of cristobalite and tridymite corresponds to the amount of opal-CT. Fig. 5 shows a good fit between real data and calculated curve to the applied model.

#### 4.3. Electron probe micro-analyzer – cathodoluminescence (EPMA-CL)

The presence and spatial distribution of opal-CT in sample D1 was assessed by element and CL mapping on the EPMA instrument. CL mapping shows that different types of silica are present in the sample (Fig. 5), but reliable quantification was not possible due to its very small grain size below the spatial resolution of the instrumentation. However, the combined amount of quartz, tridymite and cristobalite determined by XRD (56 wt.%) is consistent with the amount of  $\text{SiO}_2$  determined by EPMA (64 wt.%) in D1-01.

#### 4.4. Comparison with data from PARTNER

The PARTNER project [1] used a number of European test methods to assess the potential reactivity of aggregates for concrete. A brief outline of each method can be found in Table 3. Data for the aggregate samples included in this study are collated in Table 4.

These results show that 3 out of the 5 aggregate samples included in this paper have pessimum behavior. As defined by Hobbs [31], for a given level of alkalis, the expansion of concrete increases with the reactive aggregate content to reach a maximum value. For aggregate content superior to the maximum, the expansion decreases due to an excess of reactive silica. The proportion of reactive aggregates corresponding to the peak expansion is called the “pessimum content”. Concretes based on both coarse and fine aggregates of very fast reactive forms of siliceous aggregates like flint/chert usually do not swell. Flint or chert-containing aggregates typically show pessimum behavior from 20 to 30 vol.%, with expansion reducing to negligible for flint/chert contents of 60 vol.% or over. For pure opaline silica, which is among the most alkali-reactive forms of silica, pessimum content is typically 2–5 vol.%, and self-inhibition from around 15 vol.% and up. Brouard [32] defended the importance of correctly identifying the potentially reactive aggregates with pessimum effect. These aggregates can be used safely in concrete structures as long as these aggregates are used alone or mixed with potentially alkali-reactive aggregates. If they are mixed with non-reactive aggregates, the combination will likely lead to expansion and damage depending on the proportion of non-reactive aggregates.

The petrographic method RILEM AAR-1 [8] seems quite effective at identifying reactive materials, but may conflict with field experience in case a pessimum effect exists. The accelerated mortar bar test RILEM AAR-2 [6] was effective in all cases, except for F3 (reactive according to RILEM AAR-2, but no deleterious ASR reported in field structures). This aggregate is reported to have a marked pessimum effect, and it is probable that the difference in results between the concrete and mortar methods reflects the fact that the proportion of reactive material in the fine is within the pessimum proportion, but when the coarse and fine are tested together in concrete, the amount of reactive material exceeds the pessimum, and limited expansion is obtained. Overall, the concrete prism methods were effective in identifying both reactive and non-reactive aggregate combinations with the exception of aggregate sample D1. All laboratories except one identified this aggregate combination as non-reactive, whereas it is known from field experience to cause rapid and severe damage to structures in Denmark. It is also known, however, that this aggregate type has marked pessimum behavior, and it is presumed that the results for the concrete methods reflect the presence of an amount of

**Table 3**  
Brief outline of PARTNER test methods.

Test method	Brief outline of the method
Petrographic method RILEM AAR-1 [8]	The petrographic method comprises two techniques: macroscopic petrography, and thin-section petrography. Macroscopic petrography is used in coarse aggregate fractions > 4 mm. Thin-section petrography is applied to all fine aggregate fractions < 4 mm (point-counting method), as well as to any coarse constituent that could not be unequivocally identified by macroscopic petrography (whole rock petrography). The objective is to identify the mineral and rock constituents of the aggregate according to acknowledge nomenclature and classify the alkali-reactivity potential of each mineral and rock type identified. At the end of the test an aggregate should be classified as: I – very unlikely to be alkali-reactive; II – alkali-reactivity uncertain; III – very likely to be alkali-reactive.
Accelerated mortar bar method RILEM AAR-2 [6]	Test duration of 14 days. Mortar prisms made with the aggregate and a reference high alkali cement are stored in 1 M NaOH at 80 °C. Results of less than 0.10% are likely to indicate non-expansive materials, while results exceeding 0.20% are likely to indicate expansive materials. Results between 0.10% and 0.20% are difficult to interpret and in the absence of additional local experience shall be regarded as potentially expansive. These critical limits are still under discussion.
Concrete prism method RILEM AAR-3 [35]	Test duration of 12 months. Wrapped concrete prisms (dimensions ranging between 250 ± 50 mm and 75 ± 5 mm) made with the aggregate and a reference high alkali cement are stored in individual containers within a constant temperature room at 38 °C and measured at 20 °C. The aggregate is considered reactive if expansion is higher than 0.05% in the end of the test.
Accelerated concrete prism method RILEM AAR-4 [7]	Test duration of 20 weeks. Concrete prisms (dimensions ranging between 250 ± 50 mm and 75 ± 5 mm) made with the aggregate and a reference high alkali cement are stored in individual containers within a reactor at 60 °C and measured at 20 °C. The aggregate is considered reactive if expansion is higher than 0.03% in the end of the test.
Accelerated concrete prism method RILEM AAR-4 Alt. [7] The Danish mortar bar test TI-B51 [36,37]	Same procedure as RILEM AAR-4 but the prisms are wrapped. Test duration of 52 weeks. Mortar prisms (40 × 40 × 160 mm) made with the aggregate are stored in saturated NaCl solution at 50 °C. The aggregate is considered non-reactive if expansion is less than 0.04% after 20 weeks; late slow reactive if expansion is lower than 1.0% after 20 weeks and higher than 1.0% after 52 weeks; and fast highly reactive if expansion is higher than 1.0% after 20 weeks.
The Danish Chatterji method [38]	The degree of reaction between silica in the aggregate and KCl is determined by measuring the alkalinity after 24 h reaction compared to a non-reactive standard.
German concrete method [39]	Test duration of 9 months. Three concrete prisms (100 × 100 × 500 mm) and one cube (300 × 300 × 300 mm) are stored in a fog chamber at 40 °C with measurements taken immediately with no cooling down period. The aggregate is considered reactive if expansion is higher than 0.06% in the end of the test.
Norwegian concrete prism method [40]	Test duration of 12 months. Three concrete prisms (100 × 100 × 450 mm) made with the aggregate and a reference high alkali cement are stored in individual containers within a constant temperature room at 38 °C and 100% relative humidity and measured at 20 °C. The aggregate is considered reactive if expansion is higher than 0.04% in the end of the test.

opaline chert/flint that takes the combination past the pessimum amount when the fine and coarse aggregates are used together.

When comparing the results from PARTNER to the results obtained in this study with XRD some interesting considerations can be drawn. A recent investigation by Garcia-Diaz et al. [33] with siliceous limestones concluded that contrary to the pure siliceous aggregates, the content of silica in siliceous limestones is too low to consume a maximum of alkalis in non-expansive adsorption process and to obtain

non-expansive concretes. This is in agreement with the results obtained for the aggregate samples B1 and G1. Both have variable amounts of carbonates and higher reactivity than the aggregate sample F1. On the other hand, Zhang [5] defends that the phase in which silica occurs plays a dominant role in determining the reactivity, with disordered structures more reactive than structures containing cristobalite, which are in turn more reactive than structures containing quartz. Although more research is needed to confirm experimentally this theory, it is

**Table 4**  
Comparison of results of test methods with behavior in field sites and structures for the studied aggregates (adapted from [1,41]).

Aggregate sample	Fraction/combination	Reactivity/evaluation							
		AAR-1	AAR-2	AAR-3	AAR4/AAR-4 Alt.	TI-B51/Chatterji	German/Norwegian	Field site test after 7 years <sup>a</sup>	Reported reactivity in structures?
B1	F	R	R			R/R			Yes
	C	R							
	C + F			R	R/R		R/R	R	
D1	C + NRF			R	R/R			R	Yes, but pessimum effect
	F	R	R			R/R			
	C	R	R						
F1	C + F			? <sup>b</sup>	NR/NR		NR/–		No, but known pessimum effect
	C	R	NR			NR/R		R <sup>c</sup>	
	C + NRF			NR	NR/NR		NR/–		
F3	F	R	R			NR/R			No, but likely pessimum effect
	C	R							
	C + F			NR	NR/NR				
G1	C	R	R			R/–			Yes
	C + NRF			R	R/R		R/–	R	

F = fine aggregate; C = coarse aggregate.

NRF = non-reactive fine aggregate.

R = reactive (according to the critical limits in the different testing methods); NR = non-reactive (according to the critical limits in the different testing methods).

<sup>a</sup> The evaluation of the preliminary results from the field sites is based on measurements of crack widths after ~7 years of exposure and of expansions during the last 6 years (the expansion measurements were re-started in 2005 due to problems with the zero measurements at some field sites).

<sup>b</sup> One result strongly reactive, second non-reactive.

<sup>c</sup> First indication of reactivity in at least one field site.



interesting to observe that aggregate sample D1, where opal-CT was identified by XRD in two particles, was ranked as highly reactive by field experience but expansion after 14 days with RILEM AAR-2 was lower than other aggregate samples like F1 and G1 that show lower reactivity in the field than aggregate sample D1. Another interesting fact about aggregate sample D1 is that it has shown pessimum behavior despite its composition that is not the typical “pure siliceous aggregate”.

## 5. Summary and conclusions

This paper presents the results on selected aggregate materials from PARTNER, both alkali-reactive particles extracted from post-mortem prisms used in expansion testing as well as unreacted equivalent particles from virgin aggregate originally stored for reference. Alkali-reactive particles were first identified by optical petrography, then assessed in detail by XRD on powdered material and polished sections, and one particle was further assessed using element mapping and cathodoluminescence in an EPMA instrument. Based upon the reported results and above discussion, we draw the following conclusions:

- due to fine grain size (~3 μm average, ~5 μm maximum) of the chert/flint and siliceous limestone investigated here, optical petrography is unsuitable for reliable quantitative assessment of mineral content and/or silica speciation, nor for the identification of preferred orientation, justifying the use of XRD analysis;
- grain size and size distribution of the silica in the samples analyzed with polished sections are within the 2–5 μm range considered best suitable for XRD analysis;
- the number of silica grains in diffraction in the effective volume in polished sections is comparable with the number of silica particles in powder specimens, allowing phase quantification;
- the total volume of amorphized material as a sample preparation artifact is theorized to be less in polished sections compared to powdered sample material;
- preferred orientation could not be identified by optical petrography (too fine grain size), EBSD mapping on an SEM (probably sample preparation issues), nor by assessment of the diffractogram;
- XRD analysis of the chert/flint and siliceous limestone investigated here using polished sections provides results that are indistinguishable from results obtained using powdered material. Previous implications by Castro et al. [16] are now theoretically corroborated;
- the presence of other species of silica in addition to quartz was confirmed by cathodoluminescence using an FEG EPMA instrument. XRD analysis implies these might represent cristobalite and/or tridymite, presumably present as opal-CT.
- reliable quantification (e.g. using image analysis) was not possible due to grain size being below the spatial resolution of the FEG EPMA instrument;
- expansion data from PARTNER coincide with the presence of known deleterious alkali-reactive silica species, notably fine grained quartz;
- the identification of additional silica species other than quartz in sample D1 coincides with the unexpected pessimum behavior and very high expansion in the field although non-reactive results in several other tests have observed pessimum as reported by PARTNER project.

The results point indeed that for the studied samples (fine-grained flint/chert and siliceous limestone with grain size below ~5 μm and without preferred orientation) the assessment of mineral content by XRD using polished sections represents an advantage over traditional powder specimens. Extending the results obtained here to samples from other locations, or to other (very) fine grained lithologies (e.g. siltstone, greywacke, rhyolite) is likely to produce different results. Therefore, future work should focus on the assessment of XRD analysis using polished sections from samples of flint/chert and siliceous limestone of different origins and nature, as well as of different lithologies to clearly understand the limitations of the method. Nevertheless, used as a complementary tool to RILEM AAR-1, the

methodology suggested in this paper has the potential to improve the strength of the petrographic method.

## Acknowledgments

The first author wishes to acknowledge Fundação para a Ciência e Tecnologia ([www.fct.pt/](http://www.fct.pt/)) for the financial support through doctoral grant SFRH/BD/41810/2007.

## References

- [1] J. Lindgård, P.J. Nixon, I. Borchers, B. Schouenborg, B.J. Wigum, M. Haugen, U. Åkesson, The EU “PARTNER” Project – European standard tests to prevent alkali reactions in aggregates: final results and recommendations, *Cem. Concr. Res.* 40 (2010) 611–635.
- [2] M.A.T.M. Broekmans, Classification of the alkali-silica reaction in geochemical terms of silica dissolution, in: H. Pietersen, J. Larbi, H. Janssen (Eds.), 7th Euroseminar on Microscopy Applied to Building Materials, Delft, 1999, pp. 155–170.
- [3] M.A.T.M. Broekmans, The alkali-silica reaction: mineralogical and geochemical aspects of some Dutch concretes and Norwegian mylonites, PhD thesis, University of Utrecht, Geologica Ultraeina 217, 2002, pp. 144.
- [4] M.A.T.M. Broekmans, Structural properties of quartz and their potential role for ASR, *Mater. Charact.* 53 (2004) 129–140.
- [5] X. Zhang, B.Q. Blackwell, G.W. Groves, The microstructure of reactive aggregates, *Br. Ceram. Trans. J.* 89 (1990) 89–92.
- [6] RILEM Recommended Test Method AAR-2, Detection of potential alkali-reactivity of aggregates – the ultra accelerated mortar bar test, *Mater. Struct.* 33 (2000) 283–293.
- [7] RILEM Recommended Test Method AAR-4.1, Detection of potential alkali-reactivity of aggregates. 60 °C accelerated method for aggregate combinations using concrete prisms, (in preparation).
- [8] RILEM Recommended Test Method AAR-1, Detection of potential alkali-reactivity of aggregates – petrographic method, TC 191-ARP: alkali-reactivity and prevention – assessment, specification and diagnosis of alkali-reactivity, prepared by: Sims, I, Nixon, P, *Mater. Struct.* 36 (2003) 480–496.
- [9] M.A.T.M. Broekmans, I. Fernandes, P. Nixon, A global petrographic atlas of alkali-silica reactive rock types: a brief review, in: B. Middendorf, A. Just, D. Klein, A. Glaubitt, J. Simon (Eds.), 12th Euroseminar on Microscopy Applied to Building Materials, Dortmund, 2009, pp. 39–50.
- [10] B. Schouenborg, U. Åkesson, L. Lieberg, Precision trials can improve test methods for alkali aggregate reactions (AAR) – part of the PARTNER-project, in: M.A.T.M. Broekmans, B.J. Wigum (Eds.), 13th International Conference on Alkali-Aggregate Reactions in Concrete, Trondheim, 2008, p. 9.
- [11] D.L. Bish, R.C. Reynolds, Sample preparation for X-ray-diffraction, *Rev. Mineral.* 20 (1989) 73–99.
- [12] V.E. Buhrke, R. Jenkins, D.K. Smith, A Practical Guide for the Preparation of Specimens for X-ray Fluorescence and X-ray Diffraction Analysis, Wiley-VCH, New York, 2001.
- [13] B.D. Cullity, S.R. Stock, Elements of X-ray Diffraction, 3rd ed. Prentice Hall, Upper Saddle River, New Jersey, 2001.
- [14] H.P. Klug, L.E. Alexander, X-ray Diffraction Procedures for Polycrystalline and Amorphous Materials, 2nd ed. John Wiley & Sons, 1974.
- [15] M.A.T.M. Broekmans, Sample representativity: effects of size and preparation on geochemical analysis, in: B. Fournier (Ed.), Marc-André Bérubé Symposium on Alkali-aggregate Reactivity in Concrete 8th CANMET / ACI International Conference on Recent Advances in Concrete Technology Montréal, 2006, pp. 1–19.
- [16] N. Castro, B.E. Sorensen, M.A.T.M. Broekmans, Assessment of individual ASR-aggregate particles by XRD, in: M.A.T.M. Broekmans (Ed.), Proceedings of the 10th International Conference on Applied Mineralogy (ICAM), Springer Verlag, Heidelberg/Berlin, Trondheim, 2012, pp. 95–102.
- [17] Danish Standard Association, in: Concrete Testing – Hardened Concrete – Production of Fluorescence Impregnated Plane Sections (in Danish), DS 423.39, 2002, p. 8.
- [18] Danish Standard Association, in: Concrete Testing – Hardened Concrete – Production of Fluorescence-Impregnated Thin Sections (in Danish), DS 423.40, 2002, p. 12.
- [19] D.W. Humphries, The preparation of thin sections of rocks, minerals and ceramics, Royal Microscopical Society, Oxford Science Publications, 1992.
- [20] J. Götz, M. Plötze, D. Habermann, Origin, spectral characteristics and practical applications of the cathodoluminescence (CL) of quartz – a review, *Mineral. Petrol.* 71 (2001) 225–250.
- [21] W.A. Deer, R.A. Howie, J. Zussman, An Introduction to the Rock Forming Minerals, 2nd ed. Pearson, 1992.
- [22] D.K. Richter, T. Gotte, J. Gotze, R.D. Neuser, Progress in application of cathodoluminescence (CL) in sedimentary petrology, *Mineral. Petrol.* 79 (2003) 127–166.
- [23] J. Lindgård, M. Haugen, PARTNER report 3.1 – experience from using petrographic analysis according to the RILEM AAR-1 method to assess alkali reactions in European aggregates, in: SINTEF Building and Infrastructure, 2006.
- [24] D.K. Smith, Evaluation of the detectability and quantification of respirable crystalline silica by X-ray powder diffraction methods, *Powder Diff.* 12 (1997) 200–227.
- [25] D.K. Smith, Opal, cristobalite, and tridymite: noncrystallinity versus crystallinity, nomenclature of the silica minerals and bibliography, *Powder Diff.* 13 (1998) 2–19.



- [26] G. Beilby, *Aggregation and flow of solids, Being the Records of an Experimental Study of the Micro-structure and Physical Properties of Solids in Various States of Aggregation*, MacMillan & Co, London, 1921.
- [27] F. Bowden, T. Hughes, Physical properties of surfaces IV – polishing, surface flow and the formation of the Beilby layer, in: *Proceedings of the Royal Society*, 160A, 1937, pp. 575–587.
- [28] G. Vandervoort, *Metallography, Principles and Practice*, American Society for Metals (ASM) International, Metals Park, OH, 1999.
- [29] S. Fiore, J. Cuadros, F. Huertas, Interstratified clay minerals: origin, characterization and geochemical significance, in: *ALPEA Educational Series*, 2011, p. 175.
- [30] G.D. Guthrie, D.L. Bish, R.C. Reynolds, Modeling the X-ray-diffraction pattern of opal-Ct, *Am. Mineral.* 80 (1995) 869–872.
- [31] D.W. Hobbs, *Alkali-Silica Reaction in Concrete*, Thomas Telford Ltd., London, 1988.
- [32] E. Brouard, Potentially reactive aggregates with a pessimum effect. Pessimism effect mechanisms, review of PRP qualification tests and conditions of use of these aggregates, in: T. Drimalas, J.H. Ideker, B. Fournier (Eds.), 14th International Conference on Alkali-Aggregate Reactions in Concrete Austin, Texas, 2012, p. 10.
- [33] E. Garcia-Diaz, D. Bulteel, Y. Monnin, P. Degrugilliers, P. Fasseu, ASR pessimum behaviour of siliceous limestone aggregates, *Cem. Concr. Res.* 40 (2010) 546–549.
- [34] D.L. Whitney, B.W. Evans, Abbreviations for names of rock-forming minerals, *Am. Mineral.* 95 (2010) 185–187.
- [35] RILEM Recommended Method AAR-3, Detection of potential alkali-reactivity of aggregates: method for aggregate combination using concrete prisms, *Mater. Struct.* 33 (2000) 209–293.
- [36] TI-B51, accelerated method for detection of alkali-aggregate reactivities of aggregates, *Cem. Concr. Res.* 8 (1978) 647–650.
- [37] B. Grelk, PARTNER report 3.4 – experience from testing of the alkali reactivity of European aggregates according to two Danish laboratory test methods, in: *SINTEF Building and Infrastructure*, 2006.
- [38] S. Chatterji, A.D. Jensen, A simple chemical test method for the detection of alkali-silica reactivity of aggregates, *Cem. Concr. Res.* 18 (1988) 654–656.
- [39] Deutscher Ausschuss für Stahlbeton, Vorbeugende Maßnahmen gegen schädigende Alkalireaktion im Beton: Alkali-Richtlinie, Beuth, Berlin, 2007. (DAfStb-Richtlinie).
- [40] Norsk Betongforening, in: *Durable Concrete with Alkali Reactive Aggregates*, 21, Norsk Betongforening, 2008, p. 15.
- [41] I. Borchers, C. Müller, Seven years of field tests to assess the reliability of different laboratory test methods for evaluating the alkali-reactivity potential of aggregates, in: T. Drimalas, J.H. Ideker, B. Fournier (Eds.), 14th International Conference on Alkali-Aggregate Reactions in Concrete, Austin, Texas, USA, 2012, p. 10.

### **Potential contribution of EBDS to understand the role of quartz deformation in the alkali-reactivity of aggregates for concrete**

*Authors: Nélia Castro, Bjørn E Sorensen, Børge J Wigum, Jarle Hjelen, Wilhelm Dall*

The candidate wrote the paper and performed the petrographic analysis. EBSD analyses were performed at the Department of Materials Science and Engineering at NTNU by the co-author Wilhelm Dall in cooperation with the candidate, the co-supervisor and second author Bjørn E Sorensen, and the co-author Jarle Hjelen. Ideas and the final manuscript were discussed with all the co-authors.

*The paper was submitted to Materials Characterization (November 2012).*

Is not included due to copyright

